Bayerische Julius-Maximilians-Universität Würzburg

Fakultät für Biologie

Cellular Factors Contributing to Host Cell Permissiveness in Support of Oncolytic Vaccinia Virus Replication

Doctoral thesis

for a doctoral degree at Julius-Maximilians-Universität Würzburg

submitted by

Jennifer Reinboth

from

Altenstadt (Hessen), Germany

Würzburg, 2012

Date of Submission: .....

Dissertation Examination Committee:

Chairman: .....
Prof. Dr. Rössler

Primary Supervisor: .....
Prof. Dr. A.A Szalay

Secondary Supervisor: .....
Prof. Dr. G. Krohne

Date of Public Defense: .....

Date of Receipt of Certificates: .....

"…answers preexist,
and it is the question that needs to be discovered"

(Jonas Salk)

Für Christian, meine Familie und Freunde

Table of contents

Summary

Although remarkable progress has been made in the field of cancer research, certain types and advanced stage cancer still remain untreatable. Current cancer therapy options, such as chemotherapy, radiotherapy, hormonal therapy, or targeted therapy, are limited in regards to their long-term efficacy and are often restricted to a particular cancer type, stage, or body part. In many patients an emerging resistance to chemotherapy and targeted therapy treatments has been observed. Additionally, current available treatment options often fail to cure metastatic cancer. During the last few years, the use of oncolytic viruses (OVs) has arisen as an innovative and promising approach to treat cancer. OVs feature an intrinsic or acquired tumor tropism, leading to a tumor-specific viral life cycle ultimately causing lysis of the infected cancer cell. In this regard, vaccinia virus (VACV) has emerged as an exciting candidate, not only due to its ability to infect metastases and circulating tumor cells, but also due to its potential for gene delivery.

VACV replication efficiency is essential for antitumor activity and is directly associated with oncolytic function. In addition, the permissiveness of host cells to oncolytic VACV treatment is dependent on successful viral replication and propagation. With that, this study centers on the investigation of cellular factors that could influence VACV replication and thus predict permissiveness of host cells to VACV treatment.

In initial experiments, the well characterized VACV strain GLV-1h68 and three wild-type LIVP isolates (LIVP 1.1.1, LIVP 5.1.1, and LIVP 6.1.1) were utilized to analyze gene expression in a pair of autologous human melanoma cell lines (888-MEL and 1936-MEL) after infection. Microarray analyses, followed by sequential statistical approaches, characterized human genes whose transcription is affected specifically by VACV infection. In accordance with the literature, those genes were involved in broad cellular functions, such as cell death, protein synthesis and folding, as well as DNA replication, recombination, and repair.

In parallel to host gene expression, viral gene expression was evaluated with help of customized VACV array platforms to get better insight over the interplay between VACV and its host. Our main focus was to compare host and viral early events, since virus genome replication occurs early after infection. We observed that viral transcripts segregated in a characteristic time-specific pattern, consistent with the three temporal expression classes of VACV genes, including a group of genes which could be classified as early-stage genes. Comparing the averaged gene expression of those early genes within the different VACV isolates, we found that LIVP 6.1.1 showed the highest mean levels of gene transcription, followed by LIVP 1.1.1 and LIVP 5.1.1, and finally by the attenuated GLV-1h68 strain. Similar results were observed for viral replication efficiency of the individual isolates.

Recently we showed for the NCI-60 panel of cell lines that GFP marker gene expression of GLV-1h68 correlates with the respective viral copy number indicating that viral gene transcription can be evaluated as a parameter indicative of viral replication. Accordingly, in this work, comparison of VACV early replication and respective early gene transcription led to the identification of seven viral genes (*F15L*, *G2R*, *G5R*, *D9R*, *A5R*, *A20R*, and *A24R*) whose expression correlated strictly with replication. At least five of those are being known for their involvement in viral replication or transcription. Consequently, we considered the early expression of those seven genes to be representative for VACV replication and we therefore referred to them as viral replication indicators (VRIs).

To explore the relationship between host cell transcription and viral replication, we correlated viral (VRI) and human early gene expression. Correlation analysis revealed a subset of 114 human transcripts whose early expression tightly correlated with early VRI expression and thus early viral replication. These 114 human molecules represented an involvement in cell cycle, cell-to-cell signaling and interaction, protein ubiquitination, EIF2 signaling, and inflammatory disease. Of special interest was the analysis of the ubiquitination and proteasomal degradation pathways, since recent reports revealed the importance of the pathways for efficient reproduction and replication of orthopoxviruses. We found at least six out of 114 correlates to be involved in protein ubiquitination or proteasomal function. Another molecule of interest was the serine-threonine protein kinase WNK lysine-deficient protein kinase 1 (*WNK1*). We discovered that *WNK1* features differences on several molecular biological levels associated with permissiveness to VACV infection.

In addition to that, a set of human genes was identified with possible predictive value for viral replication in an independent dataset. The strongest positive correlations were observed for the genes lantibiotic synthetase component C-like 2 (*LANCL2*) and heterogeneous nuclear ribonucleoprotein L (*HNRNPL*). Among the strongest negative correlates were the genes encoding ATP synthase, H+ transporting, mitochondrial Fo complex, subunit B1 (*ATP5F1*), chemokine (C-C motif) ligand 5 (*CCL5*) and DEK oncogene (*DEK*).

A further objective of this work was to explore baseline molecular biological variances associated with permissiveness which could help identifying cellular components that contribute to the formation of a permissive phenotype. Therefore, in a subsequent approach, we screened a set of 15 melanoma cell lines (15-MEL) regarding their permissiveness to GLV-1h68, evaluated by GFP expression levels, and classified the top four and lowest four cell lines into high and low permissive group, respectively. Baseline gene transcriptional data, comparing low and highly permissive group, suggest that differences between the two groups are at least in part due to variances in global cellular functions, such as cell cycle, cell growth and proliferation, as well as cell death and survival. We also observed differences in the ubiquitination pathway, which is consistent with our previous results and underlines the importance of this pathway in VACV replication and permissiveness.

A great percentage of up-regulated molecules (high group) were nuclear factors. It was reported previously, that VACV is able to recruit nuclear host proteins to sites of viral replication upon infection suggesting a possible role of human transcription factors and regulators in VACV reproduction.
Moreover, baseline microRNA (miRNA) expression between low and highly permissive group was considered to provide valuable information regarding virus-host co-existence. There is evidence, that vertebrate miRNAs can directly affect viral genome replication and/or gene expression by interacting with viral mRNAs or RNA genomes. In our data set, we identified six miRNAs that featured varying baseline expression between low and highly permissive group, namely *miR-93*, *miR-29a*, *miR-487b*, *miR-148a*, *miR-107*, and *miR-32*. Subsequently, a list of human miRNA-mRNA pairings whose expression correlated inversely with strong statistical significance was established. Among them we found for example *miR-107*, which targets *WNK1* messages. *miR-107* and *WNK-1* expression levels revealed a highly significant inverse correlation, with *WNK1* being down-regulated and *miR-107* being up-regulated in the highly permissive group. However, the role of miRNAs in promoting or inhibiting the viral propagation remains to be further investigated.

Finally, copy number variations (CNVs) between low and highly permissive group were evaluated. In this study, when investigating differences in the chromosomal aberration patterns between low and highly permissive group, we observed frequent segmental amplifications within the low permissive group, whereas the same regions were mostly unchanged in the high group. A set of 2,652 genes, located in the chromosomal regions that differ in-between the two groups, revealed enrichment in a variety of pathways of the cellular immune response such as cytokine-mediated communication between immune cells, crosstalk between dendritic cells and NK cells, granzyme A signaling and others. To what extent pre-existing, not virus-induced immune-related pathways contribute to antitumor activity or permissiveness to virus infection is not clear yet.

Taken together, our results highlight a probable correlation between viral replication, early gene expression, and the respective host response and thus a possible involvement of human host factors in viral early replication. Furthermore, we revealed the importance of cellular baseline composition for permissiveness to VACV infection on different molecular biological levels, including mRNA expression, miRNA expression, as well as copy number variations. The characterization of human target genes that influence viral replication could help answering the question of host cell response to oncolytic virotherapy and provide important information for the development of novel recombinant vaccinia viruses with improved features to enhance replication rate and hence trigger therapeutic outcome.

Zusammenfassung

Einige Krebsarten, insbesondere in fortgeschrittenen Stadien, sind trotz bahnbrechender Fortschritte in der Krebsforschung immer noch unheilbar. Derzeit verfügbare Therapiemöglichkeiten, wie z.B. Chemotherapie, Strahlentherapie, Hormontherapie oder zielgerichtete Therapien, sind auf bestimmte Krebsarten und -stadien oder eine Körperregion beschränkt und wirken zudem oft nicht auf Dauer. Bei vielen Patienten wurde eine zunehmende Resistenz gegenüber Chemotherapie und zielgerichteter Therapien festgestellt. Des Weiteren versagen gegenwärtige Therapieoptionen häufig bei der Heilung metastasierender Tumore. In den letzten Jahren hat sich die Verwendung onkolytischer Viren (OVs) als vielversprechender Ansatz in der Krebsbehandlung heraus gestellt. OVs weisen einen intrinsischen oder erworbenen Tumortropismus auf, welcher einen Tumor-spezifischen viralen Lebenszyklus zur Folge hat und schlussendlich zur Lyse der infizierten Krebszelle führt. In diesem Zusammenhang hat sich das Vaccinia-Virus (VACV), als besonders attraktiv etabliert, da es nicht nur in der Lage ist Metastasen und zirkulierende Tumorzellen zu infizieren, sondern auch als Vektor zum Transfer von Genen dienen kann.
Die Replikationseffizienz von VACVs spielt eine maßgebliche Rolle für deren antitumorale Wirkung und onkolytische Effizienz. Ferner hängt die Permissivität einer Wirtszelle gegenüber der Behandlung mit onkolytischen VACVs maßgeblich von einer erfolgreichen viralen Replikation und Vermehrung ab. Darauf basierend, war der Fokus der vorliegenden Arbeit, zelluläre Eigenschaften zu erforschen, welche die VACV-Replikation beeinflussen und die Wirtszell-Permissivität gegenüber einer Behandlung mit VACV prognostizieren können.

Für initiale Genexpressionsanalysen wurden zwei autologe, humane Melanom-Zelllinien (888-MEL und 1936-MEL), sowie der ausgiebig charakterisierte VACV-Stamm GLV-1h68 und drei wildtypische LIVP Isolate (LIVP 1.1.1, LIVP 5.1.1 und LIVP 6.1.1) verwendet. Mit Hilfe von *Microarray* Analysen und einem sequenziellen statistischen Ansatz konnten humane Gene charakterisiert werden, deren Transkription eigens durch VACV-Infektion beeinflusst wird. Erwartungsgemäß zeigten diese Gene eine Anreicherung in globalen zellulären Signalwegen und Funktionen, wie z.B. Zelltod, Proteinsynthese und -faltung, DNA-Replikation, Rekombination und Reparatur.
Um einen besseren Einblick in das Zusammenspiel zwischen VACV und dessen Wirt zu erhalten, wurde die virale Genexpression parallel zur Wirts-Genexpression mithilfe einer maßgefertigten VACV-Expressions-Plattform ermittelt. Für diese Arbeit war die Untersuchung früher viraler und wirtseigener Abläufe von besonderem Interesse, da die virale Replikation zu einem frühen Zeitpunkt nach der Infektion stattfindet. Es konnte gezeigt werden, dass virale Transkripte ein

charakteristisches, zeitpunktspezifisches Expressions-Muster formen, welches mit den drei Expressions-Klassen von VACV-Genen konform geht. Eine Gruppe früher Transkripte war von besonderem Interesse für weitere Vergleichsstudien. Die gemittelte Expression dieser frühen Gene zeigte die höchsten Werte für den Klon LIVP 6.1.1, gefolgt von LIVP 1.1.1 und LIVP 5.1.1, während der attenuierte Stamm GLV-1h68 das niedrigste Transkriptionslevel aufwies. Vergleichbares wurde ebenfalls für die Replikationseffizienz der verschiedenen Virusstämme beobachtet.
Kürzlich wurde anhand der *NCI-60* Zelllinien nachgewiesen, dass die GFP-Markergen-Expression von GLV-1h68 mit der entsprechenden viralen Vervielfältigungszahl korreliert. Folglich kann die frühe virale Gentranskription als repräsentative Bestimmungsgröße für virale Replikation betrachtet werden. Darauf basierend resultierte der Vergleich von früher VACV Replikation und entsprechender früher Gentranskription in der Identifikation von sieben viralen Genen (*F15L, G2R, G5R, D9R, A5R, A20R* und *A24R*), deren Expression und Replikation stark korrelierten. Für mindestens fünf dieser sieben Gene wurde bereits eine Beteiligung an der viralen Replikation oder Transkription nachgewiesen. Aus diesem Grund wurde die frühe Expression der sieben VACV-Gene als kennzeichnend für virale Replikation angesehen und diese Gene als virale Replikations-Indikatoren (VRIs) definiert.

Zur Aufklärung von Zusammenhängen zwischen Wirts-Transkription und viraler Replikation wurde die frühe virale VRI-Expression mit der frühen humanen Genexpression in Beziehung gesetzt. Mit Hilfe von Vergleichsanalysen wurden 114 humane Transkripte identifiziert, deren frühes Expressionsmuster eng mit demjenigen der VRIs korrelierte und dementsprechend ebenso mit der viralen Replikation.
Eine Beteiligung dieser 114 Moleküle konnte für die folgenden Vorgänge nachgewiesen werden: Zellzyklus, Zell-Zell Signalgebung und Interaktion, Protein-Ubiquitinierung, EIF2-Signalgebung und entzündliche Erkrankungen. Von besonderem Interesse war die Untersuchung des Ubiquitinierungs-Signalweges und derjenige des proteasomalen Abbaus, da aktuelle Veröffentlichungen die Relevanz dieser Signalwege für die Reproduktions- und Replikationseffizienz von Orthopockenviren ans Licht gebracht haben. Von den 114 Korrelaten spielen mindestens sechs eine Rolle in der Protein-Ubiquitinierung oder in der proteasomalen Signalgebung. Ein weiteres Molekül, welches besonderes Interesse weckte, war die Serin-Threonin Proteinkinase WNK Lysin-defizientes Protein 1 (*WNK1*). Für *WNK1* wurden Unterschiede, die mit der VACV-Infektions-Permissivität zusammenhängen, auf verschiedenen molekularbiologischen Ebenen nachgewiesen.
Desweiten wurde in dieser Arbeit eine Anzahl humaner Gene identifiziert, welche virale Replikation in einem unabhängigen Datensatz prognostizieren konnten. Die stärksten Korrelationen wurden für die Gene lantibiotische Synthetase-Komponente *C-like* 2 (*LANCL2*) und das heterogene nukleare Ribonukleoprotein L (*HNRNPL*) nachgewiesen. Unter den negativen Korrelaten wurden wiederum

die Gene ATP-Synthase, H+-transportierend, mitochondrial Fo-Komplex, Untereinheit B1 (*ATP5F1*), Chemokin (C-C Motiv)-Ligand 5 (*CCL5*) und das DEK-Onkogen (*DEK*) identifiziert.

Eine weitere Zielsetzung dieser Arbeit war es, molekularbiologische Unterschiede, welche mit Infektions-Permissivität von Zellen assoziiert sind, auf Basisebene zu ergründen. Diese könnten dabei helfen, zelluläre Komponenten zu identifizieren, welche einen so genannten permissiven Phänotyp kennzeichnen. Aus diesem Grund wurden in einem weiteren Versuchsansatz 15 Melanom-Zelllinien (15-MEL) bezüglich ihrer Permissivität gegenüber GLV-1h68 anhand von GFP Expression untersucht. Die vier Zelllinien mit der höchsten und diejenigen vier mit der niedrigsten Permissivität wurden je einer Gruppe zugeordnet (hochpermissive und niedrigpermissive Gruppe). Die Gruppen hoher und niedriger Permissivität wurden bezüglich ihrer Basislevel-Transkription verglichen. Unterschiedlich exprimierte Gene waren, zumindest zum Teil, in globale zelluläre Prozesse involviert, wie z.B. Zellzyklus, Zellwachstum und -proliferation, sowie Zelltod und -überleben. Im Einklang mit vorherigen Beobachtungen, wurden des Weiteren Abweichungen im Ubiquitinierungs-Signalweg entdeckt, was die Relevanz dieses Signalweges für die Replikation von VACV und für Wirtszellpermissivität noch weiter hervorhebt. Unter den am stärksten hochregulierten Genen in der hochpermissiven Gruppe wurde ein Großteil nukleärer Faktoren gefunden. Frühere Veröffentlichung belegen, dass VACV in der Lage ist nukleäre Wirtsfaktoren zu den Orten viraler Replikation zu rekrutieren, weshalb eine Beteiligung humaner Kernfaktoren an viraler Reproduktion denkbar wäre.

Darüber hinaus wurde angenommen, dass die Untersuchung von microRNA (miRNA) Basislevel-Expression von hoch- und niedrigpermissiver Gruppe weiteren Aufschluss über Virus-Wirts Interaktionen geben kann. Es ist bekannt, dass in Vertebraten miRNAs die virale Genom-Replikation und/oder Genexpression direkt beeinflussen können durch Interaktion mit viraler mRNA oder RNA-Genomen. In dieser Arbeit wurden sechs miRNAs identifiziert (*miR-93*, *miR-29a*, *miR-487b*, *miR-148a*, *miR-107* und *miR-32*), deren Basislevel-Expression zwischen niedrig und hochpermissiver Gruppe differiert. Im Anschluss wurde außerdem eine Liste humaner miRNA-mRNA-Paarungen etabliert, welche eine statistisch signifikante inverse Korrelation in ihrem Expressionsverhalten aufwiesen. Darunter wurde z.B. *miR-107* gefunden, welche gegen *WNK1* Transkripte gerichtet ist. Die Expressionslevels von *miR-107* und *WNK-1* wiesen eine signifikante inverse Korrelation auf, wobei *WNK1* nieder- und *miR-107* hochreguliert war in der hochpermissiven Gruppe. Die genaue Rolle von miRNAs in der Förderung oder Inhibierung viraler Propagation ist noch nicht vollständig verstanden und erfordert weitere Erforschung.

Abschließend wurden Veränderungen der Kopienzahl von Genen (*copy number variations*, CNVs) im Vergleich zwischen niedrig- und hochpermissiver Gruppe untersucht. Betrachtung chromosomaler

Veränderungen zeigte eine Anreicherung von Segment-Amplifikationen in der niedrigpermissiven Gruppe, während gleiche Abschnitte der hochpermissiven Gruppe größtenteils keine Veränderungen aufwiesen. In den chromosomalen Regionen, welche Unterschiede in der Kopienzahl zwischen den zwei Gruppen aufwiesen, wurden 2652 Gene lokalisiert. Diese waren in einer Vielzahl von Signalwegen der zellulären Immunabwehr angereichert, wie z.B. Cytokin-vermittelte Kommunikation zwischen Immunzellen, *Crosstalk* zwischen dendritischen Zellen und Natürlichen Killerzellen sowie Granzym A-Signalgebung. In welchem Ausmaß nicht-virusinduzierte Immun-Signalwege zur antitumoralen Wirkung oder zur Infektions-Permissivität beitragen ist noch nicht aufgeklärt.

Zusammenfassend konnte in dieser Arbeit eine mutmaßliche Korrelation zwischen viraler Replikation, früher Genexpression und der entsprechenden Wirtsantwort gezeigt werden und somit eine mögliche Beteiligung humaner Wirtsfaktoren an der viralen Replikation. Zusätzlich wurden wichtige Aspekte der Basiskomposition von Zellen für die Permissivität gegenüber VACV-Infektion auf verschiedenen molekularbiologischen Ebenen aufgedeckt, einschließlich mRNA-Expression, miRNA-Expression sowie Kopienzahl-Variationen. Die Charakterisierung humaner Zielgene, welche die virale Replikation beeinflussen, könnte dabei helfen, die Wirtszellantwort auf onkolytische Virotherapie aufzuklären und wichtige Informationen zu liefern für die Entwicklung neuartiger rekombinanter Vaccinia-Viren mit verbesserten Eigenschaften und verbesserter Replikationseffizienz und somit einem gesteigerten Therapieerfolg.

1 Introduction

1.1 Cancer – Statistics and biology

The term cancer describes a disease or a group of diseases in which abnormal cells proliferate uncontrolled and acquire the ability to migrate through the blood and lymph system and invade other organs. Despite decades of extensive research, cancer remains one of the leading causes of death worldwide. It was estimated by the IARC (International agency for research on Cancer) that in 2008 about 12.7 million incident cases of cancer occurred of which 7.6 million cases resulted in cancer-related death [1]. In female individuals, breast cancer is the most frequently occurring cancer and accounts for 14% of cancer deaths in women. In contrast to that lung cancer is the leading cancer type in males, comprising 23% of cancer-related deaths.

Cancer is characterized by a pronounced heterogeneity and variability not only in the way that it presents itself, but also at molecular levels. It is a complex disease which arises in a multi-step process through accumulation of genetic alterations in genes involved in the control of essential cellular processes such as cell survival and proliferation. Ultimately, the acquirement of genetic changes leads to unregulated, excessive cell growth and thus to tumor formation. Despite the heterogeneity of the disease, different types of cancer feature common acquired capabilities defined as “the hallmarks of cancer” (Hanahan and Weinberg) [2]. These are comprised of the following biological abilities: self-sufficiency in proliferation signals, evading anti-growth signals, circumvention of cell death, unlimited replicative potential, promoting angiogenesis, inducing tissue invasion and metastasis formation, reprogramming of energy metabolism, and avoiding immune destruction [3]. Furthermore tumors have acquired the capability to sustain their “tumor microenvironment” which is mainly comprised of non-transformed cells.

The factors contributing to cancer formation can be divided into two main categories, environmental and life style factors, and genetic epidemiology. Cancer-associated lifestyle and environment include tobacco smoking [4], overweight, dietary deficiencies, lack of physical activity, reproductive and hormonal factors, pathogens as well as occupational and urban carcinogens [5-7].
Carcinogenesis starts with the genetic and epigenetic alterations in healthy cells resulting in a selective survival and growth advantage [8]. Sequential alterations in two classes of genes are mainly responsible for triggering the transformation into neoplastic cells.
In homeostatic concentrations these genes regulate proper cell growth stimulation (proto-oncogenes) and inhibition (tumor suppressor genes). Proto-oncogenes encode for growth factors, growth factor

receptors, transcription factors, signal transducers, chromatin remodelers, and apoptosis regulators [9]. Mutations in these genes result in the transformation into oncogenes which in turn produce a hyperactive form or an exceeding amount of the growth regulatory protein [10]. In contrast to that, tumor suppressor genes become cancerous through inactivating "loss-of-function" mutations which result in a lack of inhibitory signaling.

Besides disruption of cell growth signaling, cancerous cells feature a malfunction in cell cycle control [10]. Augmented activity of stimulatory cyclins and cyclin-dependent kinases (CDKs) as well as inactivation of inhibitory proteins (p53 [11-13], pRB [14], p16 [15], p15 [16]) are related to excessive cell proliferation and thus progress into malignancy. Furthermore, telomerase activity and evasion of apoptosis contribute to tumor formation. Normal healthy cells are characterized by a genetic safety net which is missing in cancer cells and leads to induction of apoptosis when the cell is damaged or control mechanisms are abnormal in any kind. In addition to that, after a certain number of doublings normal cells initiate senescence due to shortening chromosome endings (telomeres). Malignant cells however circumvent to enter into a senescent state by systematical replacement of segments at the chromosome termini, carried out by an enzyme called telomerase [17]. Recently it was reported that also aberrant expression of small non-coding RNA, such as microRNAs, plays a role in carcinogenesis [18-23].

In addition to carcinogenesis through accumulation of somatic mutations, germ-line mutations can predispose a person to cancer development [24, 25]. The inheritance of a "cancer gene" leads to a ubiquitous expression of this gene and thereby making the carrier more vulnerable to acquire another cancer-causing mutation since all body cells are predisposed.

1.1.1 Melanoma

Melanoma is the most aggressive and deadly form of skin cancer. It is caused by a malignant proliferation of the pigment-producing cells of the skin, the so called melanocytes.

Each year there are about 160,000 incident cases of melanoma worldwide [1]. The disease is predominantly affecting the fair-skinned population whereas dark-skinned people show a lower risk of developing melanoma. In addition to pigmentation phenotype, risk factors include congenital naevi, geographical parameters, immunosuppression, and most importantly natural and artificial high-intensity ultra violet (UV) radiation [26-30].

There are two pathways that are mainly responsible for contracting cutaneous melanomas, a melanocyte proliferation associated pathway and a sunlight exposure-triggered one [31].

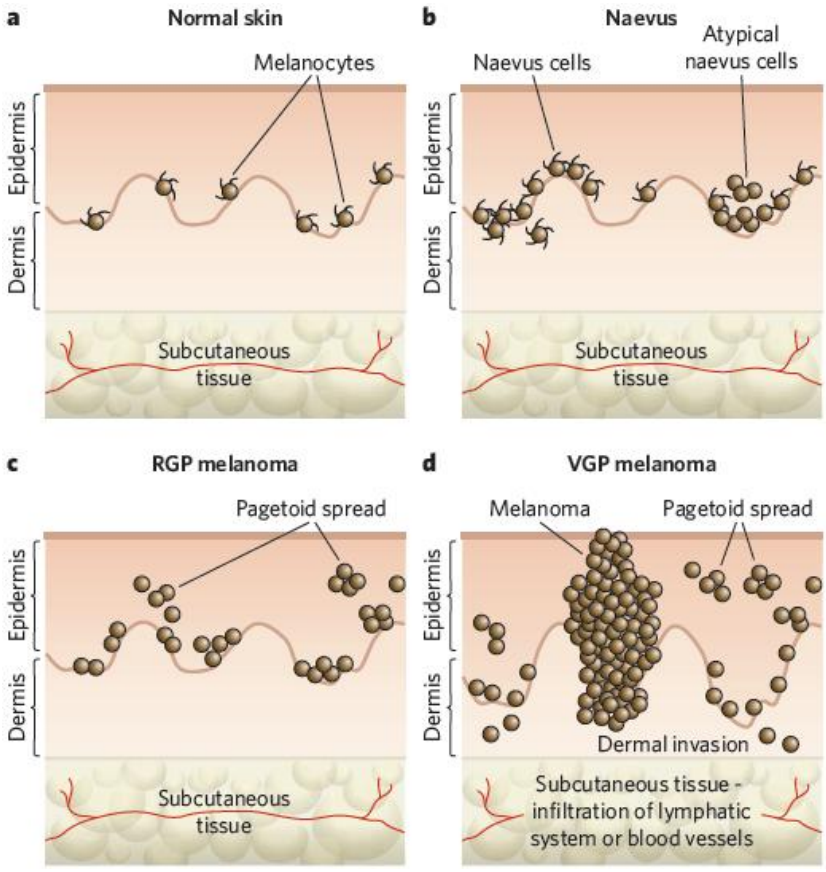

Figure 1-1: Melanocyte transformation – from benign to malignant

(a) Normal skin - evenly spread dendritic melanocytes throughout the epidermis base. (b) Naevus – Proliferation of dendritic melanocytes lead to formation of benign melanocytic naevi. (c) Radial-growth-phase (RGP) melanoma - melanocytes spread laterally into the epidermis (primary state of malignancy). (d) Vertical-growth-phase (VGP) melanoma – dermal invasion of cells. Infiltration of the blood and lymphatic system leads to development of metastatic malignant melanoma. (Figure from Gray-Schopfer *et al*., 2007 [32]).

Disruption of the intracellular signaling in melanocytes results in their proliferation and spread and thus in formation of a usually benign naevus (Figure 1-1 b). Progression into radial-growth-phase (RGP) melanoma is considered as the first step into malignancy (Figure 1-1 c). In addition to that RGP cells can progress into the vertical-growth phase (VGP) which is characterized by invasion of cells into the dermis (Figure 1-1 d). Subsequent infiltration of the vascular and lymphatic systems leads to formation of metastases the hallmark of metastatic malignant melanoma.

1.1.1.1 Melanoma genetics – an overview

Genetic etiology of melanoma includes the alteration of factors involved in crucial cell-signaling pathways. Among them is the mitogen-activated protein kinase (MAPK) signaling pathway operating through small GTPase Ras and a three-tiered kinase cascade composed of Raf, MEK, and ERK [33]

(Figure 1-2). This pathway regulates cell proliferation, differentiation, and survival-related gene expression.

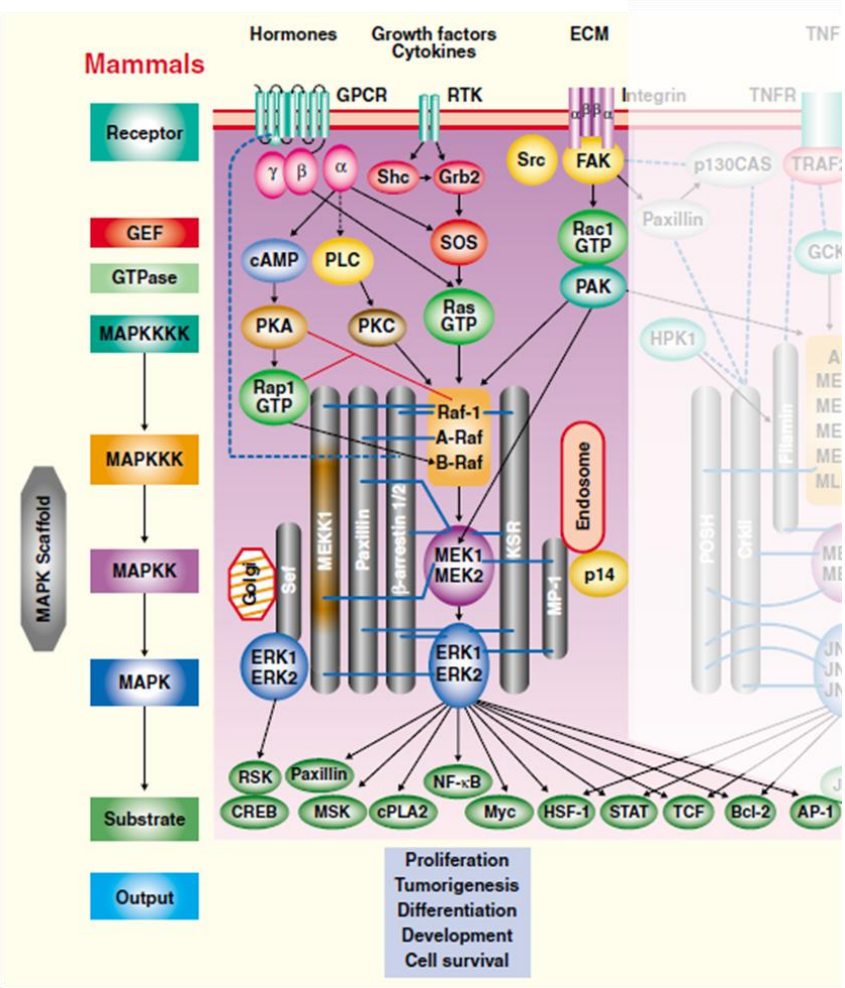

Figure 1-2: Ras/Raf/MEK/ERK signaling cascade in mammals

(Figure modified from Qi *et al*., 2005 [33])

Hyperactive ERK is present in roughly 90% of human melanomas and considered as a key regulator of melanoma cell proliferation [34]. ERK activation occurs either through autocrine growth factors [35] or in about 15 to 30% of melanomas by gain-of function mutations in the *NRAS* member of the *Ras* gene family (*NRAS*, *HRAS* and *KRAS*). However, the most frequently occurring mutation in the Ras/Raf/MEK/ ERK signaling pathway occurs in *BRAF* with a mutation rate of 50 to 70% in melanomas [36]. Mutated BRAF (substitution at position 600, ^{V600E}BRAF) promotes constitutive ERK signaling, leading to enhanced cell survival and proliferation [37]. Downstream effectors affected by mutated ^{V600E}BRAF include VEGF [38] (angiogenesis), cyclin D1 [39] and p16^{INK4a} [40, 41] (cell cycle regulators) amongst others.

Another signal transduction pathway with relevance in melanoma is the phosphoinositide-3-OH kinase (PI(3)K) pathway [42]. PI(3)K signaling is hyper-activated in many melanomas and plays a

role in controlling cell proliferation, growth, survival, and motility. The lipid phosphatase PTEN (phosphate and tensin homologue) acts as an inhibitor of PI(3)K signaling and shows loss-of-function mutations in 5 to 20% of late-stage melanomas [43]. In contrast to that, PI(3)K effector protein kinase B (PKB, also called Akt) reveals an overexpression in a high proportion of melanomas [44]. Another key regulator in melanoma is the microphthalmia-associated transcription factor (MITF) which regulates the expression of melanogenic factors such as tyrosinase or melanoma-associated antigen recognized by T cells-1 (MART-1) [45]. MITF stimulates downstream pathways in a level-dependent manner with only an intermediate level promoting proliferation [32].

Some genetic alterations that occur frequently in melanoma target the apoptosis pathway, i.e. the overexpression of B cell leukemia/lymphoma 2 (*Bcl-2*), nuclear factor-κB (*NF-κB*) and *Akt3*. In addition to that, upregulation of the β-catenin pathway through activating alterations in β-catenin (*CTNNB1*) [46] or inhibiting mutations in adenomatous polyposis coli (*APC*) [47] promote cell survival.

Another mechanism leading to melanoma development is bypassing senescence by inactivating key pathways. The tumor suppressor $p16^{INK4a}$ is part of a major genomic locus (the INK4b–ARF–INK4a locus) involved in predisposition for melanoma. Loss of $p16^{INK4a}$ leads to inactivation of the $p16^{INK4a}$-CDK4/6-RB senescence barrier thereby enabling the entrance into S phase.

Susceptibility to skin cancer can also be increased through loss-of-function mutations in the human melanocortin-1 receptor (MC1-R), which have been associated with physical predispositions such as fair skin, red hair, freckles and decreased ability to tan [48].

In addition to structural genetic changes, also epigenetic alterations contribute to the malignant transformation of melanocytes [49]. Epigenetics describe heritable alterations in gene expression that do not arise from changes in the primary nucleotide sequence. Epigenetic modifications include DNA methylation and histone modifications. Hypo- and hypermethylation of gene sequences especially the promoter sequence influences the expression level of the respective gene. Histone modifications influence the packing structure of the chromatin and thus the accessibility of DNA sequences for expression.

1.1.1.2 Cell lines 888-MEL and 1936-MEL

In 1988 a patient at the National Institutes of Health (NIH) was diagnosed with metastatic cutaneous melanoma. Tumor resection in 1989 served as a source for generating a melanoma cell line designated 888-MEL. After combined immunotherapy (*IL-2 & tumor infiltrating lymphocytes -TIL*) the patient experienced a complete regression of all metastases. Several recurrences occurred within about a decade and cell lines were established from each resection (1290-MEL, 1858-MEL, 1936-MEL and

1962-MEL). Relapses in 2001 were more aggressive and unresponsive to immunotherapy. Two melanoma cell lines were generated out of biopsies from this period designated 1936-MEL and 1962-MEL. Karyotype analyses of the generated cell lines revealed drastic changes in metaphase chromosomes of 1936-MEL compared to the previous cell isolates. High instability of 1936-MEL resulted in various chromosomal rearrangements as well as triploid or near tetraploid metaphases [50, 51].

The two cell lines 888-MEL (from initial tumor) and 1936-MEL (from last occurring, unresponsive relapse) served as an ideal autologous model for this study, exhibiting the same clonal origin.

1.1.2 Cancer management

The path of cancer management starts with the prevention of cancerogenesis. Amongst others, the avoidance of risk factors, practicing a healthy life style, regular check-ups especially in the second half of life and genetic testing contribute to circumvent or delay cancer development. Once a patient is diagnosed with cancer, treatment options have to be evaluated based on type and stage of the cancer, the patient's overall health, potential side effects of the treatment, and on the patient's general preferences. The most common primary cancer management options include surgery, radiation therapy, and chemotherapy. At the same time, applied palliative care helps to manage cancer-related or treatment-induced pain and affliction as well as emotional distress.

First-line therapy for most solid cancers is surgery, a procedure in which the main tumor and surrounding tissue is removed. Surgical biopsies of the tumor can be used to determine the histology and stage of disease [52]. In general, an adjuvant therapy is applied in addition to the main treatment. It is also possible to administer a treatment such as radiation before the main treatment, a so called neoadjuvant therapy. Radiation therapy uses ionizing radiation (IR) such as high-energy photons (x-rays and γ-rays) or electrons to destroy cancer cells by damaging their DNA beyond repair. The other very commonly applied adjuvant treatment is chemotherapy. A chemotherapeutic substance is a drug which inhibits cell proliferation and growth of actively growing cells such as cancer cells. Unlike radiation therapy and surgery, chemotherapy is a systemic treatment. The effectiveness of chemotherapy is limited by the fact that the drug cannot distinguish between normal dividing cells and cancerous cells and is thus also toxic to some healthy cell populations. There are over 100 different drugs which can be categorized by their mechanism of action or their target (folate antagonists, pyrimidine and purine antimetabolites, DNA adductors, mitotic inhibitors, etc.). Depending on the type and stage of the disease, one drug or a combination of drugs is administered utilizing a patient-adjusted dose or multiple doses.

Novel drugs have more cancer cell-specific mechanisms of action thereby causing less severe side effects. Among them is endocrine therapy, also known as hormone therapy, which acts through inhibition of a hormone or its receptor to reduce the hormone level in the body. Its application is usually indicated to treat cancers of the prostate, breast, thyroid, and reproductive system.

In addition to that, immune therapeutic approaches have made huge progress over the last decade and have become a crucial part in the treatment of a variety of cancers. This therapy option aims to either modify the host immune system or uses components of the immune system to fight cancer. The immune system recognizes a diversity of over-expressed tumor proteins. Established immune therapies such as monoclonal antibodies, immune adjuvants, and cytokines trigger antitumor immunity. Further vaccines used against oncogenic viruses can prevent their cancer-promoting effects [53]. In contrast to cancer-causing viruses such as Epstein-Barr virus [54-56] or human papillomavirus [57, 58], there are so called oncolytic viruses which serve as a novel treatment option against cancer (Section 1.1.2.1).

1.1.2.1 Oncolytic virotherapy

Despite extensive research, cancer, particularly at advanced stages, remains untreatable. For this reason, novel therapeutic strategies are underway. A promising approach is the use of oncolytic viruses (OVs). Oncolytic virotherapy exploits the natural or artificial tumor tropism of certain viruses to specifically target, replicate in and lyse tumor cells without harming healthy somatic cells [59, 60].

Cases about complete or temporary remissions of cancer patients who had contracted a viral infection are documented back from the mid-1800s. In 1904, George Dock presented his observations on a leukemia patient who experienced a temporary complete remission after catching an influenza virus infection [61]. Over decades research groups pursued the idea of cancer-killing viruses by investigating the effects of a variety of viruses in tumor-bearing animals [62, 63]. Preclinical studies with oncolytic viruses showed promising progress in combating cancer; however success was restricted by infection-related issues caused by the wild-type viruses. Advances in tumor biology, microbiology, genetics, and virology paved the way for the development of genetically attenuated oncolytic viruses with increased tumor selectivity.

Viruses and tumor cells share certain necessities for replication and development, respectively. Consequently, transformed cells are more prone for virus infection. They are actively dividing cells and provide therefore all nucleotides and other factors needed for viral replication. In addition to that, apoptotic pathways are inhibited in malignant cells thereby allowing the completion of the viral cycle before cell death occurs. Some replication-competent viruses such as Newcastle disease virus (NDV) and vesicular stomatitis virus (VSV) feature inherent tumor selectivity [64] whereas other viruses need to be genetically altered to restrict their replication to conditions only found in cancer cells. This

applies to adenovirus (Ad), Herpes simplex type-1 (HSV-1) and poxviruses such as vaccinia virus (VACV). Alternative approaches focus on usage of tumor-specific promoters for transcriptional control of essential viral genes.
Another aspect of great importance for oncolytic virotherapy is antitumor efficacy which comprises several mechanisms of action. One of these mechanisms is direct viral oncolysis which results from the viral replication cycle [65]. Others include immune-mediated oncolysis [66], expression of cytotoxic proteins [67], and destruction of the tumor vasculature [68, 69]. In addition to that, OVs can be used as a vehicle for gene delivery through insertion of therapeutic transgenes into the viral genome. One group of transgenes is summarized as gene-directed enzyme prodrug therapy (GDEPT), also called "suicide gene therapy", where non-cytotoxic prodrugs are converted into cytotoxic drugs [70-73]. Other groups of therapeutic genes code for pro-apoptotic factors [74], immune-promoting factors [75-80] or they target angiogenesis [69].

After decades of extensive research and based on increasing preclinical success, by now a variety of clinical trials is underway using different viral vectors [81, 82]. In 2005, the first oncolytic virus, an Ad mutant, was approved in China for patients with head and neck squamous cell carcinoma [83].

1.2 Vaccinia virus

1.2.1 Poxviridae – Taxonomy

The poxvirus family is subdivided into two subfamilies, the *Chordopoxvirinae*, which infect vertebrates, and the *Entomopoxvirinae*, which only infect insects. Both families in turn are subdivided into genera based on similarities in host range, morphology etc. [84]. Members of the *Orthopoxvirus* genus, which belongs to the *Chordopoxvirinae* subfamily, are able to infect humans and other mammalian species [85, 86]. Amongst others, they include variola virus (VARV), the causative agent of smallpox and VACV, the smallpox vaccine. The natural host of VACV as well as its origin remains elusive.

1.2.2 History of poxviridae and their application in oncolytic virotherapy

Over centuries variola virus (*variola major*) a member of the poxvirus family, was responsible for waves of epidemic outbreaks of smallpox. This acute infectious disease caused millions of deaths worldwide. In the late 18-hundreds Edward Jenner discovered the protective effects of cowpox regarding infection with smallpox-causing variola virus (VARV) and established a vaccination against

the disease [87]. Based on Jenner's discovery and following a worldwide vaccination campaign the World Health Organization (WHO) declared smallpox to be eradicated in 1980 [88, 89]. The agent used for the vaccination program differed from the original cowpox vaccine and was named vaccinia virus (VACV). The exact origins of vaccinia virus are obscure, but it shows close relation to cowpox virus and might therefore be a hybrid of cowpox and VARV [90].

In the 1980's, VACV had emerged as an increasingly interesting tool for other biological and medical applications. Due to its historical importance as smallpox vaccine, VACV biology and pathogenesis was investigated in great detail thereby establishing an enormous safety profile for this virus. In addition to that the large double-stranded DNA genome of VACV enables insertion of up to 25 kb of foreign DNA [91] without loss of infectivity, and because of its high infection efficiency, VACV has emerged as an attractive tool for gene delivery [92]. The virus replication is carried out entirely in the cytoplasm of its host cell. This compartmentalization of host and viral DNA synthesis averts the risk of genomic integration [93]. A further advantage of VACV is that it can be easily produced in relatively high titers and stored in different conditions (frozen or as powder) for an extended period of time. In addition to the attributes mentioned above, the high immunogenicity of the virus makes it especially attractive for the use as cancer therapeutic. VACV features a fast and efficient replication cycle, is able to infect and replicate in a variety of human cell types [94], and is easy to attenuate. It was reported previously that for example deletion of vaccinia growth factor (VGF) and/or thymidine kinase (TK) resulted in tumor-selective replication of the mutant viruses [95]. TK-deleted VACV mutants depend on a TTP source for viral DNA synthesis, leading to a preferential viral replication in metabolically active cells such as cancer cells with only minimal infection of normal tissues [95-97].

Consequently, a variety of recombinant viruses derived from different VACV strains (Modified Vaccinia Ankara (MVA), Lister (LIVP), Western Reserve (WR), Copenhagen (COP), New York Vaccinia virus (NYVAC) and others) has been developed, and investigated in the laboratories.
Preclinical success was observed for many different solid cancers such as prostate [69, 98], pancreatic [69, 99], lung [100, 101], breast [100-102], brain tumors [103, 104] and other cancers.
Based on promising preclinical results a set of recombinant VACVs was approved for clinical trials in humans (Excerpt table 1-1) [105].

Table 1-1: Excerpt of ongoing clinical trials with oncolytic VACV

Phase	Condition	Intervention	Sponsor
1	Melanoma; Breast Cancer; Head and Neck Squamous Cell Cancer; Liver Cancer; Colorectal Cancer; Pancreatic Adenocarcinoma	Vaccinia virus (vvDD-CDSR)	University of Pittsburgh
1/2	Peritoneal Carcinomatosis	GL-ONC1 (GLV-1h68)	Genelux Corporation
2	Carcinoma, Hepatocellular	Recombinant Vaccina GM-CSF (JX-594)	Jennerex Biotherapeutics
3	Prostate Cancer Metastatic	Recombinant Vaccinia Virus Vaccine PROSTVAC-V/F-TRICOM + GM-CSF vs. placebo	BN ImmunoTherapeutics
2	Ovarian Cancer; Fallopian Tube Cancer; Peritoneal Cancer	Recombinant MVA 5T4 TroVax®;	University College, London; Oxford BioMedica

(Source: http://clinicaltrials.gov)

However, despite the tremendous success of VACV as an oncolytic therapeutic, there are certain tumors which do not respond to oncolytic virotherapy. The reason for the variances in response of tumors to virus treatment in pre-clinical models as well as the permissiveness of respective cell lines to VACV replication (Figure 1-3) [101] is still poorly understood. Worschech *et al.* [101] revealed that for the most part *in vitro* permissiveness of a given cell line to GLV-1h68 infection correlates with *in vivo* responsiveness of the corresponding tumor xenograft.

	Responders [R]	**T.I.**
1858-MEL	Melanoma	90.1
888-MEL	Melanoma	88.0
MIA PaCa-2	Pancreatic Carcinoma	80.1
A549	Lung Carcinoma	62.8
OVCAR-3	Ovarian Adenocarcinoma	56.2
Panc-1	Pancreatic Carcinoma	50.9
DU-145	Prostate Carcinoma	48.4
GI-101A	Breast Carcinoma	27.9

	Poor/Non-Responders [NR]	**T.I.**
MDA-MB-231	Breast Adenocarcinoma	21.6
SiHa	Cervical Squamous Cell Carcinoma	15.6
1936-MEL	Melanoma	13.7
NCI-H1299	Breast Adenocarcinoma	-2.3
HT-29	Colorectal Carcinoma	-19

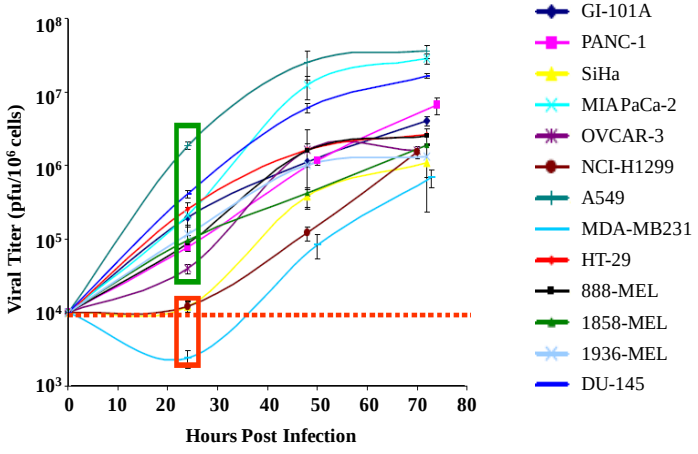

Figure 1-3: Therapeutic index (T.I.) of responding and non-responding tumor xenografts and *in vitro* GLV-1h68 replication efficiency in different human cancer cells lines

Therapeutic index (T.I.) of tumor-bearing nude mice (8 animals per group), determined through integration of the areas between median growths of control vs. treated xenografts (left). Time-course of GLV-1h68 infection (24, 48, and 72 hpi) in different human cancer cells lines (right). Determination of viral titers via plaque assay analyses (n=3). Two replication patterns: GLV-1h68-replication occurs even at early time points (green box) and no virus replication within the first 24 hours (red box). Figure modified from Worschech *et al.*, 2009 [101].

1.2.3 Morphology of vaccinia viruses

VACV is a complex DNA virus with a single linear double-stranded (ds) DNA molecule of about 192 kbp encoding for approximately 200 non-overlapping genes. Both genome endings exhibit inverted terminal repeats (ITRs) which consist of identical sequences with opposite directionality [106]. Within the ITRs the two DNA strands are connected in an AT-rich hairpin loop which reveals incomplete base-pairing [107]. In addition to that the ITRs contain a short (<100 bp), highly conserved region that is essential for concatemer resolution during replication [108, 109].

Virus particles of VACV are brick-shaped structures with dimensions of 360 x 270 x 250 nm. The particles are comprised of a lipid membrane surrounding the dumbbell-shaped core (Figure 1-4) which contains the virus DNA genome and about 50 polypeptides, more than half of which being directly involved in early mRNA synthesis [93].

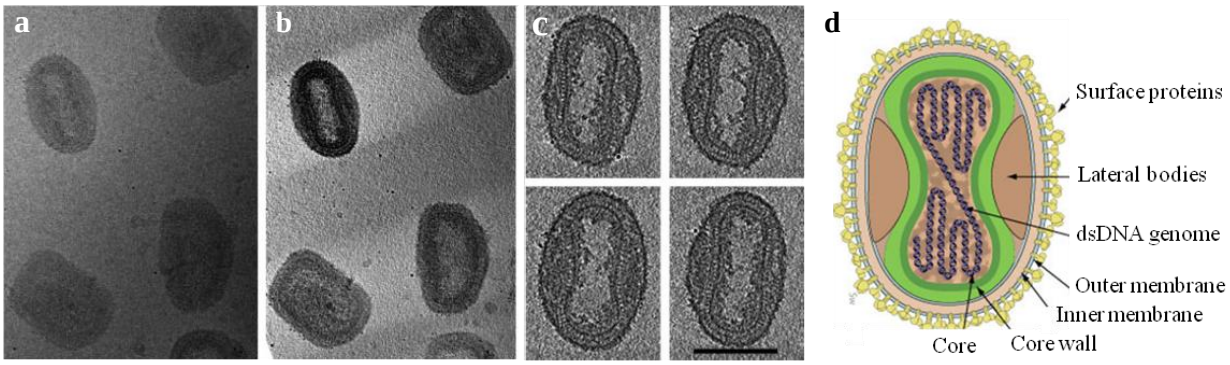

Figure 1-4: Morphology of IMV particles

(a-c) Isolated IMVs preserved by rapid freezing. Viewed by cryo-EM. (a) IMV particles in varying orientations. (b) *x–y* section through the tomographic reconstruction of the area from figure a. (c) Four *x–y* sections of a single particle. Scale bar: 200 nm (Figure modified from Cyrklaff *et al.*, 2005 [110]). (d) Schematic cross-section of an IMV particle (Figure modified from http://viralzone.expasy.org).

During morphogenesis VACV forms four distinct virions in the course of infection which differ in number of surrounding membranes, location within the cell, time of production, and dissemination preferences. The mature virion (MV) also referred to as intracellular mature virus (IMV) is surrounded by a single membrane and remains inside the cell until lysis. The other virions are surrounded by an additional membrane and are named according to their locations as follows: intracellular enveloped virion (IEV), cell-associated enveloped virus (CEV) and extracellular enveloped virus (EEV). The outer membrane of all enveloped forms provides characteristic structural, antigenic, and functional properties when compared to IMVs [111].

1.2.4 Vaccinia virus life cycle

VACV, like all other members of the poxvirus family conducts its life cycle exclusively within the cytoplasm of the host cell (Figure 1-5 a) [93]. The VACV genome comprises approximately 200 genes with some of them being highly conserved and encode for products involved in cell entry, gene expression, DNA replication, and virion assembly. Less conserved genes are arranged close to the genome termini and are involved in specific host interactions. The nomenclature of the VACV open reading frames (ORFs) are based on HindIII restriction endonuclease genome fragments and assigned with a capital letter. Furthermore an Arabic number indicates the position within the HindIII fragment and L or R give information about the direction of transcription, to the left or to the right, respectively. The respective proteins are designated in the same way, but without the letter for transcriptional directionality [112].

1.2.4.1 Vaccinia virus cell entry

The two types of infectious particles of VACV (IMVs and EEVs) enter a host cell through endocytosis, more precisely by activation of macropinocytosis. The mechanisms how macropinocytosis is induced and the fusion process vary among the particle types [113]. The general aim of both particles is to introduce their genetic material plus related protein machinery in a replication competent state into the host cell.

MV attachment is mediated by four viral proteins, namely D8 (binds chondroitin sulfate [114]), A26 (binds laminin [115], as well as A27 and H3 (bind to heparin sulfate [116-118]). In contrast to that, attachment molecules for EEVs have not been identified, yet [119]. EEVs have to get rid of their outer membrane by fusion with either the plasma or the endosomal membrane [120]. MVs and EEVs are both internalized via macropinocytosis, a signal-induced process with involvement of several host cell factors [121, 122]. Finally, the viral membrane fuses with the endosomal one resulting in the release of the viral core into the cytoplasm. The fusion is mediated by a large viral protein complex which assembles in the MV or MV-like membrane and is designated entry/fusion complex (EFC) [123]. Up to now, nine proteins (A16, A21, A28, G3, G9, H2, J5, L5 and O3) are considered to be integral components of the EFC [124]. Moreover, two proteins (F9 and L1) are thought to be EFC-associated.

1.2.4.2 Vaccinia virus replication

After virus entry the DNA-containing core structure is released into the cytoplasm and transported via microtubules to the sites where disassembly, DNA release and transcription take place [125, 126].

Soon after virus entry early mRNAs are transcribed within the core [127] and presumably extruded through pore-like structures in the core membrane [110]. Early virus proteins in turn are responsible for core uncoating, the release of the viral genome, and comprise essential factors of DNA synthesis. VACV DNA replication is restricted to special endoplasmic reticulum (ER)-enclosed cytoplasmic foci, so called viral factories [128, 129]. Viral DNA synthesis begins about 1 to 2 hrs post infection (hpi) and leads to the generation of roughly 10,000 copies of the viral genome in each infected cell. It is a highly autonomous process, since VACV encodes for factors of nucleotide biosynthesis such as thymidine kinase (J2), thymidylate kinase (A48) and ribonucleotide reductase (F4/ I4) as well as for enzymes and DNA-binding proteins directly involved in the replication procedure [130]. Among the key proteins involved in DNA replication that have been identified so far are the viral DNA polymerase (E9) [131-135], a processivity factor (heterodimer: uracil DNA glycosylase (D4) and A20) [136-138], the D5 protein (putative primase/NTPase/helicase) [139, 140], a DNA ligase (A50) [141, 142], and the I3 single-stranded DNA binding proteins (SSB) [143, 144]. In addition to that there is a panel of accessory factory involved in DNA replication with function in replication support (H5) [145], DNA recombination/repair (G5) [146], maturation (Holliday junction resolvase A22) [147, 148], and encapsidation of the genome (I6 and A32) [149, 150]. Finally, the serine/threonine protein kinase B1 [151] is necessary to phosphorylate and thereby resolve the inhibitory binding of a host protein (BAF) to viral DNA [152, 153].

The working model of VACV DNA replication suggests that replication initiation starts with the introduction of a nick close to the genome termini [154, 155]. This incision provides a free 3'-hydroxyl terminus that serves as a primer for the trimeric replication complex consisting of the DNA polymerase and the heterodimeric processivity factor (D4 and A20) [156] and it is further associated with the NTPase/helicase D5 (Figure 1-5 b) [157]. Subsequently, the newly synthesized strand folds back on itself and replication proceeds toward the hairpin endings which results in an intermediate with self-complementary termini (Figure 1-5 b, c). Self-priming hairpin structures facilitate the replication of the remainder of the genome. Additional rounds of replication before resolution of the arisen tail-tail dimers result in the formation of branched concatemers [93]. This replication model proposes that only leading strand synthesis is applied. Furthermore, recombinational strand invasion and priming may play a part in the generation of these complex multi-branched molecules. Concatemers are resolved into unit-length molecules [158] at the cruciform concatemer junction. It has been reported that resolution might be linked to transcription due to the presence of a late promoter within the resolution sequence [159, 160]. The concatemer resolution occurs quickly and is most likely mediated by a viral holiday junction resolvase (A22) [147]. After DNA synthesis the genome is packaged into nascent virions with involvement of a putative ATPase (A32) and a telomere binding protein (I6) [130].

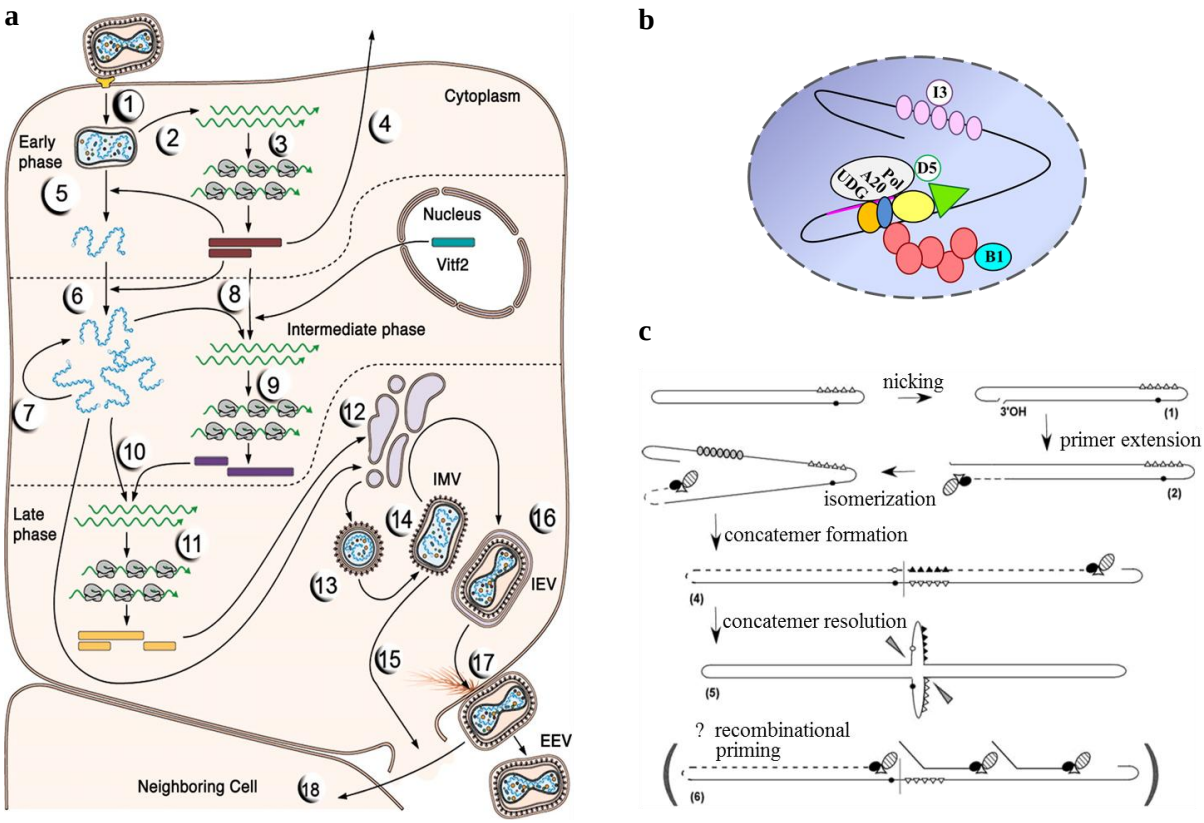

Figure 1-5: Overview of vaccinia virus replication and life cycle

(a) Life cycle of vaccinia virus in 18 steps: (1) EEV entry. (2) Core release; early mRNA synthesis. (3) Early protein synthesis. (4) Portion of early proteins (proliferation stimulators and immune evasion factors) is secreted. (5) Release of viral DNA genome. (6, 7) Viral DNA synthesis. (8, 9) Transcription of intermediate-phase genes. (10, 11) Transcription of late-phase genes. (12, 13) Assembly – formation of immature virion (IV). (14) Maturation into mature virion (IMV). (15) IMV release during cell lysis. (16) Subset of particles acquires second membrane – formation of intracellular enveloped virion (IEV). (17) IEV transport to cell surface via microtubules – formation of cell-associated virions (CEV). (18) Dissociation from cell membrane – formation of extracellular enveloped virions (EEV). Figure from Harrison et al., 2004 [161]. (b) Organization of replication complex and accessory factors (Figure modified from P. Traktmann [162]). (c) Current working model of VACV DNA replication. Steps: Nicking, primer extension, isomerization, concatemer formation, concatemer resolution, possible recombinational priming events (Figure modified from Boyle *et al*., 2009 [130]).

1.2.4.3 Vaccinia virus gene expression

The mechanisms of gene transcription are highly conserved among the members of the poxvirus family. During their unique cytoplasmic life cycle the viral genome is expressed into roughly 200 proteins in case of VACV which are involved in gene expression, DNA synthesis, virion morphogenesis and host defense/immune evasion [93]. VACV genes are composed of continuous ORFs and expressed by the viral DNA-dependent RNA polymerase (RPO) in a cascade-like manner and are therefore subdivided into three temporal classes: early, intermediate, and late-stage [127]. The

viral RPO contains at least 8 subunits ranging from 7 to 147 kDa, named accordingly RPO 7, RPO 18, RPO 19, RPO22, RPO 30, RPO 35, RPO 132, and RPO 147 encoded by the viral genes G5.5R, D7R, A5R, J4R, E4L, A29L, A24R, and J6R, respectively. The exact role of the different subunits has not been investigated, yet. However it is suggested that the large subunits RPO 132 and RPO 147 catalyze nucleotide accretion, due to their sequence homologies with the corresponding large subunits of cellular RNA polymerases [93]. Half of the RPOs in VACV virions reveal an additional factor, namely RNA polymerase-associated protein of 94 kDa (RAP94) which is required exclusively for the transcription of early genes.

The viral core contains the complete transcription machinery which enables the synthesis of viral early mRNAs shortly after infection. Early gene products include enzymes and factors necessary for DNA replication and for transcription of intermediate class genes as well as for a set of immune-regulatory factors which avert virus recognition and antiviral defense [163]. Intermediate mRNAs in turn encode for DNA-binding/packaging proteins, non-enzymatic core-associated proteins, and factors needed for the transcription of late genes. Lastly, late gene transcripts encode components of the EFC, structural components (i.e. IMV-membrane-associated proteins), and early transcription factors (TFs) which are packaged into nascent virions for the next round of infection. Figure 1-6 b summarizes the distribution of the 3 temporal gene classes within functional categories.

Despite the, for the most part, self-sufficient life cycle of VACV, the virus remains dependent on the host cell protein synthesis apparatus to translate viral mRNAs into polypeptides [164].

1.2.4.3.1 Early-stage gene transcription

As mentioned previously, VACV early mRNAs are synthesized within the viral core just minutes after virus infection via the pre-packaged multisubunit RPO as well as a set of factors and enzymes such as RAP94, 2'-O-methyltransferase, mRNA capping enzyme, poly(A) polymerase, nucleotide phosphohydrolase I (NPH I), and topoisomerase. About half of the VACV genes, an estimate of 118 genes [165], are considered to belong to the early class [166]. Early promoters feature an almost universal G residue at -21 or -22 which is surrounded by a variable AT-rich sequence [167]. Initiation of transcription is mediated by a viral heterodimer composed of D6 and A7 and designated the VACV early transcription factor (VETF) [168, 169]. The VETF is interacting with the nt -12 to -29, and the nt +7 to +10 regions of the early promoter, thereby flanking the transcription start site [170]. The VETF promoter interaction leads to the recruitment of the RPO to the initiation site. It is assumed that an ATPase activity associated with VETF [171] induces the subsequent dissociation of the VETF promoter complex via ATP hydrolysis thereby liberating the transcription start site for the RNA polymerase. Of special importance for early gene transcription is RAP94 (VACV H4), which is essential for the interaction of VETF and RPO [172]. Following initiation the RPO and associated

factors mediate RNA polymerization. The elongation process concludes when the RPO passes the termination signal TTTTTNT (with N being any nucleotide) and creates the mRNA 3'-ends about 20-50 bp downstream of this sequence [173]. At least two *trans*-acting factors, the capping enzyme and NPH I are necessary for transcription termination and mRNA release through an ATP hydrolysis-mediated reaction [174, 175]. Capping of nascent mRNA takes place after the transcript is about 30 nt long [176]. Polyadenylation is performed by a virus-encoded heterodimer VP55 and VP39. [177].

1.2.4.3.2 Intermediate-stage gene transcription

Genes that belong to the intermediate class are expressed after DNA replication is initiated, but before late gene transcription occurs. Intermediate transcripts are detectable by approximately 100 min and peak at 120 min post VACV infection [127]. Both, the expression of intermediate and late genes depend on viral DNA synthesis and are therefore designated as post-replicative (PR) genes. There are thought to be about 93 PR genes, 53 of which are considered to belong to the intermediate class and 38 to the late [178]. In contrast to early transcription initiation, the start of intermediate transcription requires both viral and host factors. Among the viral factors involved in intermediate transcription are the viral RPO, capping enzyme in a role that is independent of mRNA capping [179], VACV intermediate transcription factor (VITF) 1 which shows homology to eukaryotic transcription elongation factor SII (TFIIS) and is encoded by E4L (a.k.a. RPO 30) [180], and finally the heterodimer VITF-3 composed of A8 and A23 [181]. An additional factor required for transcription of intermediate genes is VITF-2, a heterodimer composed of the two host-derived cellular proteins, Ras-GTPase activating protein SH3-domain-binding protein (G3BP) and Cytoplasmic Activation/ Proliferation-associated Protein 1 (Caprin-1or p137) [182, 183]. The exact function of intermediate and late promoter elements in terms of transcription initiation remains elusive. The promoters feature a TAAAT motif where the RPO presumably initiates transcription as well as an essential upstream element. During the initiation the RPO slips repeatedly on the three T-residues of the template strand which leads to the formation of a novel 5'-poly(A) leader with so far unknown function [127, 184, 185]. It was shown recently that the cellular transcription factor TATA-binding protein (TBP) plays a role in targeting the core elements of intermediate and late promoters and the activation of subsequent gene transcription from these promoters [186]. Moreover, it has been reported that about half of the intermediate and late promoters reveal a binding element for the cellular transcription factor YinYang 1 (YY1) at the transcriptional start site (initiator element, INR) [127, 187]. Contrary to the initially assumed activating function of YY1 it was shown recently that YY1 acts as a negative regulator of intermediate and late VACV promoters [187].

Up-to-date the mechanisms of intermediate and late transcription termination are not fully understood. The RPO seems to terminate at multiple sites leading to transcripts with broad 3'-end heterogeneity independent of the size of the transcribed gene [188]. Multiple interacting factors have been identified to either promote RNA elongation or transcript release and it is therefore assumed that the termination of post-replicative transcripts is somewhat balanced between transcription elongation maintenance and support of transcript release [189, 190]. Among the candidates are, the A18 protein with its DNA helicase activity possibly interacting with a host factor, the G2 protein, with a suggested role in transcription elongation and interaction with H5, as well as the predicted positive elongation factor J3.

1.2.4.3.2 Late-stage gene transcription

The transcription of the about 38 late genes [178] occurs subsequent to the synthesis of intermediate transcripts with messages being detectable by 140 min post infection [127]. VACV late promoters are bipartite just like intermediate ones, with a transcription initiator element containing the TAAAT motif and an A-T-rich upstream element [191], but with a shorter interjacent sequence [192]. As discussed for intermediate mRNAs also late transcripts contain a poly(A) leader of variable length generated through RPO slippage [185]. Late transcription requires de novo synthesis of the viral RPO [193] and further depends on at least three virus-encoded TFs, namely A1, A2, and G8 also referred to as VLTF-1, VLTF-2, and VLTF-3, respectively [194, 195]. Additionally, a transcription stimulatory function has been reported for the H5 polypeptide (VLTF-4) [196]. Moreover, a set of host proteins is implicated to play a role in VACV late transcription. Among them is the TF VLTF-X [197] featuring affinity for poly(T) tracts and the transcription stimulating cellular heterogeneous nuclear ribonucleo-proteins A2/B1 (hnRNP A2) and RBM3 [198]. Dellis *et al*. investigated protein-protein interactions among VACV late TFs and suggested the formation of a late gene transcription complex with the following relations: A2–G8, A2–RBM3, A1–G8, H5–A2, and H5–G8 [199]. Since intermediate and late promoters show similar bipartite conformation and are interchangeable through extension or truncation of the intermediate sequence between the two promoter elements, it seems plausible that core elements are recognized and bound by the same factor(s). In fact, as described for intermediate transcription, the TBP seems to also interact with late promoter core elements [186]. The elongation and termination mechanisms for late transcription appear to be comparable with those for intermediate mRNAs. The factors A18, G2, and J3 mediate the release of the late transcripts which reveal highly heterogeneous 3'-ends [189].

All factors involved in VACV gene transcription identified so far are summarized in Figure 1-6 a.

a

Function	Protein	VACV gene
RNA polymerase	Rpo147	J6R
	Rpo132	A24R
	Rpo35	A29R
	Rpo30	E4L
	Rpo22	J4R
	Rpo19	A5R
	Rpo18	D7R
	Rpo7	G5.5R
	RAP94	H4L
Early transcription factor	ETF	D6R, A7L
Early transcription termination	Capping enzyme	D1R, D12L
	NPH 1	D11L
Intermediate transcription factor	VITF-3	A8R, A23R
	Capping enzyme	D1R, D12L
	Rpo30	E4L
	P137/G3BP	Cellular
	TBP	Cellular
Late transcription factor	VLTF-1	G8R
	VLTF-2	A1L
	VLTF-3	A2L
	VLTF-4	H5R
	VLTF-X	Cellular
	hnRNP A2/RBM3	Cellular
	TBP	Cellular
Intermediate and late transcription termination	Release factor	A18R
	Elongation factor	J3R
	Elongation factor	G2R

b

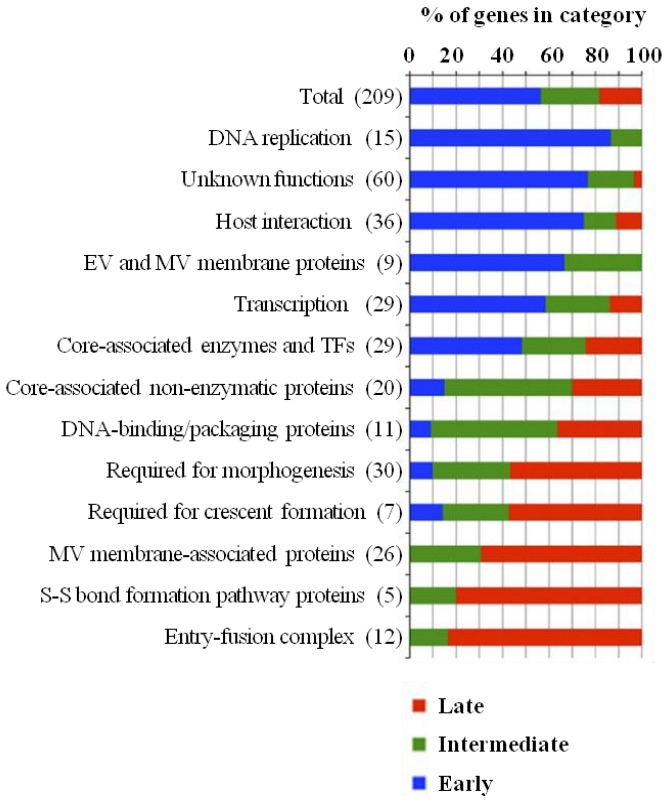

Figure 1-6: Expression-class distribution within functional categories and VACV transcription mediators

(a) Proteins involved in VACV transcription (table modified from Broyles *et al*., 2010 [192]). (b) Gene function categories broken down into early, intermediate, and late fraction (Figure modified from Yang *et al*., 2012 [178]).

1.2.5 Vaccinia virus-host interactome

1.2.5.1 Immune evasion

Upon VACV infection various virus-induced alterations of host cellular function occur to benefit the production of virus progeny and avert virus recognition and antiviral defense. VACV infection induces a profound shutdown of host DNA, RNA, and protein synthesis. In accordance with that, Yang *et al*. [165] observed that 4 hpi the proportion of viral RNAs accounts for about 25 to 55% of the total. In contrast to that, at 2 hpi a small set of cellular mRNAs was up-regulated with enrichment in the following functional classes: NF-κB cascade, signal transduction, apoptosis, and ligand-mediated signaling. Furthermore, viral protein functions are implicated in manipulating many cellular processes including cell cycle, apoptosis, and formation of the cytoskeleton.

A great portion of VACV-host interactions comprises molecular mechanisms that facilitate to evade anti-poxvirus defense reactions. VACV immune-modulating factors are produced in the first stage of infection and interfere with the host's virus detection and antiviral immunity mechanisms on several

different levels. Poxviruses cause acute infections and their defense strategies are therefore mainly directed against the universal early nonspecific (innate) host immune reactions. Among them are inflammatory reactions, interferon production, host cell apoptosis, virus inactivation by the complement complex amongst others [200]. On the other hand, the secondary specific (adaptive) immune response is slower developing and mediated by a variety of cytokines, such as interferon-γ, interleukins (IL), and tumor necrosis factor (TNF). The genes encoding for host range factors are located in the variable termini of the virus genome which explains the variation in host range of different VACV strains. Even though the mechanisms utilized to circumvent host defense are comparable, the target molecules vary between the different strains. Consequently, not all of the mechanisms and focus molecules described below apply to all VACV strains to equal amounts.

Proteins of the IL-1/Toll-like receptor (TLR) superfamily respond to viral infections and activate intracellular signaling pathways that activate the NF-κB TF which in turn triggers the transcription of target genes that encode cytokines, chemokines, factors of the complement system, immune receptors etc. The VACV genes A46R and A52R encode factors containing a TIR (Toll/IL-1 receptor) motif which allows interactions with adapter molecules such as MyD88, IRAK2 and TRAF6 and thus prevent downstream signaling and consequently suppress NF-κB activation [201]. Among the most potent preventers of host immunity are the viral interferon (IFN) inhibitors E3 and K3. IFNs are produced within host cells in response to dsRNA molecules, synthesized during viral infection and induce an antiviral defense state. The viral E3 protein can bind to dsRNA and thus antagonize dsRNA-induced signaling pathways that regulate antiviral responses such as protein kinase R (PKR) and 2',5'-oligoadenylate synthetase (OAS) function [202, 203]. The VACV K3L gene in turn encodes a homologue to the alpha subunit of eukaryotic initiation factor 2 (eIF2α) which competes with endogenous target molecules for protein kinase-mediated phosphorylation [204]. To circumvent the effects of IFN many poxviruses also produce a soluble IFN-γ receptor analog (VACV B8R) [205] and an inhibitor of the IFNα/β receptor (VACV B19R) [206].

Inflammation plays also a central role in the early defense against viral infection [207] with IL-1β, IL-18, TNF, and IFN-γ cytokines as key players in inducing inflammatory reactions. A variety of VACV gene products suppress inflammatory responses at different stages. Inhibition of caspase 1 activity by SPI-2 prevents the conversion of pro-IL-1β into IL-1β and some strains encode for proteins which acts as a soluble IL-1β receptor (COP B16R). Furthermore, it was reported that some VACV strains suppress the proinflammatory effect of IL-18 by expressing an IL-18-binding protein [208], or avoiding the impact of TNF by producing a type II TNF receptor analog (COP C22L/B28R). Another viral mechanism of action includes the binding of CC chemokines and thus the inhibition of chemokine-receptor interactions and subsequent signal transduction [209]. Furthermore, poxviruses inhibit, modulate, and exploit several levels of the complement system which is composed of various effector proteins and soluble regulatory proteins [210].

Important anti-viral host defense mechanisms also include programmed cell death (apoptosis) [211-213]. Since viruses need to keep their host cell alive for production of viral progeny and later dissemination, viral anti-apoptotic effectors with different modes of action are expressed early upon infection. Apoptosis is primarily executed by cysteine proteases called caspases with one of them (caspase 9) being targeted by COP F1 [214]. In addition to that COP C12 and N1 play a role as antiapoptotic factors [200] supposedly by manipulating other cell death pathways within the cell.

Poxviruses reveal a number of additional strategies to circumvent anti-viral host responses. In summary poxviruses feature a multi-factorial, multi-step system to control the host's antiviral state.
A short excerpt of poxvirus modulatory molecules and the respective affected pathways is summarized in table 1-2 exemplary for the VACV COP strain.

Table 1-2: Poxvirus immune-modulatory molecules and affected pathways

Viral protein	VAC-COP	Pathways
TNF receptor CrmB	C22L (B28R)	Cytokine pathway
eIF2α homolog	K3L	Cytokine pathway, Anti-apoptotic
IFN-γ receptor	B8R	Cytokine pathway
IFN α/β binding proteins	B19R	Cytokine pathway
Putative type I interferon antagonists	C7L, K1L	Cytokine pathway
dsRNA-binding protein	E3L	Cytokine pathway, Anti-apoptotic
IL-1β receptor	B16R	Cytokine pathway
Toll-like/IL-1 receptor inhibitor	A46R, A52R	Cytokine pathway
Chemokine binding protein	C23L (B29R)	Chemokine pathway
3β-hydroxysteroid dehydrogenase	A44L	Immune modulatory
Semaphorins	A39R	Immune modulatory
Viral growth factor	C11R	Immune modulatory
Complement inhibition	C3L	Immune modulatory
CD47-like protein	A38L	Immune modulatory
SPI-1	C12L	Anti-apoptotic
SPI-2/CrmA	B13R/B14R	Anti-apoptotic
SPI-3	K2L	Anti-apoptotic

(Modified from Seet et al., 2003 [210])

1.2.5.2 Host factors in vaccinia virus life cycle (not immediately immune-related)

In addition to host immune evasion poxviruses use other virus-host interactions to benefit from its surroundings. It starts with the first step of poxvirus host cell entry, more precisely the binding of viral particles (MVs and EVs) to the cell which occurs via particle-type-specific cellular attachment factors in the plasma membrane [113]. Subsequent uptake via macropinocytosis is a signaling-induced process which involves many cellular factors (i.e. EGFR signaling and VPEF/FAM21) [113].
For particle transport and spread VACV takes advantage of the host cell cytoskeleton. The recruitment of kinesin leads to microtubule-mediated transport [215-217] to sites of DNA synthesis and transcription as well as transport of newly synthesized virions to the cell surface.

As described previously, VACV recruits cellular factors to the sites of mRNA intermediate and late transcription to mediate certain steps during transcript generation. Among them are TBP, P137/G3BP, hnRNP A2/RBM3 and VLT-X (Table 1-1). Additionally, virus protein synthesis is dependent on the host cell translation machinery. VACV messages are structurally similar to host mRNAs, featuring an m7G cap at their 5'-terminus [218, 219]. For this reason and to secure maximal viral protein synthesis, VACV stimulates the formation of eIF4F complexes [220, 221] which are an important component of eukaryotic translation initiation regulation [222]. In addition to promoting eIF4F assembly VACV initiates the redistribution of host translation factors eIF4E and eIF4G to the viral replication compartments [223, 224]. Zaborowska *et al*. [225], described recently that the VACV ssDNA-binding protein I3 is involved in the recruitment of host translation initiation factor eIF4G. Enrichment of host translation factors in viral compartments not only promotes virus protein synthesis, but decreases translation of host mRNAs at the same time due to the absence of these factors at sites of host protein production. This effect is further intensified through increased host mRNA turnover, mediated by two VACV encoded decapping enzymes D9 and D10 [226, 227].

At the plasma membrane virions induce actin tail formation, important for cell-to-cell dissemination [228]. Actin polymerization is regulated by interaction of several cellular and viral proteins. Cellular tyrosine (tyr)-protein kinase Src is activated by binding of the viral factor B5 [229]. Src phosphorylates tyr residues of VACV A36 which leads to generation of binding sites for cellular adapter proteins Nck and Grb2 [230]. Nck forms a complex with WASP interacting protein (WIP) and N-WASP [231-233] and eventually N-WASP leads to activation of the actin-polymerizing activity of the Arp2/3 complex [234, 235]. Actin tail formation is further promoted by the transient recruitment of AP-2 and clathrin [236]. The rate of actin-mediated virus dissemination is presumably regulated by interactions of host SH2-containing 5'-inositol phosphatase 2 (*SHIP2*) and viral A34 [237].

The role of virus-host interactions in the formation of virus-modified membranes is not fully understood. It was shown before that for example p37 (COP F13L) [238] is involved in enveloping IMVs with TGN (trans-Golgi network)-derived membranes [239, 240] through interaction with host proteins [241]. Intracellular trafficking of vesicles and membranes also requires the interaction with host factors such Rab proteins [242]. Bartel *et al.* [243] published a 2-gel plus MALDI-PSD-TOF MS-based proteome analysis of vaccinia virus-infected HEK 293 cells and discovered, amongst other things, that all energy metabolism-related alterations in the human proteome profile indicated an elevation in glycolysis rate and in oxidative phosphorylation, thereby meeting the virus' demand for energy during replication.

Numerous interactions of human proteins and their potential viral binding partner have been suggested via yeast-two-hybrid (Y2H) technology or other screening methods [244, 245]. However, due to an increased number of "false positives" and "false negatives" associated with different detection technologies the interpretation of these results remains challenging.

1.3 Aim of the study

The main goal of this thesis was to investigate interactions between oncolytic vaccinia viruses (VACV) and host cells to identify cellular factors and parameters related to VACV infection that might influence viral replication and thus contribute to, or predict *in vitro* permissiveness of host cells to infection.

Although, VACV has emerged as an attractive tool in oncolytic virotherapy with promising success, yet, little is known about causes for variations in permissiveness of host cell lines and tumors to infection and oncolysis. Analysis of the NCI-60 panel of cell lines revealed that the replication efficiency of the same virus strain (GLV-1h68) is quite heterogeneous among different cancer cell lines [246]. Further, it was shown previously that viral replication efficiency correlates directly with antitumor efficacy [247]. In the present work, it was therefore of interest to investigate the influence of host factors on viral replication efficiency and thus host cell susceptibility to VACV infection.

Recently, a series of VACV Lister wt clones, derived from the mixed population of the GLV-1h68 parental strain, was characterized regarding replication efficiency, toxicity and therapeutic effect in nude mice (*unpublished*). Among them, three isolates revealed natural genetic attenuations (LIVP 1.1.1, LIVP 5.1.1, and LIVP 6.1.1).

For the first part of the study, two previously characterized autologous melanoma cell lines (888-MEL and 1936-MEL) [50, 51] with similar *in vitro* permissiveness to GLV-1h68 infection [101] should be tested for permissiveness to these 3 wt VACV clones as well as to the attenuated GLV-1h68 control strain [102]. An initial goal was to correlate viral replication efficiency with viral gene transcription levels.

Further, it was of interest to point out expressional differences among different VACV wt isolates and GLV-1h68 as well as general time-dependent variances (early vs. late) in viral gene transcription and replication. At the same time human gene expression of infected cells should be evaluated and correlated with viral replication and transcription to elucidate the relationship between host cell transcription and viral replication/transcription. One main focus of the gene expression studies was to explore in particular events occurring early after infection since replication is initiated within the first 2 hours after VACV infection [129].

Finally, the findings obtained via expression analysis within the two autologous melanoma cell lines should be applied to an independent data set to investigate the predictive strength of the results. Therefore the well characterized breast cancer cell line GI-101A and the adenocarcinoma cell line HT-29 [101] are considered appropriate as well as a set of 5 VACV recombinants (GLV-1h70, GLV-1h71, GLV-1h72, GLV-1h73, GLV-1h74) with known differences in replication due to replacement of expression cassettes from GLV-1h68 with short non-coding DNA sequences [247] plus GLV-1h68 as control.

The focus of the second part of the study was to highlight cellular differences between highly permissive and less permissive cell lines on different molecular biological levels. Baseline expressional differences prior to VACV infections were thought to provide important information regarding the existence of a "permissive phenotype".

A panel of 15 melanoma cell lines should be screened regarding VACV permissiveness. Based on the results of the screening, cell lines should be divided into a low and a highly permissive group. Subsequent analysis should be focused on emphasizing baseline differences in mRNA expression, miRNA expression and DNA copy number variations in-between these two groups prior to infection.

Data obtained from the second study should also be overlaid with the results of the first part to get a better global understanding of correlations between cellular composition and expressional baseline with viral replication state.

In summary, this second part of the study should include a comprehensive evaluation and comparison of factors that might promote vaccinia virus replication and thus contribute to permissiveness of a given cell line to vaccinia virus treatment.

2 Material and Methods

2.1 Material

2.1.1 Devices

Table 2-1

Device	Manufacturer
Bioanalyzer 2100	Agilent technologies, Santa Clara, CA, USA
Biological Safety Cabinet, Class II Type A2	NuAire, Plymouth, MN, USA
Centrifuge, Sorvall Legend XTR, TX-750 Rotor	Thermo Fisher Scientific, Asheville, NC, USA
Forma SeriesII Water Jacketed CO_2 Incubator	Thermo Fisher Scientific, Asheville, NC, USA
GeneChip® Fluidics Station 450	Affymetrix, Inc., Santa Clara, CA , USA
GeneChip® Hybridization Oven 640	Affymetrix, Inc., Santa Clara, CA , USA
GeneChip® Scanner 3000 7G	Affymetrix, Inc., Santa Clara, CA , USA
GenePix 4000B Microarray Scanner	Molecular Devices, LLC, Sunnyvale, CA, USA
High-Resolution Microarray Scanner	Agilent technologies, Santa Clara, CA, USA
Invertoscope ID 03	Carl Zeiss Microscopy,LLC, Thornwood, NY, USA
LabChip® GX	Caliper Life Sciences, PerkinElmer, Santa Clara, CA, USA
Microcentrifuge 5415 R	Eppendorf, Westbury, NY, USA
MicroONE Mini Centrifuge	TOMY TECH U.S.A. via CS Bio Co., Menlo Park, CA, USA
PTC-225 Peltier Thermal Cycler	MJ Research, Life Science, Hercules, CA, USA
MoFlo Astrios Cell Sorter	Beckman Coulter, Inc., Atlanta GA, USA
NanoDrop 8000 and 2000 Spectrophotometer	Thermo Fisher Scientific, Asheville, NC, USA
Neubauer Counting Chamber	Marienfeld GmbH, Lauda-Königshofen, Germany
Orbital Vortexer Minishaker	IKA® Works, Inc., Wilmington, NC, USA
Sonicator	Heat Systems-Ultrasonic, Farmingdale, NY, USA
Thermomixer® R	Eppendorf, Westbury, NY, USA
Titer Plate Shaker	Thermo Fisher Scientific, Asheville, NC, USA
Vortex-Genie 2® Laboratory Mixer	Daigger, Vernon Hills, IL, USA

2.1.2 Reagents

Table 2-2

Reagent	Manufacturer
2-Propanol	Sigma, Sigma-Aldrich, St. Louis, MO, USA
Antibiotic-Antimycotic Solution (Penicillin/Streptomycin/Amphotericin)	Corning cellgro, Mediatech, Inc., Manassas, VA, USA
AutoMACS® Running Buffer	Miltenyi Biotec, Auburn, CA, USA
Carboxymethylcellulose (CMC)	Sigma, Sigma-Aldrich, St. Louis, MO, USA
Ciprofloxacin (10 mg/mL)	Hospira, Inc. Lake Forest, IL, USA
Crystal Violet	Sigma, Sigma-Aldrich, St. Louis, MO, USA
50x Denhardt's blocking solution	Sigma, Sigma-Aldrich, St. Louis, MO, USA
Deoxyribonucleotide (dNTP) Mix	Amersham Pharmacia Biotech, Piscataway, NJ, USA
Diethylpyrocarbonate (DEPC)-Treated Water	Quality Biological, Inc., Gaithersburg, MD, USA
Dimethyl Sulfoxide (DMSO)	Sigma, Sigma-Aldrich, St. Louis, MO, USA
Dulbecco's Modified Eagle Medium (DMEM), High Glucose	Gibco ®, life technologies, Grand Island, NY, USA
Dulbecco's Phosphate-Buffered Saline (DPBS), No Calcium, No Magnesium	Gibco ®, life technologies, Grand Island, NY, USA
Ethyl Acohol, 200 Proof	Warner Graham Company, Cockeysville, MD, USA
Ethylenediaminetetraacetate (EDTA)	Quality Biological, Inc., Gaithersburg, MD, USA
Fetal Bovine Serum (FBS), Heat-Inactivated	Gibco ®, life technologies, Grand Island, NY, USA
Formaldehyde (37%)	Sigma, Sigma-Aldrich, St. Louis, MO, USA
Formamide	Sigma, Sigma-Aldrich, St. Louis, MO, USA
Fungizone® Amphotericin B (250 µg/mL)	Gibco ®, life technologies, Grand Island, NY, USA
HEPES (N-2-hydroxyethylpiperazine-N'-2-ethanesulphonic acid)	Corning cellgro, Mediatech, Inc., Manassas, VA, USA
Human Cot I DNA (1 mg/ml)	Gibco ®, life technologies, Grand Island, NY, USA
L-Glutamine:Penicillin:Streptomycin (GPS)	Gemini Bio-products, West Sacramento, CA, USA
Paraformaldehyde (16%)	Electron Microscopy Sciences, Hatfield, PA, USA
Poly d(A)	Amersham Pharmacia Biotech, Piscataway, NJ, USA
Ribonuclease H (RNase H)	Invitrogen, life technologies, Grand Island, NY, USA
RNAprotect® Cell Reagent	QIAGEN, Inc., Valencia, CA
RNase AWAY	Molecular BioProducts, Inc., Thermo Fisher Scientific, Asheville, NC, USA
RNasin® Ribonuclease Inhibitor	Promega Corporation, Madison, WI, USA

Roswell Park Memorial Institute-(RPMI-) Medium 1640, L-glutamine	Gibco ®, life technologies, Grand Island, NY, USA
Saline-Sodium Citrate (SSC) 20X	K·D Medical Inc., Columbia, MD, USA
Sodium Dodecyl Sulfate (SDS) 10%	Quality Biological, Inc., Gaithersburg, MD, USA
Trypan Blue Stain 0.4%	Invitrogen, life technologies, Grand Island, NY, USA
Trypsin:EDTA (0.5%:0.53 mM Solution)	Gemini Bio-products, West Sacramento, CA, USA
Yeast tRNA	Sigma, Sigma-Aldrich, St. Louis, MO, USA

2.1.3 Items

Table 2-3

Item	Manufacturer
36 k Human Array and 827 miRNA Array, (Manufactured in house)	Department of Transfusion Medicine, NIH, Bethesda, MD, USA
Agilent 2 × 105 K arrays	Agilent, Agilent technologies, Santa Clara, CA, USA
Aspirating Pipets, Disposable (2 ml)	VWR International LLC., Philadelphia, PA, USA
Barrier Tips (10 µl, 20 µl, 200 µl, 1000 µl)	Neptune, San Diego, CA, USA
Cell Culture Flasks (75 cm^2, 175 cm^2)	SARSTEDT, Inc., Newton, NC, USA
Cell Scraper	Crystalgen Inc., Commack, NY, USA
Costar® Multiple Well Plates, TC-Treated	Corning, Inc., Corning, NY, USA
Costar®, Serological Pipets, Disposable (5 ml, 10 ml, 25 ml)	Corning, Inc., Corning, NY, USA
Cover Slips for Microarray Slides (22 x 60 mm)	Thermo Fisher Scientific, Asheville, NC, USA
Cryo Freezing Container	Nalgene, Thermo Fisher Scientific, Asheville, NC, USA
Cryo Tubes (1.8 ml)	Nunc, Thermo Fisher Scientific, Asheville, NC, USA
Falcon™ Cell Culture Dishes (60 mm)	BD, Becton Dickinsons, Franklin Lakes, NJ, USA
Falcon™ Tubes, Conical (15 ml, 50 ml)	BD, Becton Dickinsons, Franklin Lakes, NJ, USA
Falcon™ Tubes, Round-Bottom (5 ml)	BD, Becton Dickinsons, Franklin Lakes, NJ, USA
Filter Units (90 mm, 1000 ml)	Nalgene, Thermo Fisher Scientific, Asheville, NC, USA
GeneChip® Customized Probe Arrays (VACGLa520445F)	Affymetrix, Inc., Santa Clara, CA , USA
Magnetic Stand for 96-well plates	Applied Biosystems™, life technologies, Grand Island, NY, USA
PCR Strips (0.2 ml)	Denville Scientific, Metuchen, NJ, USA
Posi-Click Tube (1.7 ml)	Denville Scientific, Metuchen, NJ, USA

2.1.4 Kits

Table 2-4

Kit	Manufacturer
Advantage cDNA Polymerase Mix	Clontech Laboratories, Inc., Mountain View, CA, USA
Agilent RNA 6000 Nano Kit	Agilent technologies, Santa Clara, CA, USA
GeneChip® 3' IVT Express Kit	Affymetrix, Inc., Santa Clara, CA , USA
GeneChip® Hybridization, Wash, and Stain Kit	Affymetrix, Inc., Santa Clara, CA , USA
GeneChip® Sample Cleanup Module	Affymetrix, Inc., Santa Clara, CA , USA
HT DNA LabChip® Kit	Caliper Life Sciences, PerkinElmer, Santa Clara, CA, USA
MEGAscript® T7 Kit	Ambion, life technologies, Grand Island, NY, USA
miRCURY LNA™ microRNA Array, Power labeling kit	EXIQON, Woburn, MA, USA
miRNeasy Mini Kit	QIAGEN, Inc., Valencia, CA
RNA Fragmentation Reagents	Ambion, life technologies, Grand Island, NY, USA
QIAamp® DNA Mini Kit	QIAGEN, Inc., Valencia, CA
SuperScript™ II Reverse Transcriptase	Invitrogen, life technologies, Grand Island, NY, USA
ULS™ aRNA Labeling Kit (with Cy3 and Cy5)	Kreatech, Inc., Durham, NC, USA

2.1.5 Synthetic oligonucleotides (primer)

Table 2-5

Primer	Sequence
Oligo dT(15)-T7 Primer	5' AAA CGA CGG CCA GTG AAT TGT AAT ACG ACT CAC TAT AGG CGC $T_{(15)}$ 3'
Ramdom Hexamer Primer	dN_6
TS (template switch) Oligo Primer	5' AAG CAG TGG TAA CAA CGC AGA GTA CGC GGG 3'

2.1.6 Software

Table 2-6

Microsoft Word 2007	
Microsoft Excel 2007	
BRB-ArrayTools 4.1.0, Microsoft Excel Add-In (http://linus.nci.nih.gov/BRB-ArrayTools.html) [248]	
Partek Genomics Suite ®	
Cluster 3.0 (Michael Eisen, Stanford University) [249]	
TreeView (Michael Eisen, Stanford University) [249]	
Ingenuity® Systems	
Agilent Feature Extraction	
Kaluza Cytometry Software (Beckman Coulter, Inc. Brea, CA).	
Device-specific software to generate, process and save data:	2100 Bioanalyzer
	GeneChip® Fluidics Station 450
	GeneChip® Scanner 3000 7G
	High-Resolution Microarray Scanner
	LabChip® GX
	MoFlo Astrios Cell Sorter
	NanoDrop 8000 Spectrophotometer

2.1.6 Composition of buffers and media

Table 2-7

Solution/ Medium	**Composition**	
CMC Overlay Medium	7.5 g	CMC
	500 ml	DMEM High Glucose (4.5 g/l)
	1%	Antibiotic-Antimycotic Solution
	5%	FBS
Crystal Violet Staining Solution	1.3 g	Crystall Violet
	50 ml	Ethyl Acohol
	300 ml	Formaldehyde (37%)
	650 ml	H_2O_{bidest}
Freezing Medium	10%	DMSO
	90%	FBS

CV-1 Culture Medium	500 ml	DMEM High Glucose (4.5 g/l)
	1%	Antibiotic-Antimycotic Solution
	10%	FBS
CV-1 Infection Medium	500 ml	DMEM High Glucose (4.5 g/l)
	1%	Antibiotic-Antimycotic Solution
	2%	FBS
NCI-60 Cell Culture Medium	1000 ml	RPMI
	10%	FBS
	16 ml	HEPES
	1%	Antibiotic-Antimycotic Solution
	1%	Ciprofloxacin (10 mg/mL)
		(added after passing through filter unit)
NCI-60 Cell Infection Medium	1000 ml	RPMI
	2%	FBS
	16 ml	HEPES
	1%	Antibiotic-Antimycotic Solution
	1%	Ciprofloxacin (10 mg/mL)
Melanoma Cell Culture Medium	1000 ml	RPMI
	10%	FBS
	16 ml	HEPES
	1%	GPS
	1‰	Ciprofloxacin (10 mg/mL)
	1%	Fungizone
		(added after passing through filter unit)
Melanoma Cell Infection Medium	1000 ml	RPMI
	2%	FBS
	16 ml	HEPES
	1%	GPS
	1‰	Ciprofloxacin (10 mg/mL)
	1%	Fungizone
		(added after passing through filter unit)

2.1.7 Cell lines

Table 2-8

CV-1	African green monkey kidney fibroblasts	American Type Culture Collection (ATCC)
1936-MEL 888-MEL	Autologous human melanoma cell lines	Sequential sub-cutaneous metastases in patient 888 at the National Institutes of Health (NIH) [50, 51]
GI-101A	Human metastatic breast tumor cell line	Provided by Dr. A. Aller (Rumbaugh-Goodwin Institute for Cancer Research, Inc., Plantation, Florida, USA
HT-29	Human colorectal adenocarcinoma cell line	ATCC
HCT-116 HCT-15	Human colon carcinoma cells	NCI-Frederick Cancer Center, DCTD Tumor/Cell Repository
2492-MEL 2744-MEL 2155-MEL 2075-MEL 2224-MEL 3107-MEL 2448-MEL 2523-MEL 3104-MEL 2805-MEL 2458-MEL 2427-MEL 2035-MEL 1866-MEL 3025-MEL	Human metastatic melanoma cell lines	Lesions from patients treated at the Surgery Branch, National Cancer Institute (NCI), Bethesda, MD. Kindly provided by Dr Steven A Rosenberg

2.1.8 Vaccinia virus isolates

2.1.8.1 Recombinant vaccinia viruses

In this work three recombinant *Genelux Virus* (GLV) isolates, derived from wild-type (wt) Lister strain (LIVP), were used for various experiments, namely GLV-1h68, GLV-1h134, and GLV-1h261. The viruses were constructed via insertional mutagenesis of three transgene expression cassettes into the LIVP genome.

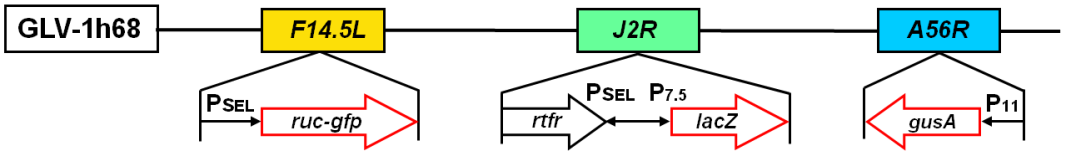

Figure 2-1: Recombinant VACV GLV-1h68

The VACV GLV-1h68 contains an insertion of *Renilla* luciferase (*RUC*) and green fluorescent protein (*GFP, Aequorea*) gene fusion in the *F14.5L* locus under control of an *early/late* promoter $P_{E/L}$. Further an expression cassette coding for β-galactosidase (*lacZ*) was introduced into the thymidine kinase (*TK*) locus *J2R* under control of the $P_{7.5}$ promoter. Moreover, the human transferrin receptor (*rtfr*) was inserted in reverse orientation into the *TK* locus. Finally, the β-glucuronidase (*gusA*) gene was cloned into the hemagglutinin (*HA*) locus *A56R* under control of the promoter p11 (Figure 2-1) [102].

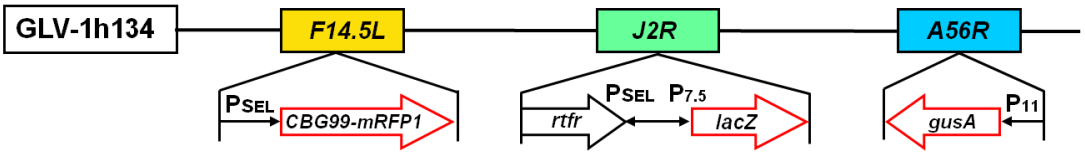

Figure 2-2: Recombinant VACV GLV-1h134

GLV-1h134 differs from GLV-1h68 only by an insertion of click beetle green (*CBG*) 99–red fluorescent protein fusion (CBG99-mRFP1) into the F14.5L locus instead of *RUC-GFP* (Figure 2-2).

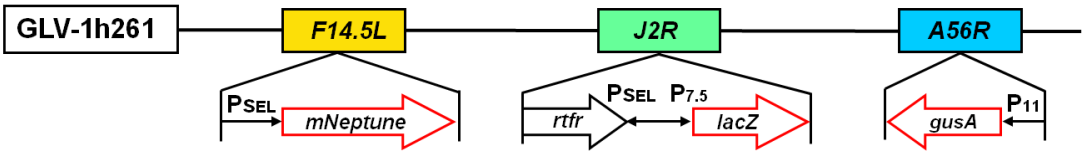

Figure 2-3: Recombinant VACV GLV-1h261

The recombinant VACV GLV-1h261 features the same transgene insertions into J2R and A56R loci as GLV-1h68 and GLV-1h134. It differs from these two isolates by an insertion of the mNeptune cDNA into the *F14.5L* locus (Figure 2-3).

A series of recombinant VACV isolates, namely GLV-1h70, GLV-1h71, GLV-1h72, GLV-1h73, and GLV-1h74 was engineered by replacing expression cassettes from GLV-1h68 with short non-coding DNA sequences (Figure 2-4) [247].
All recombinant virus isolates were designed, generated, and isolated by Dr. Qian Zhang and Dr. Nanhai G. Chen, Genelux Corp., San Diego, USA and provided for Dr. Szalay's research program at the University of Wuerzburg, Germany and at the NIH, Bethesda, MD, USA.

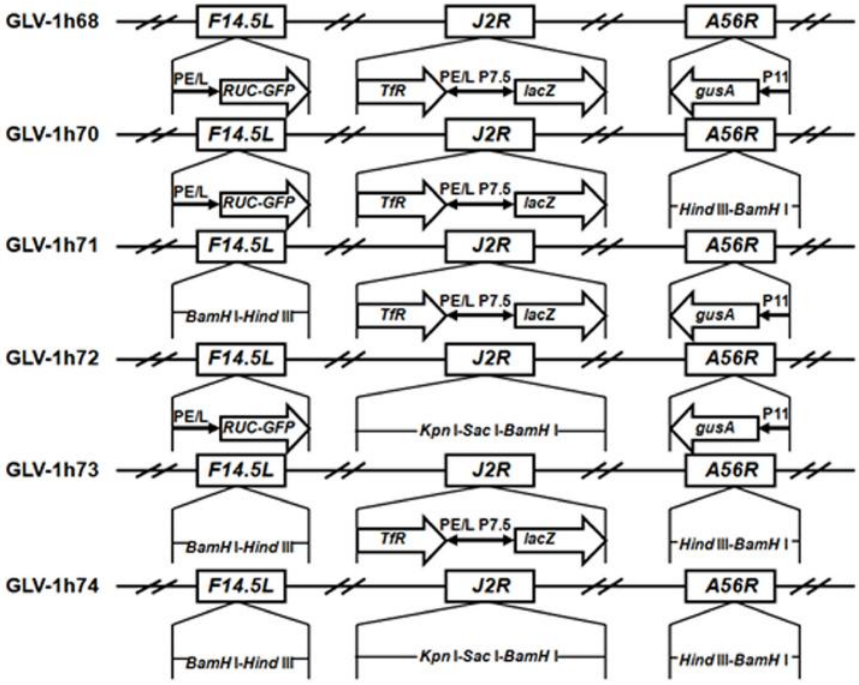

Figure 2-4: Recombinant VACVs GLV-1h68, 1h70, 1h71, 1h72, 1h73, and 1h74
(Figure from Chen et al., 2011 [247])

2.1.8.2 Wild-type vaccinia virus isolates

Different wild-type (wt) clones were picked from the mixed population of the LIVP strain by Dr. Nanhai G. Chen, Genelux Corp., San Diego, USA. Three isolates (LIVP 1.1.1, LIVP 5.1.1, and LIVP 6.1.1) with natural attenuations due to point mutations and deletions were used for this work.

2.2 Methods

2.2.1 Cell culture

2.2.1.1 Culturing of adherent human cancer cells

All cell culture experiments were performed under a class II biological safety cabinet in sterile conditions. The cell culture media were supplemented with antibiotics and fungizone (ciprofloxacin, penicillin, streptomycin, amphotericin B) to prevent bacterial and fungal contaminations. Moreover, all items were disinfected with 70% ethyl alcohol before usage under the safety cabinet. CO_2 incubators were used to maintain the cells under optimum growth conditions (37 °C, 95% relative humidity, 5% CO_2). Cell culture flasks, dishes and plates are made of sterilized polystyrene, treated for optimal cell attachment. The culture medium contains the pH indicator phenol red which helps to control for pH, cell metabolites, and nutrients by change in color (red to yellow). The composition of the culture medium was optimized for each cell line. Culture medium was changed every two to three days as appropriate. To prevent cell growth inhibition and the formation of multi-layers the cells were passaged before reaching 100% confluence.

2.2.1.2 Cell passaging

In cell culture, passaging is an essential process to maintain cells in culture for a longer time by preventing senescence and cell death due to high cell density. Before reaching 100% confluence a small fraction of cells is split and transferred into a new vessel. First the culture medium is aspirated from the culture vessel followed by a washing step with PBS to remove cellular debris. Subsequently, cells are detached by trypsin-EDTA and an incubation time of up to 5 minutes at 37 °C. Trypsin is an endopeptidase which hydrolyses peptide bonds preferentially C-terminal of the amino acids lysine and arginine. Cell detachment can be supported by rocking the culture vessel. The reaction can be stopped by addition of fresh culture medium. After resuspending of the detached cells by pipetting, an appropriate portion of the cell suspension is transferred into a new vessel and fresh medium is added.

2.2.1.3 Cell counting

For many applications in cell culture it is required to determine the cell concentration. A device to determine the cell number manually is the Neubauer counting chamber (hemocytometer). The chamber consists of a microscope slide with an engraved grid and a cover slip. The counting grid is composed of four main squares with 16 sub-grids each. Depth and area of chamber and grid are

known and enable to determine the number of particles in a certain volume. Living and dead cells can be distinguished by adding Trypan blue to the cell suspension which stains dead cells and debris but doesn't pass the intact cell membrane of living cells. Trypan blue and cell suspension are mixed in a 1-to-1 ratio and 10 µl of the well-mixed cell suspension are applied to the chamber. The suspension is sucked under the cover slip via capillary action. To guarantee accuracy the cell number of all 4 main grids is counted with help of a microscope. The cell number is calculated as follows:

$$\frac{number\ of\ cells\ counted}{number\ of\ main\ squares\ counted} \times 10^4 \times dilution\ \ factor = \frac{cell\ number}{ml}$$

2.2.1.4 Confluence test

For most cell culture experiments a confluence of 100% is not desired since cell characteristics, especially global gene expression patterns change significantly in confluent cells when compared to sub-confluent cells [250]. Cell proliferation varies drastically in-between different cancer cell lines and for the most part independently from the tissue they originated from. For this reason it is essential to perform a confluence test for each cell line in an experiment to investigate cell proliferation characteristics. To do so cells are seeded at different concentrations (for example 1 x 10^5, 3 x 10^5 and 5 x 10^5) in a certain culture vessel. If the cell number is determined at the same time an appropriate number of wells has to be seeded at same cell concentrations. After 24 hrs the confluence is determined via microscope and cells can be counted according to 2.2.1.3. In case of a time course experiment it could also be of interest to check confluence at 48, 72 or even at 96 hrs.

2.2.1.5 Freezing and thawing cells

For long or short term storage cells can be frozen in freezing medium which minimizes damage to the cell during the freezing process. Cells with a confluence of 90 to 100% were washed once with PBS and subsequently detached with help of trypsin-EDTA. Culture medium was used to stop the enzymatic reaction of trypsin. After determining the cell concentration the cells were harvested by centrifugation (1400 rpm, 5 min). The pellet was resuspended in freezing medium to a concentration of 2 x 10^6 to 2 x 10^7 cells/ ml and aliquoted in cryo tubes. The tubes were placed as rapidly as possible into a cryo freezing container filled with 100% isopropyl alcohol thereby providing the desired -1 °C/minute cooling rate. The cooler was placed into a -80 °C freezer for at least 24 hours. Finally the vials were stored in liquid nitrogen.

Thawing of cells should also be performed as rapidly as possible to obtain a good survival rate. Cell culture medium was pre-warmed to 37 °C and 10 ml aliquots filled into 50 ml reaction tubes. Cryo tubes were removed from the liquid nitrogen tank and placed directly into a 37 °C water bath just until the content was completely thawed. The content of the cryo vial was transferred immediately into the medium-filled reaction tubes to minimize the toxic effects of DMSO on the cells. After centrifugation, the cell pellet was resuspended in fresh medium and the cell suspension seeded into a culture vessel. An additional washing step with culture medium can be performed before transferring the cells into the culture vessel. After 16 to 24 hours the medium was replaced by fresh culture medium and cells cultivated at 37 °C and 5% CO_2.

2.2.2 Virological methods

2.2.2.1 VACV infection of human cancer cells

For the infection with VACV, cells were cultured to a confluence of 70 to 90%. The viral dose used for an experiment was application-specific and is calculated as ratio of infectious viral particle to total cell number, also referred to as *multiplicity of infection* (MOI). An MOI of 1 indicates that theoretically every cell is infected by one virus particle, whereas at an MOI of 0.5 every other cell should be infected. The amount of virus needed for infection at a certain MOI is calculated as follows:

$$\frac{[Total\ cell\ number\ x\ MOI\ x\ (Single\ infection\ volume)^{-1}]\ x\ Total\ infection}{Virus\ stock\ titer} = Virus\ volume$$

For the infection(s) the VACV-containing cryo vial was thawed quickly in a 37 °C water bath. Subsequently, viral aggregates were dissolved by sonication. Therefore the virus tubes were placed in a 4 °C sonication bath and sonicated 3 times for 30 seconds with 30 seconds break (on ice) in-between. Following, the tubes were vortexed and spun down briefly. The previously calculated amount of virus was mixed with the appropriate volume of infection medium (culture medium with 2% FBS) and applied carefully on the cell layer. Every 20 min the culture vessel was rocked gently to ensure an even distribution of viral particles. After one hour the infection medium was aspirated and the adherent cells carefully washed twice with PBS followed by supply with fresh culture medium.

2.2.2.2 Vaccinia virus titration via plaque assay

The number of viral particles in a suspension or stock solution can be determined via plaque assay. Firstly, CV-1 cells were grown in 24-well plates to a confluence of 100%. Subsequently, the infected samples or virus stocks were thawed and sonicated in a 4 °C sonication bath 3 times for 30 seconds with 30 seconds break (on ice) in-between. Appropriate serial dilutions were made using low FBS (2%) DMEM. Following, the medium was aspirated from the wells and cells infected in duplicate or triplicate with 250 µl of the virus dilutions. CMC overlay medium (1 ml/ well) was added after one hour and plates placed in the incubator (37 °C, 5% CO_2). After two days the cells were stained by adding 250 µl crystal violet to each well for several hours at room temperature (RT) and subsequent rinsing in a water bath. Spots with diminished staining (plaques) were observable on the dried plates. The number of plaques was counted manually and the viral titer calculated according to the following formula:

$$\frac{\textit{Number of plaques}}{\textit{Dilution factor x infection volume}} = \textit{Virus titer (pfu/ml)}$$

2.2.2.3 Viral replication assay

The replication efficiency of vaccinia virus is dependent on the utilized virus isolate and the host cell line in which the virus is replicating. To analyze the replication behavior of a virus isolate in a certain cell line, cells were infected with this particular virus and the virus titer determined at different time points. To do so, cells were grown to 90% confluence and infected in 6-well plates with each virus of interest at an MOI of 0.01 or 10 as appropriate. Cells were harvested at 2, 6, 10, 24, and 48 hours post infection (hpi) in triplicate. Viral particles were released by applying 3 freeze & thaw cycles. Viral titers were determined by standard plaque assays on CV-1 cell monolayers.

2.2.2.4 Infection of human cancer cells for flow cytometry

Flow cytometry enables an indirect measurement of GLV-1h68 infection and replication [251] via measurement of the *gfp* marker gene expression. To analyze the permissiveness of different cell lines to GLV-1h68 infection, cells were grown in 6-well plates to a confluence of up to 90%. Following, infection was performed as described in 2.2.2.1 at an MOI of 1 in 500 µl/well in 6-well plates for 20 hrs. The infection was stopped with 1.5 ml culture medium. After stopping the infection and harvesting the cells, samples were fixed and prepared for analysis via flow cytometer (2.2.3.2).

2.2.3 Molecular biological methods

2.2.3.1 Microarray

DNA microarrays serve as a platform to analyze the expression of thousands of genes simultaneously. Among other things, microarray technology enables the analysis of transcriptional changes within a cell under different conditions or in-between healthy and diseased cells. Arrays are solid glass or nylon supports onto which DNA fragments are fixed (printing, spotting, direct synthesis), with each spot on the array representing a particular gene. The technology is based on the principle of specific complementary binding (hybridization) of an mRNA or cDNA molecule to the DNA sequence from which it originated.

There are two basic types of microarray experiments, two-color (Figure 2-5 a) and one-color (Figure 2-5 b) experiments. For a two-color experiment (slide-based) RNA from the samples to be compared is extracted, transformed into cDNA via reverse transcription, and labeled with different fluorescent dyes (for example, Cy3 and Cy5). Co-hybridization of equal amounts of the two differently labeled samples to the immobilized probes takes places in a competitive manner. During the scanning process of the chip, the fluorophores excite at a certain wavelength after being hit by a laser. The output of the scanner represents the ratio of the fluorescence intensities of both colors. If both samples hybridize equally to a probe the ratio of the signal will appear yellow on the array. Increased relative Cy3 signal or Cy5 signal will appear in green and red, respectively, and represent down or up regulation of this particular gene. Two-color experiments enable a direct comparison between two different samples in a single experiment whereas one-color experiments require two separate experiments for sample comparison. In one-color experiments the cDNA is labeled with a single color (i.e., biotin + streptavidin/phycoerythrin, Affymetrix) and hybridized to the microarray without a reference sample. In this case the output is an absolute value of hybridization and is compared with other experiments to obtain information about expressional variation.

2.2.3.1.1 Generation and isolation of total RNA for microarray

For RNA isolation 5 x 10^6 cells were seeded in 60 mm dishes one day before infection. Infection was performed as described in 2.2.2.1 using 1 ml diluted virus for a 1 hr infection period and adding 3 ml culture medium after washing twice with PBS. At selected time points cells were harvested by scraping and centrifuging the cell suspension (3000 rpm, 5 min). After discarding the supernatant the cell pellet was resuspended in at least 5 volumes of QIAGEN RNAprotect Cell Reagent. Total RNA (ttRNA) was isolated with the QIAGEN miRNeasy Mini kit and quality and quantity of the RNA were determined with the Agilent Bioanalyzer 2100 and Nanodrop (2.2.3.1.2).

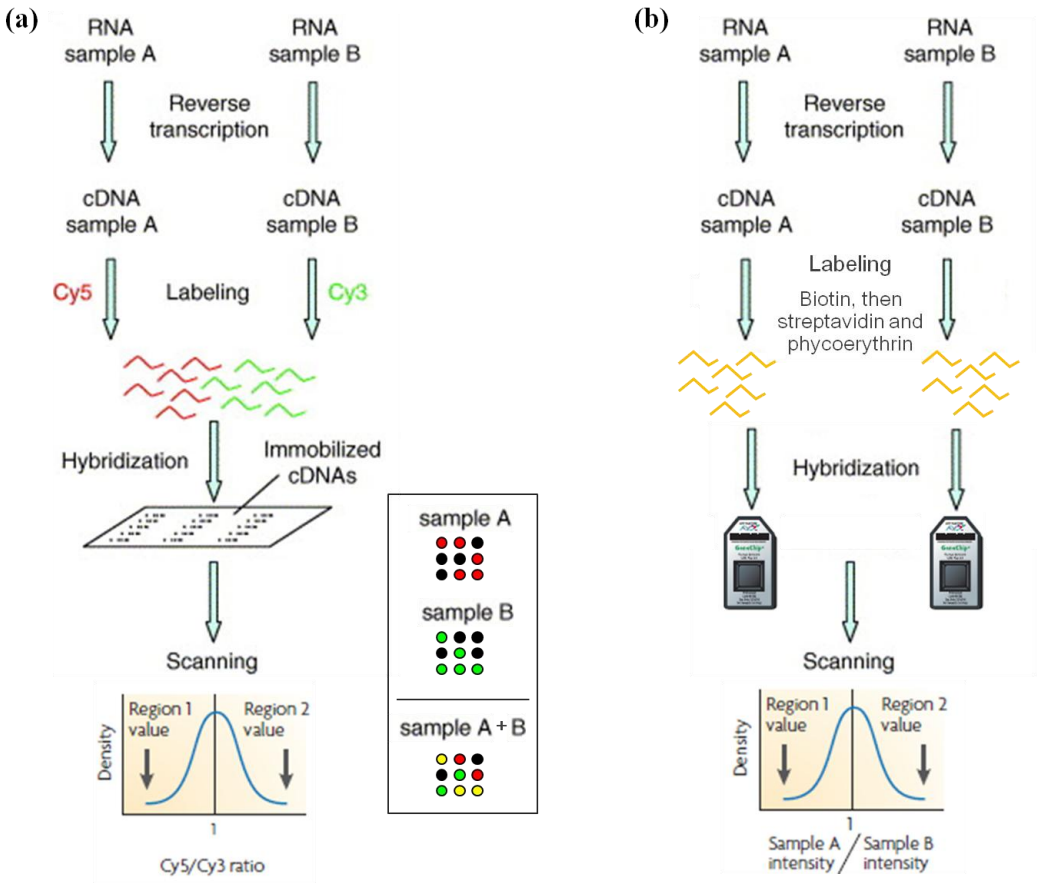

Figure 2-5: Outline of a two-color and one-color microarray experiment

(a) Two-color experiment: RNA of two samples (A and B) is converted into cDNA via reverse transcription, labeled with two fluorophores of different absorption/emission wavelength (i.e. Cy3 and Cy5) and hybridized to the immobilized cDNA probes on the array. The arrays are scanned and results indicated as ratio of the fluorescence intensities of both dyes. The example in the box shows an overexpression of genes from sample A in red, sample B in green, equal expression in A+B in yellow and lack of expression in black. (b) One-color experiment: cDNA is generated as described for (a), but labeling is performed with a single color and samples are hybridized separately to individual arrays. The output after scanning reflects single absolute value of hybridization (Figure modified from Ranz et al., 2006 [252] and Gresham *et al*., 2008 [253]).

2.2.3.1.2 RNA quality and quantity control evaluation

High quality, purity, and integrity of RNA are crucial for successful downstream applications such as microarray gene expression experiments. For this reason RNA integrity was assessed using the Agilent's Bioanalyzer 2100 or Caliper Life Sciences LabChip GX system, prior to running microarray experiments. Both systems analyze RNA integrity via electrophoretic separation and calculate a RNA Integrity Number (RIN, Agilent) or RNA Quality Score (RQS, Caliper Life Science) under consideration of the entire electropherogram. The RQS is defined by the following equation:

$$QS = A + \left(1 - \frac{FastRegion\ Area}{Total\ Area}\right) \times X_1 + \left(\frac{18S\ Area + 28S\ Area}{Total\ Area}\right) \times X_2 + \left(\frac{28S\ Height}{18S\ Height}\right) \times X_3$$

Modified from Caliper Life Sciences, Application Note 402 *A, X_1, X_2, and X_3 are constants

RIN and RQS are comparable with maximum deviation < 10% and are expressed on a scale from 1 for degraded RNA to 10 for fully intact RNA. Samples featuring a RIN/RQS ≥7 are considered high quality and appropriate for downstream microarray analysis [254]. RNA quality can further be estimated by looking at the shape of the two main peaks (ribosomal RNA, rRNA).

Further RNA concentration and purity can be quantified by Nanodrop spectrometer technology. The purity of a RNA sample is assessed by the absorbance ratios at 260 nm + 280 nm ($A_{260/280}$) and at 260 nm + 230 nm ($A_{260/230}$). RNA and other nucleic acids have their absorbance maximum at 260 nm. Protein, phenol, and other contaminants have absorbance at or near 280 nm, whereas carbohydrates and phenol (TRIzol/ QIAzol), and other aromatic compounds absorb near 230 nm. The $A_{260/280}$ and $A_{260/230}$ ratios give information about contamination of RNA samples by one or multiple of these compounds. RNA samples are considered "pure" with an $A_{260/280}$ ratio ≥ 2 and an $A_{260/230}$ ratio ≥ 2 to 2.2.

2.2.3.1.3 RNA amplification for microarray

a) RNA amplification for 36 k human array platform

In a PCR reaction amplified RNA (aRNA) was generated from ttRNA by first mixing 2 µg total RNA in 9 µl DEPC water with 1 µl (0.1-0.25 µg/ µl) oligo dT(15)-T7 primer, 1 µl of RNasin, denaturing by heating the mix to 70 °C for 3 min, and priming during the cool down process. At RT the following reagents were added for each reaction before incubation the reaction mix at 42 °C for 90 min in a thermo cycler:
4 µl 5 x First strand buffer, 1 µl (0.1- 0.5 µg/µl) TS oligo primer, 2 µl 0.1 M DTT, 2 µl 10 mM dNTP, and 1 µl Superscript II (200 U/µl). The second cDNA strand was synthesized by adding 108 µl of DEPC water, 15 µl Advantage PCR buffer, 3 µl 10 mM dNTP mix, 1 µl of RNase H (2 U/µl) and 3 µl Advantage cDNA Polymerase mix. The PCR reaction was divided in a 5 min mRNA digestion step (37 °C), a 2 min denaturing step (94 °C), a 1 min specific priming step (65 °C), and a 30 min extension step (75 °C). Enzyme reactions were terminated by adding 10 µl 0.5 M EDTA to the reaction. The ds cDNA was purified from non-incorporated dNTP, primers and inactivated enzymes by using Affymetrix GeneChip Sample Cleanup Module. Subsequently, the cDNA is transcribed into cRNA in an overnight *in vitro* transcription (IVT) at 37 °C. IVT-reaction-mix: 2 µl of each 75 mM NTP (A, G, C and UTP), 2 µl reaction buffer, 2 µl enzyme mix (RNase inhibitor and T7 phage RNA

polymerase), and 8 µl ds cDNA. The cRNA was cleaned-up by using Affymetrix GeneChip Sample Cleanup Module and RNA yield determined via Nanodrop.

In the second amplification cycle 1 µg of aRNA was diluted in 8 µl DEPC water and 1 µl (2 µg/µl) random hexamer (dN6) and the mix was heated to 70 °C for 3 min. After cooling the reaction down, the following reagents were added: 4 µl 5 x First strand buffer, 1 µl (0.5 µg/ µl) oligo dT-T7 primer, 2 µl 0.1 M DTT, 1 µl RNAsin, 2 µl 10 mM dNTP and 2 µl Superscript II (Reaction cycle : 42 °C, 90 min). During the second cycle, second cDNA strand synthesis and cDNA clean-up was performed in the same way as for the first cycle. The reagent volumes for the second cycle IVT were doubled compared to the first IVT. Finally the cRNA was purified by using Affymetrix GeneChip Sample Cleanup Module and RNA yield was determined via Nanodrop. The aRNA was either stored at -80 °C or used directly for labeling and hybridization.

b) RNA amplification for customized VACV array platform

For viral expression analysis on a customized Affymetrix platform, ttRNA was amplified into sense RNA by using the GeneChip® One-Cycle Target Labeling and Control kit (discontinued in 2010) or GeneChip® 3' IVT Express Kit according to the manufacturer's instructions.

2.2.3.1.4 Microarray performance

a) Microarray performance for 36 k human array platform

Array quality was documented as previously described [255]. As a reference for human arrays, peripheral blood mononuclear cells (PBMCs) from 4 normal donors were pooled. For hybridization of the 36 k human array, a two color system was applied. Both reference and sample aRNA were labeled directly with Cy3 and Cy5, respectively by using ULS aRNA Fluorescent Labeling kit.
Labeled sample and reference aRNA were pooled and following RNA fragmentation reagents were added. Co-hybridization was performed by first adding a blocking solution consisting of 1-2 µl poly d(A), 2 µl yeast tRNA, and 15 µl KREAblock buffer. The mixture was heated to 99 °C for 3 min for heat denaturation and then temporarily stored at 42 °C. Secondly, 2 x hybridization buffer was prepared as follows: 30 µl formamide, 12.5 µl SSC (20x), and 2 µl SDS (10%) were mixed and pre-warmed at 42 °C for at least 5 min. Afterwards, the hybridization buffer was mixed with the sample/ blocking buffer solution and 67 µl applied to the array slides. Then, the array slides were incubated for 20 hrs in a 42 °C water bath followed by washing steps and finally slides were scanned via an Agilent scanner.

b) Microarray performance for customized VACV array platform

VACV gene expression was analyzed using a customized VACV array platform (VACGLa520445F, Affymetrix, CA) with 308 probes representing 219 genes. Those genes cover the genome of GLV-1h68, including the *Renilla* luciferase-*Aequorea* green fluorescent protein fusion gene, *E.coli* beta-glucuronidase, and 337 human or mouse "housekeeping" genes (393 probes) [102]. Fragmented, labeled aRNA (6.5 µg) was hybridized to the VACV array platforms. After 16 hrs incubation in the hybridization oven at 45 °C, the arrays were washed and stained in the Fluidics station using the GeneChip® Hybridization, Wash, and Stain Kit (Affymetrix). Finally, the arrays were scanned using the GeneChip® Scanner 3000 7G (Affymetrix).

2.2.3.2 MicroRNA array

MicroRNAs (miRNAs) are short non-coding RNA molecules which function in translational regulation within eukaryotic cells. The miRNA's mechanism of action is based on complementary imperfect base pairing with sequences in the 3'untranslated region (UTR) of target mRNAs, thereby repressing their expression [256, 257]. Human miRNA arrays are used to generate complete miRNA expression profiles which provide information about expression regulation between different samples. Total RNA (ttRNA) was isolated by using the QIAGEN miRNeasy Mini kit and quality and quantity of the RNA were determined with the Agilent Bioanalyzer 2100 and Nanodrop. For miRNA labeling the EXIQON miRCURY LNA™ microRNA Array, power labeling kit was utilized according to the manufacturer's instructions. In the first step a CIP (Calf Intestinal Alkaline Phosphatase)-based system was used for removal of 5'-phosphates from miRNA termini. In the second step, miRNAs in the ttRNA sample and the reference (EBV-immortalized 1558 melanoma cell line) were labeled with fluorescent dyes Hy5 and Hy3, respectively. Before hybridization, sample miRNA and reference miRNA are mixed in a 1:1 volume ratio and mixed with hybridization (hyb) buffer (3 µl 50x Denhardt's blocking solution, 3 µl yeast tRNA, 30 µl human Cot I DNA (1 mg/ml), 10 µl 20x SSC, 3 µl 10% SDS, and 33 µl water). The mix was heated at 70 °C for 3 min, spun down at 14,000 x g for 1 min, and dispensed onto the gasket slide well immediately after. The in-house manufactured miRNA slides representing probes of 827 unique miRNAs from human, mouse, rat, and virus were placed onto the gasket slide. The hyb chamber was loaded into the hyb oven at 42 °C and 20 rpm rotation overnight followed by washing steps and scanning via Genepix 4000 B microarray scanner.

2.2.3.3 Array comparative genomic hybridization (CGH)

Array comparative genomic hybridization (aCGH) is a technique that allows a high-resolution screening of the genome for segmental DNA copy number variations. This technique finds application in obtaining a global understanding of cancer and the role of genetic aberrations such as amplifications and deletions in cancer development and diagnosis.

Genomic DNA from human advanced melanoma cell lines (15-MEL) and from PBMCs of a healthy female donor was isolated with help of the QIAamp® DNA Mini Kit. Starting material were 1.5 µg genomic DNA of sample and reference. DNA was fragmented, labeled, purified, and hybridized to Agilent 2 × 105 K arrays according to the Agilent Oligonucleotide Array-Based CGH for Genomic DNA Analysis (version 6.2.1). Washing and scanning was assessed via Agilent Scanner immediately after hybridization. Data was extracted using Agilent's Feature Extraction Software.

2.2.3.4 Flow cytometry

Flow cytometry is a technology which enables to count, examine, and sort cells or other single particles in suspension. Physical and biological characteristics of single cells such as size, granularity as well as expression of intracellular and cell surface proteins can be evaluated simultaneously by their light scatter and fluorescence properties. In general, a precisely defined fluid stream of single cells gets hit by a laser beam. Consequently, the cell deflects the incident laser light and emits fluorescence which is detected and recorded through an optoelectronic system. The light scatters in both forward and side direction. The former is detected by a lens called forward scatter channel (FSC) and gives information about particle size whereas the latter hits a side scatter channel (SSC) which in turn provides information about granularity. FSC and SSC generate electronic signals proportional to the optical signals striking them.

Besides the physical properties of a cell, information can be obtained about cell surface markers, cell death, protein expression, intracellular molecules etc. via fluorochrome-labeled antibodies or internal fluorescence (expression of fluorescent proteins). Optical filters allow the detection of the emitted fluorescence of a compound in a wavelength-specific manner. The amount of fluorescent signal detected is proportional to the number of fluorochrome-labeled molecules on a cell. Flow cytometry can not only be used for molecular biological but also for clinical applications.

2.2.3.2.1 Sample preparation for flow cytometric analysis

The cell lines to be investigated were infected as described in 2.2.2.4. After stopping the infection and harvesting the cells, the suspension was transferred into FACS tubes. Subsequently, cells were fixed by adding 500 µl PFA (16%) to the suspension which equates to one fourth of the total volume, followed by vortexing and incubation for 15 min at RT. After fixation the PFA was removed from the suspension by repeating the following washing step twice:
Centrifugation at 1400 rpm 5 min (RT), discarding supernatant by carefully inverting the tube, gently dissolving the pellet in back-flow drop, adding 1 ml of autorinse. After two cycles the suspension was centrifuged once more at 1400 rpm for 5 min, the supernatant discarded, and the pellet dissolved. Subsequently, 300 µl autorinse were added and the tubes covered with a lid and aluminum foil. Samples were stored at 4 °C until analysis with the flow cytometer.

2.2.3.2.2 Analysis of flow cytometry data

For flow cytometric analysis, cells were uniformly suspended into single-cell suspensions at a density of 1 million cells/ ml PBS and passed through a MoFlo Astrios cell sorter. GFP, RFP, and mNeptune were excited using lasers tuned to 488 nm, 532 nm, and 640 nm with their emission detected using bandpass filters set at 513/26, 576/21, and 671/30 nm, respectively. Spectral overlap among the fluorescence signals was digitally compensated using appropriate single color control samples. Flow cytometry raw data was analyzed using Kaluza software.

2.2.4 Statistical methods

Human array transcriptional data were uploaded to the mAdb databank (http://nciarray.nci.nih.gov) and analyzed using BRBArrayTools developed by the Biometric Research Branch, National Cancer Institute (http://linus.nci.nih.gov/BRB-ArrayTools.html) [248] or Partek Genomics Suite software (St Louis, MO) as appropriate. VACV transcription was analyzed using Partek Genomics Suite software.
Data established from human in-house arrays was processed with BRBArrayTools including a quality-control for imperfect spots (Spot filter), normalization via median log-ratio subtraction, and specification of the maximum intensity ratio plus the truncation of larger intensities ratios to this maximum. Unsupervised human data analysis was performed using the Stanford Cluster program and results were visualized with TreeView software [249] or Partek Genomic Suite software as appropriate. Adequate filtering was applied to the sample-set to secure presence of gene expression values in 80% to 100% of the samples according to downstream applications. Gene ratios were mean

centered across all samples and displayed according to uncentered correlation algorithm and a complete linkage model. Time dependent changes in human transcriptional patterns by different cell lines where identified by determination of time dependent variances across non-infected samples. Time independent changes in human transcripts related to viral infection were identified by weighting variance in the infected sample as described in the results section (3.1.1.2.1).
Data retrieved from Affymetrix platforms was normalized using a Robust Multichip Average (RMA) approach. Class comparison between groups of arrays was assessed with analysis of variances (ANOVA). P-value cut-offs were applied as appropriate with 5%, 1%, or 0.5% confidence intervals. Correlation among different transcriptional parameters within the same or across platforms (human or VACV) were done according to Pearson's correlation analysis.

Copy Number Analysis was performed according to the, from Partek Genomic Suite suggested, parameters. Copy number variations were measured via two-color system comparing melanoma cell lines to healthy diploid reference genomic DNA. Data was expressed as sample to reference intensity log2 ratios. Amplifications were defined as segments with log2 ratios greater than 0.15 and deletions as segments with log2 ratios less than -0.3. Regions with significant differences were determined using the Segmentation Model algorithm of the Partek Genomic Suite to detect copy number states. Segments were defined as regions that differed from neighboring regions by at least 2 signal-to-noise ratios (SNRs) in at least 10 markers. Regions identified were annotated with gene symbols through import of the annotation file from the NCBI RefSeq genome browser (build *Hg19*).

Viral titers obtained from plaque assay analyses were expressed as mean (n=3) ± SD (standard deviation) and compared via parametric unpaired student's *t*-test.

3 Results

3.1 Correlates between host and viral transcriptional program associated with different oncolytic vaccinia virus isolates

[*The majority of the results in part 3.1 have been published in the research article "Reinboth et al., Correlates between host and viral transcriptional program associated with different oncolytic vaccinia virus isolates, Hum Gene Ther Methods, Oct 2012"* [258]]

In this study, we investigated how interactions between VACV and host contribute to the permissiveness of a host cell to infection. It was shown previously that the kinetics of *in vitro* viral replication correlates with *in vivo* oncolytic function [101]. Therefore, in this study we investigated events related to VACV infection to identify host genes that might predict and/or influence viral replication and indicate permissiveness of cancer cells to VACV infection. Therefore, we analyzed *in vitro* transcription of distinct viral preparations to identify potential markers of permissiveness.

Two previously characterized autologous cell lines (888-MEL and 1936-MEL) derived from a single patient with metastatic cutaneous melanoma [50, 51], were tested for permissiveness to the attenuated VACV GLV-1h68 strain and 3 wild-type (wt) VACV isolates: LIVP 1.1.1, LIVP 5.1.1, or LIVP 6.1.1. 888-MEL were established from a tumor resection in 1989 when the cancer was still responsive to immunotherapy with interleukin-2 and tumor-infiltrating lymphocytes. More than a decade later after several recurrences, 1936-MEL was generated from subsequent metastases when the cancer had become unresponsive to immunotherapy [51].

3.1.1 VACV-dependent changes in host cell transcription over time

3.1.1.1 VACV-caused effects on human gene expression over time

In an initial time course experiment host gene expression of the two melanoma cell lines was analyzed after infection with the attenuated VACV GLV-1h68 and the wt isolate LIVP 1.1.1. Five time points were chosen (2, 6, 10, 24, and 48 hpi) to cover early, intermediate, and late events after VACV infection and to obtain an overview about the significance of specific time points in terms of virus-host interaction. Further it was of interest to see whether the attenuated and the wt virus show

different impact on the host gene expression. Therefore 888-MEL and 1936-MEL were infected with GLV-1h68 and LIVP 1.1.1 at an MOI of 0.01. RNA from infected and non-infected cells was isolated at 2, 6, 10, 24, and 48 hpi and RNA quality and integrity assessed as described in. All RNA samples showed high purity and integrity with an average 260/280 ratio of 2.16, an average 260/230 ratio of 2.11 and a mean RQS of 7.8. Following, total RNA was amplified, purified, labeled, and hybridized to human probe arrays. Host gene expression was evaluated with help of 36 k human microarray platforms and subsequent data analysis via BRB ArrayTools, cluster 3.0 and tree view software (Figure 3-1). Gene functions and pathways were analyzed via IPA software.

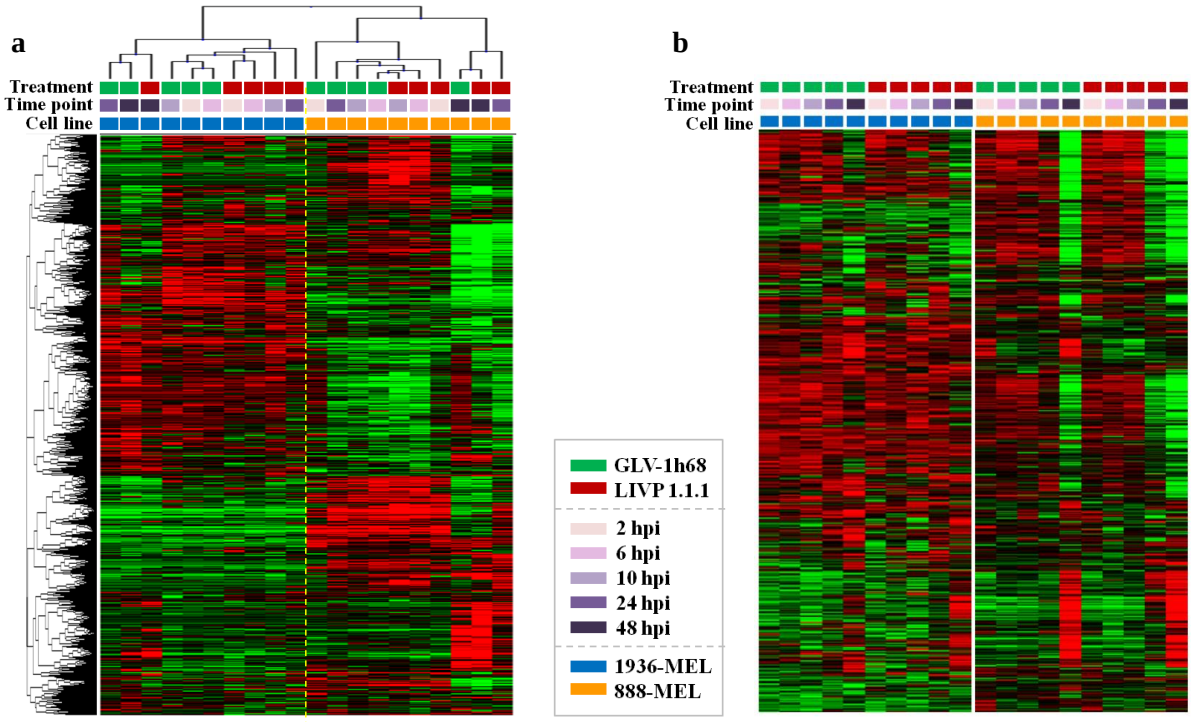

Figure 3-1: Time course of human gene expression following GLV-1h68 and LIVP 1.1.1 infection

Time course expression profile of 888-MEL and 1936-MEL cells after infection with GLV-1h68 or LIVP 1.1.1 (MOI 0.01) on a 36 k human array platform. (a) Heatmap is based on unsupervised clustering of 11,055 genes that passed the filtering criteria (80% presence call across the experimental set, ≥ 2-fold). Gene expression data was normalized across the entire array, genes mean-centered followed by hierarchical clustering (complete linkage). (b) Following normalization, experiments were ordered according to time point and cell line. Expression values were mean-centered separately for each cell line. Heatmap is based on unsupervised gene clustering of 4,241 genes that passed the filtering criteria (95% presence call across the experimental set, ≥ 2-fold).

The transcriptional profile of 888-MEL and 1936-MEL after VACV infection showed an expected clear separation of the two cell lines in discrete array clusters due to the individual nature of each cell line (Figure 3-1 a). Furthermore a separation of the late time point samples, especially 48 hpi, from the early ones could be observed. Sorting the samples according to cell line and time point and separate mean centering of genes per cell line revealed that at 48 hpi the transcriptional profile was

dramatically altered (up or down-regulated) when compared to earlier time points. These late effects were present independent of cell line or virus strain utilized, but were more prominent in 888-MEL. Additionally, we observed that effects caused by VACV infection occur earlier when using wt isolates compared to GLV-1h68 (Figure 3-1 b).

3.1.1.2 Infected and uninfected samples segregate together according to time in culture

To further investigate virus-induced host transcriptional patterns we included two additional wt VACV isolates (LIVP 5.1.1 and LIVP 6.1.1) besides wt LIVP 1.1.1 and attenuated GLV-1h68. At the same time we also investigated the expression profile of time point-specific uninfected control samples. Based on the results obtained before (3.1.1.1) the time points 2, 10, and 48 hpi featured the clearest spectrum of time course-specific expressional variances. For this reason subsequent microarray experiments were based on these three time points. 888-MEL and 1936-MEL were infected with GLV-1h68, LIVP 1.1.1, LIVP 5.1.1, and LIVP 6.1.1 at an MOI of 0.01 or mock-infected with infection medium. RNA isolation, quality, and integrity assessment as well as microarray performance was carried out as described above.

Using the human array platform, we first investigated the culture-dependent kinetic changes in transcription, independent of infection (control samples). Unsupervised clustering segregated infected and respective uninfected samples together according to time in culture suggesting that this parameter dominated the global transcriptional profile (Figure 3-2). This variation resulted in a lack of segregation between infected and uninfected samples as indicated with red asterisks in Figure 3-2. In each cell line a distinct cluster separately from all other samples was only observed for all infected 48 hpi samples.

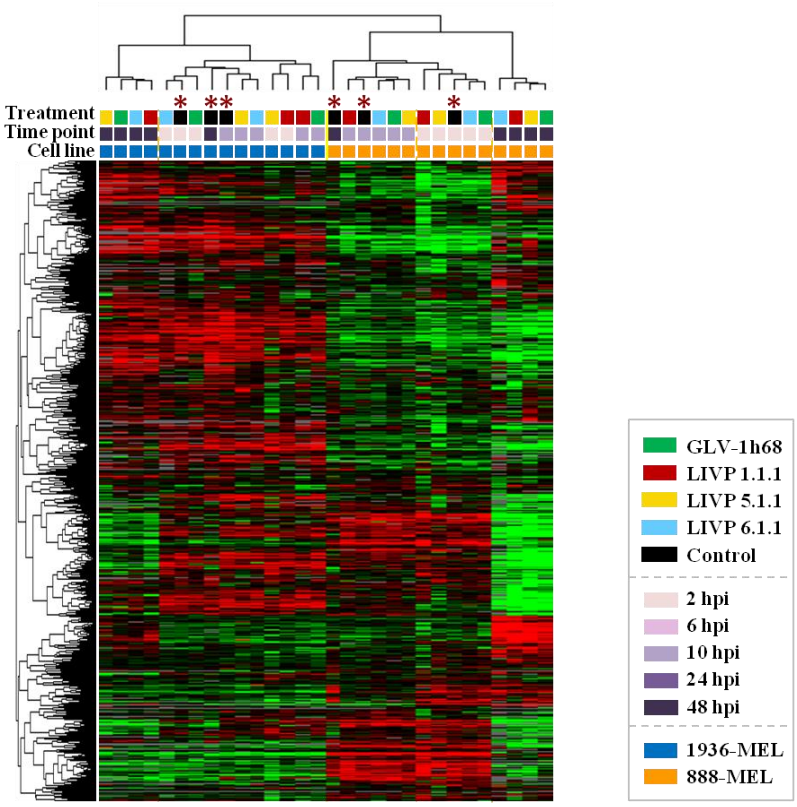

Figure 3-2: Transcription profile of infected and uninfected 888-MEL and 1936-MEL cells at 2, 10, and 48 hpi
Transcription profile of uninfected and infected (MOI 0.01: GLV-1h68, LIVP 1.1.1, LIVP 5.1.1, and LIVP 6.1.1) 888-MEL and 1936-MEL cells on a 36 k human array platform. Heatmap is based on unsupervised clustering of 4,238 genes that passed the filtering criteria (95% presence call across the experimental set, ≥ 2-fold). Gene expression data was normalized across the entire array, genes mean-centered followed by hierarchical clustering (complete linkage). Dark red asterisks = control samples.

3.1.1.2.1 A multistep filter reveals transcriptional changes specific to VACV infection

To eliminate the dominant effect of time in culture and to highlight the transcriptional changes specific to VACV infection, we applied a multistep filter (Figure 3-3 a).

First, the standard deviation (SD) was calculated for each gene in uninfected samples (2, 10, and 48 hpi) considering the whole unfiltered data set. The analysis was performed separately for each cell line assuming cell-specific variation in gene expression during culture. A cut-off SD >0.25 was used which identified 8,300 genes stably expressed by uninfected samples. This set of genes was applied to re-cluster infected and uninfected samples. The results still did not segregate uninfected from infected samples. Thus, we applied a second filter to include only transcripts with high SD in the infected samples, therefore, eliminating transcripts stably expressed by both infected and uninfected cells. To identify a maximum number of infection-specific genes for each cell line, the SD cut-off was determined separately for each of them by a stepwise increase (intervals of 0.05) starting from a value

of 0.3 and re-clustering samples until uninfected samples built a separate cluster resulting in a SD > 0.4 and > 0.7 for 1936-MEL (Figure 3-3 b) and 888-MEL (Figure 3-3 c) respectively. In the end, 480 infection-specific genes were identified for 1936-MEL and 507 genes for 888-MEL.

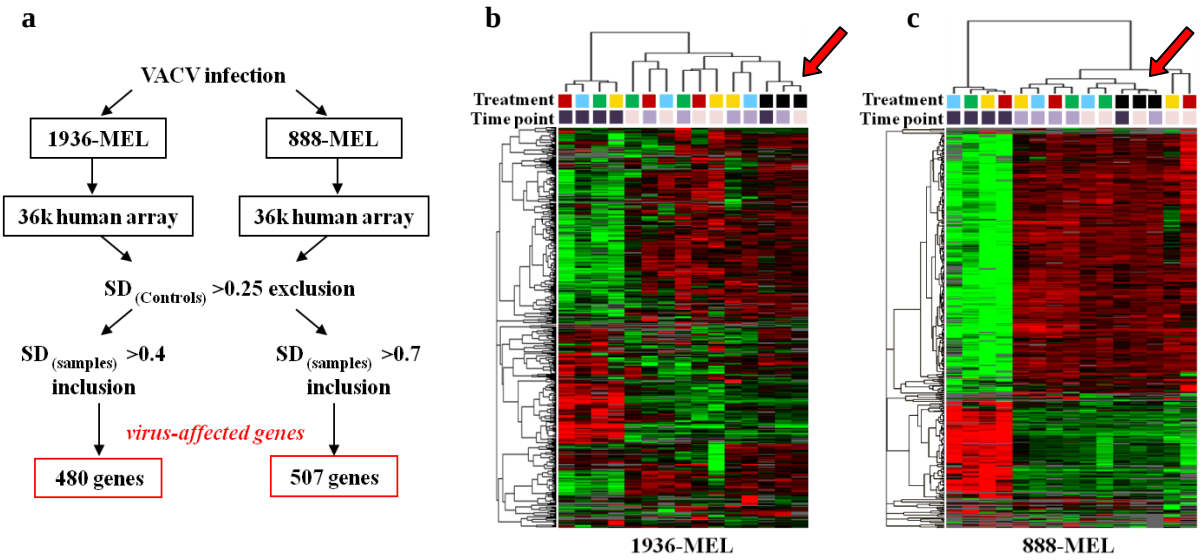

Figure 3-3: Multistep filter identified infection-specific genes for 1936-MEL and 888-MEL

(a) Flow chart of multistep filter. SD was calculated for each gene in uninfected samples (2, 10, and 48 hpi), separately for 888-MEL and 1936-MEL (cut-off SD > 0.25). Secondly, only genes with increased SD in infected samples (SD > 0.7 and > 0.4 for 888-MEL and 1936-MEL, respectively) were included. Heatmap of (b) 480 infection-specific genes in 1936-MEL and (c) 507 infection-specific genes in 888-MEL. Control samples formed a separate cluster from infected samples (red arrow).

Comparison of transcriptional patterns at 2 and 10 hpi between the two cell lines revealed a clearer clustering according to time in 888-MEL and a less consistent pattern in 1936-MEL consistent with a less predictable responsiveness of this cell line to VACV infection in functional assays.

3.1.1.3 VACV effects on human gene transcription

With the resulting gene pool, we investigated VACV effects on human gene transcription on the two autologous cell lines. The transcriptional profile at 48 hpi showed a dramatic alteration in gene expression with more prominent fraction of genes being down- than up-regulated (Figure 3-3 b, c). Ingenuity pathway analysis (IPA) revealed that these genes are involved in broad cellular functions such as cell death, cellular growth and proliferation, protein synthesis and folding, and DNA replication, recombination and repair (Figure 3-4).

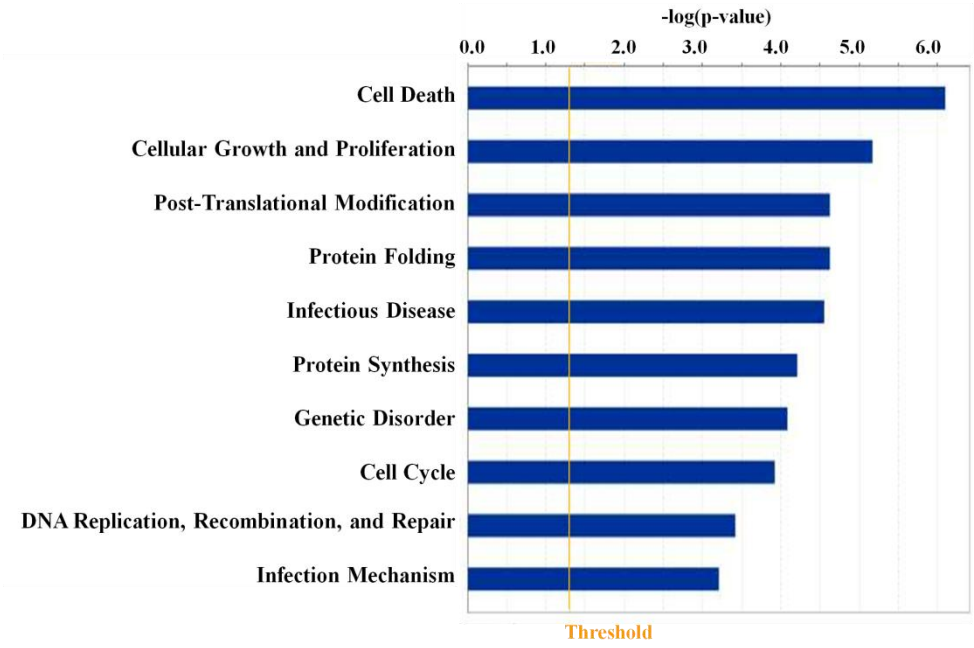

Top Networks

Associated Network functions

RNA Post-Transcriptional Modification, DNA Replication, Recombination, and Repair, Cellular Assembly and Organization
DNA Replication, Recombination, and Repair, Energy Production, Nucleic Acid Metabolism
Cellular Function and Maintenance, Genetic Disorder
Gene Expression, Protein Synthesis, Cell Cycle, Post-Translational Modification

Figure 3-4: Host canonical pathways and networks 48 hours post VACV infection

888-MEL and 1936-MEL cells were infected with 4 different VACV isolates at an MOI of 0.01 (GLV-1h68, LIVP 1.1.1, LIVP 5.1.1, and LIVP 6.1.1). Transcriptional profiles were generated via 36 k human array platforms. Virus-affected host genes were identified via a multistep filter (SD exclusion/ inclusion). Canonical pathways and top networks were identified by Ingenuity Pathway Analysis (IPA).

3.1.2 Vaccinia virus - dependent changes in viral gene transcription

Next, we were interested in characterizing the respective time point-specific viral transcriptional patterns of the different VACV isolates by using a custom-made VACV probe array platform (VACGLa520445F, Affymetrix). Based on the results obtained from the human gene expression studies, we concluded that 2 and 10 hpi are the most informative time points to investigate initial events at an early stage of infection since the drastic up or down-regulation of genes after 48 hours could conceal import slight expressional alterations. The same total RNA obtained from 888-MEL and 1936-MEL after infection with the different VACV isolates, which was utilized for human gene expression experiments, was now used as starting material for analyzing the respective VACV gene

expression. This allowed us to analyze viral and host gene expression simultaneously. The total RNA was amplified, purified, labeled, and hybridized to customized VACV array platforms. Data analysis and data visualization of the one-color VACV arrays was performed with help of Partek Genomics Suite and gene functions and pathways evaluated via IPA.

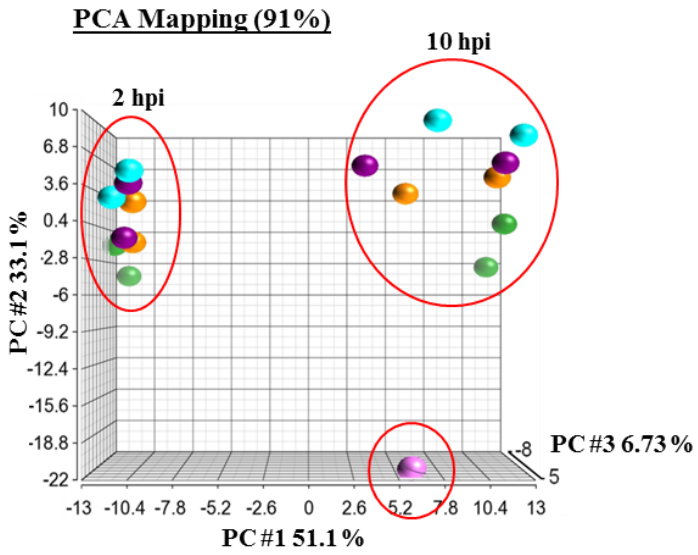

Figure 3-5: Principal components analysis (PCA) of the VACV microarray data

888-MEL and 1936-MEL cells were infected with 4 different VACV isolates (GLV-1h68, LIVP 1.1.1, LIVP 5.1.1, and LIVP 6.1.1) in separate experiments (MOI 0.01) or were treated with virus-free infection medium as negative control. Total RNA was isolated, amplified, purified, and labeled before generating transcriptional profiles via custom-made VACV array platforms. Infection period (2 or 10 hpi) and infectional status appeared to be the major source of variation, as indicated by red ellipsoids. The different colors specify the VACV isolate utilized. Green = GLV-1h68; Purple = LIVP 1.1.1; Yellow = LIVP 5.1.1; Light blue = LIVP 6.1.1; Pink = untreated controls.

During the scanning part of the microarray performance distinct data files were generated and the so-called CEL-files uploaded into Partek Genomics Suite. To investigate the main sources of variation regarding gene expression patterns of the different samples a principle component analysis (PCA) was performed. PCA is a statistical technique for finding patterns in high dimensional data sets. In Figure 3-5 a clear separation between samples taken at 2 hpi and 10 hpi and uninfected samples was evident demonstrating that the infection period as well as the infectional status acts as the major source of variation, emphasized by red ellipsoids.

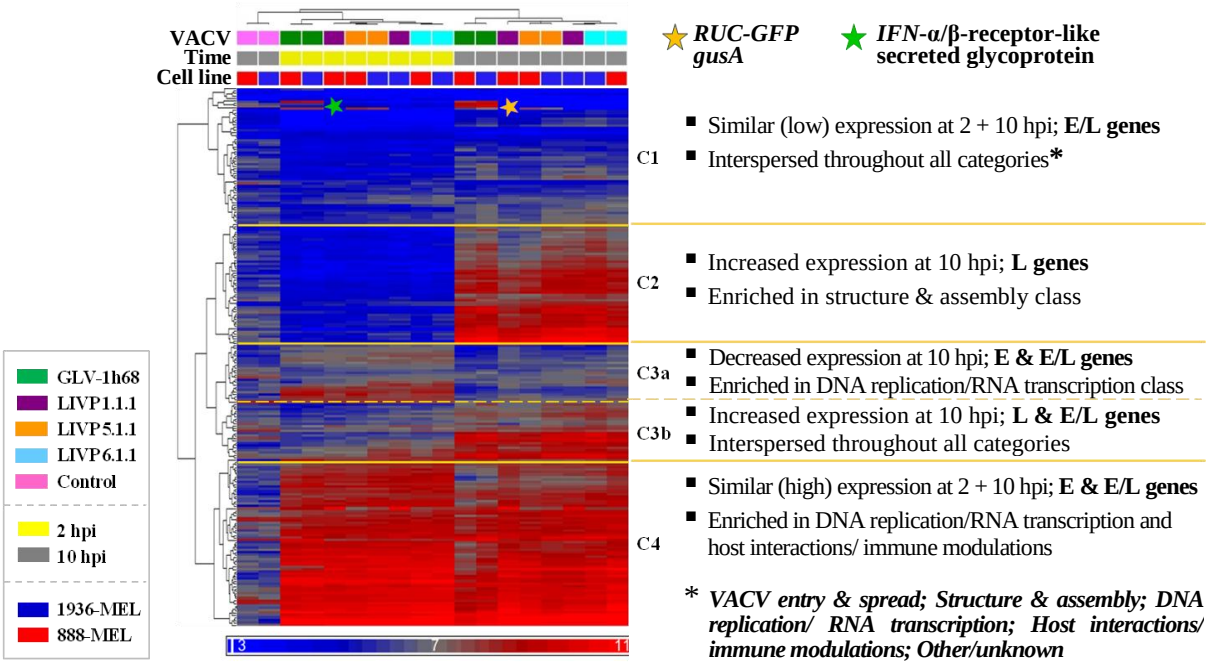

Figure 3-6: VACV-isolate-specific changes in gene transcription over time

888-MEL and 1936-MEL cells were infected with the VACV isolates GLV-1h68, LIVP 1.1.1, LIVP 5.1.1, and LIVP 6.1.1 in separate experiments (MOI 0.01) or were treated with virus-free infection medium as negative control. Total RNA was isolated, amplified, purified, and labeled before generating transcriptional profiles via custom-made VACV array platforms. Transcription profile incl. sub-cluster classification of 4 VACV isolates (2 and 10 hpi) and negative control (10 hrs). Yellow asterisk: *RUC-GFP* = *Renilla* luciferase - green fluorescent protein *(Aequorea)* fusion; green asterisk: *gus A* = β-glucuronidase. C1, C2, C3a, C3b, C4 = Cluster 1, 2, 3a, 3b, 4.

In a next step we analyzed transcriptional patterns via hierarchical clustering of all samples and genes. The 219 VACV genes represented in the VACV platform segregated in 3 array clusters and 4 main gene clusters C1, C2, C3a/3b, and C4 (Figure 3-6). VACV-infected arrays clustered according to time elapsed, following VACV infection while the uninfected arrays segregated separately. Cluster formation confirmed the distinct separation between samples taken at 2 or 10 hpi as demonstrated before via PCA (Figure 3-5). GLV-1h68 contains 3 marker gene insertions (*RUC-GFP*: *Renilla* luciferase - green fluorescent protein (*Aequorea*) fusion, *lacZ*: β-galactosidase and *gus A*: β-glucuronidase cDNA) two of which are present in the VACV chip (*RUC-GFP*, *gusA*). At 10 hpi both genes were expressed at high levels in cell line preparations infected with GLV-1h68 (Figure 3-6, yellow asterisk). Additionally, the viral IFN-α/β-receptor-like secreted glycoprotein (*B19R*, VACV Copenhagen) which is not present in full length in the genome of the wt clones was expressed exclusively by GLV-1h68 (Figure 3-6, green asterisk).

The four gene clusters revealed a transcriptional pattern representative of the three promoter classes of VACV (early, early-late, and late). Moreover, we subdivided the ORF products in five functional categories: VACV entry and spread, VACV structure and assembly, VACV DNA replication and

RNA transcription, host interactions and immune modulations, and a final category representing genes with other or unknown functions. Genes present in cluster C1 showed similar low expression levels at 2 and 10 hpi and included all functional categories. The only exceptions were the 2 marker genes *RUC-GFP* and *gusA*, *B11R* with unknown function and *B19R*, mentioned above. We found an enrichment of late genes in cluster C2 consistent with highly increased transcriptional levels at 10 hpi. Functional annotations revealed that these genes encode predominantly structural components and enzymes involved in assembly of viral particles. Cluster C3a was enriched of early transcripts. Expectedly, proteins encoded by genes present in C3a regulate DNA replication and RNA transcription. An enrichment of early-late and late genes was found in cluster C3b. The expressional pattern revealed notable expression at 2 hpi but this was more pronounced at the later time point. C3a and C3b emerged as the clusters with the most heterogeneity among cell line preparations infected with different VACV constructs. Finally, cluster C4 represented early-late transcription with consistently high expression values especially at 2 hours. These genes mainly encode proteins involved in modulation of the host immune response.

3.1.3 Vaccinia virus isolate-specific changes in transcription and correlation with viral replication

3.1.3.1 Viral replication analysis

We previously observed that the kinetics of *in vitro* viral replication correlates with *in vivo* oncolytic function [101]. For this reason we determined viral replication efficiency over time for all 4 isolates (GLV-h68, LIVP 1.1.1, LIVP 5.1.1 and LIVP 6.1.1) by time course plaque assay analyses.
888-MEL and 1936-MEL cells were infected at an MOI of 0.01 and harvested at 2, 6, 10, 24, and 48 hpi. Viral titers were determined in triplicate by standard plaque assays on CV-1 cell monolayers.

3.1.3.1.1 VACV replication efficiency of GLV-1h68 and wt isolates

To further characterize the different VACV wt isolates, we performed a time course analysis determining viral titers over time and comparing those with the well-characterized GLV-1h68 strain [102]. Using plaque assay analysis, we observed that all LIVP clones analyzed replicated more efficiently compared to GLV-1h68 especially at later time points (Figure 3-7 a).

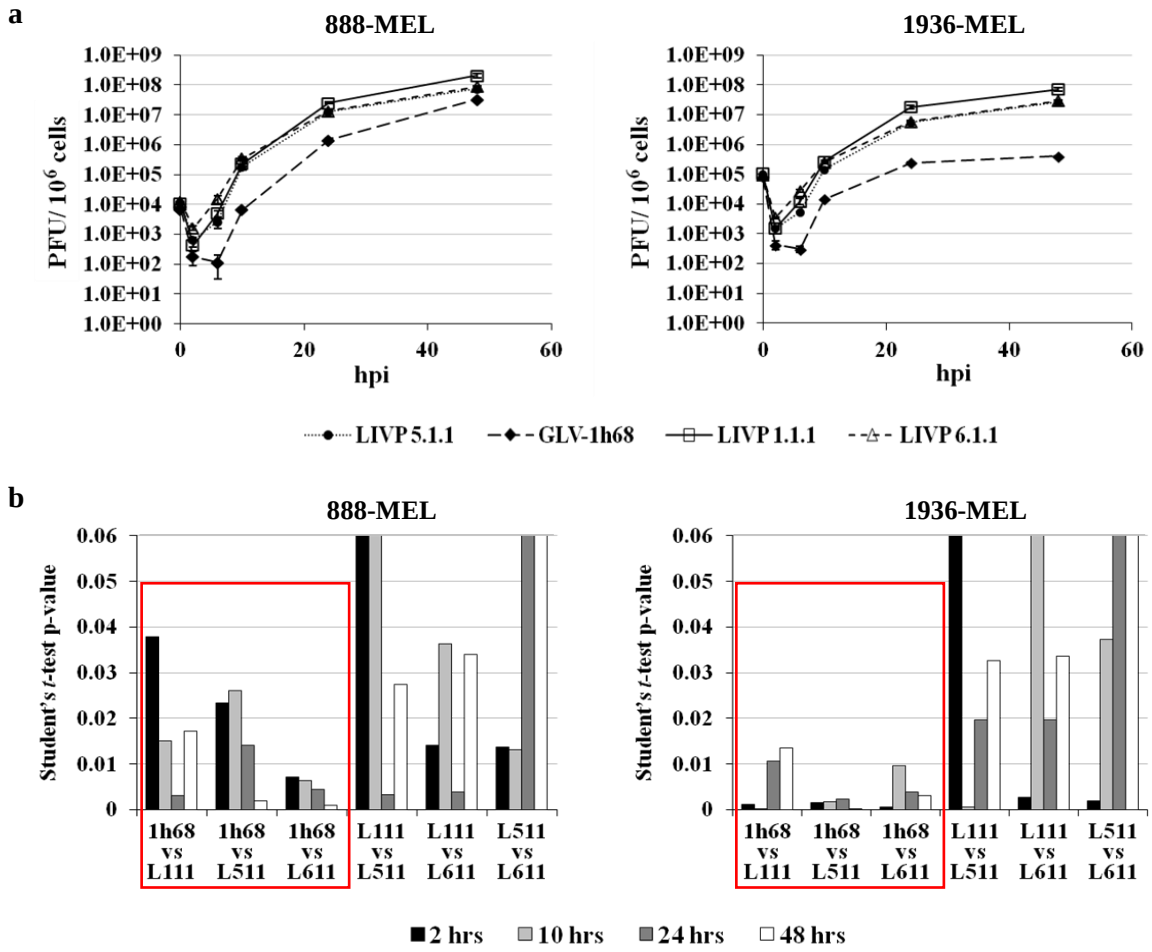

Figure 3-7: Replication characteristics of GLV-1h68 and wt VACV isolates in 888 and 1936-MEL

Viral titers in 888-MEL (a, left panel) and 1936-MEL cells (a, right panel) 2, 6, 10, 24, and 48 hrs post GLV-1h68, LIVP 1.1.1, LIVP 5.1.1, or LIVP 6.1.1 infection (MOI 0.01) determined via plaque assay. (b) Student's *t*-test comparing replication efficiencies of all virus isolates with each other. Average titers and standard deviations (SD) were determined from triplicates (n = 3). Red boxes = GLV-1h68 vs. wt VACV isolates.

At 2 hpi the viruses ranked according to their replication from lowest to highest titer as follows: GLV-1h68, LIVP 5.1.1/LIVP 1.1.1, and LIVP 6.1.1. The ranking was consistent for both melanoma cell lines. With progression of the infection, the number of plaque forming units became closer among all LIVP isolates with a widening gap compared to GLV-1h68. The differences between the viral titers obtained by infection with the different VACV isolates were emphasized with a Student's *t*-test. Comparisons between the titers of attenuated GLV-1h68 virus and the ones obtained with the different wt isolates were statistically significant ($p \leq 0.05$) at all time points and independent of the cell line utilized (Figure 3-7 b, red boxes).

3.1.3.1.2 The role of multiplicity of infection for virus effects

Of particular interest was also the replication behavior when synchronizing the infection by using a high multiplicity of infection (MOI). Therefore 888-MEL were infected with the 4 different VACV isolates (GLV-h68, LIVP 1.1.1, LIVP 5.1.1, and LIVP 6.1.1) at an MOI of 10 and harvested at 2, 6, 10, 24, and 48 hpi. Viral titers were determined by standard plaque assays on CV-1 cell monolayers.

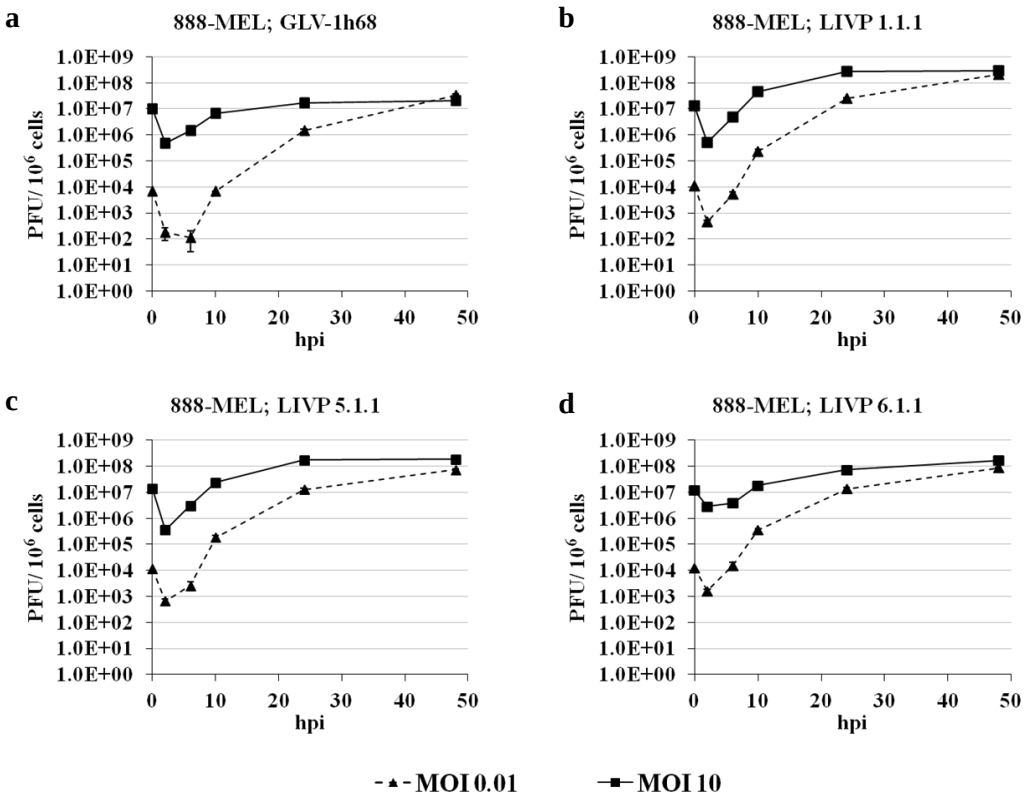

Figure 3-8: Replication progression of different VACV isolates in 888-MEL at low (0.01) and high (10) MOI
Viral titers in 888-MEL 2, 6, 10, 24 and 48 hrs post GLV-h68 (a), LIVP 1.1.1 (b), LIVP 5.1.1 (c) or LIVP 6.1.1 (d) infection at MOI 0.01 (dashed line) and MOI 10 (continuous line) determined by plaque assay. MOI = multiplicity of infection.

Expectedly, infection with a high MOI (10) led to an early saturation of the host cells with virus particles (Figure 3-8). However, the maximum titers were comparable to the ones observed after infection at an MOI of 0.01, but achieved earlier when applying the higher viral dose independent of the VACV isolate utilized (Figure 3-8 a-d). The results demonstrate that a low MOI appears to be more suitable to analyze progression of viral replication and for correlation with possible gene expressional changes.

3.1.3.2 Ranking of VACV gene transcription level and correlation with replication

We showed recently that GFP marker gene expression of GLV-1h68 correlates with the respective viral copy number in A375, DU-145, and A549 cells indicating that viral gene expression can be evaluated as a parameter representative of viral replication [246]. Based on that, we wanted to investigate whether the same was true when comparing GLV-1h68 and the wt VACV isolates.

As mentioned before, at early time points after infection the viruses ranked according to their replication efficiency from lowest to highest titer as follows: GLV-1h68, LIVP 5.1.1/LIVP 1.1.1, and LIVP 6.1.1. To compare viral transcription with replication according to plaque forming units, we ranked viral isolates according to their overall transcriptional activity. Within each gene cluster category (Figure 3-9 a, enlarged image: Figure 3-6), we averaged the intensity values of all genes for each virus at each time point. Averaged VACV gene expression was ranked from lowest to highest for each virus. The sub-clusters C3a and C3b were considered separately and in combination as representative of early gene transcription (2 hpi). The sub-clusters C2, C3b, C4, C2/C3b, and C2/C3b/C4 were analyzed to assess late gene expression (10 hpi).

3.1.3.2.1 VACV isolate-specific changes in transcription at 2 hpi

We focused subsequent analyses on gene sub-clusters revealing the most pronounced differences among LIVP 1.1.1, LIVP 5.1.1, LIVP 6.1.1, and GLV-1h68 at 2 hpi. At this time point GLV-1h68 displayed the lowest mean levels of gene transcription in all sub-clusters analyzed, whereas LIVP 6.1.1 showed the highest values at 2 hpi independent of cell line tested (Figure 3-9 b). LIVP 5.1.1 and LIVP 1.1.1 displayed comparable intermediate transcription levels and were, therefore, ranked together (rank 1 = LIVP 6.1.1, rank 2 = LIVP 5.1.1 and LIVP 1.1.1, and rank 3 = GLV-1h68). As mentioned above cluster C3a was enriched of early transcripts. Although, cluster C4 also reflects high early expression levels, there were no clear differences among VACV isolates at 2 hpi. Based on the equal gene expression of all VACV isolates in cluster C4 at 2 hpi, this cluster appeared to be ineligible to point out differences between the viruses. For this reason, gene cluster C3a emerged as the most representative sub-cluster to study VACV at 2 hpi.

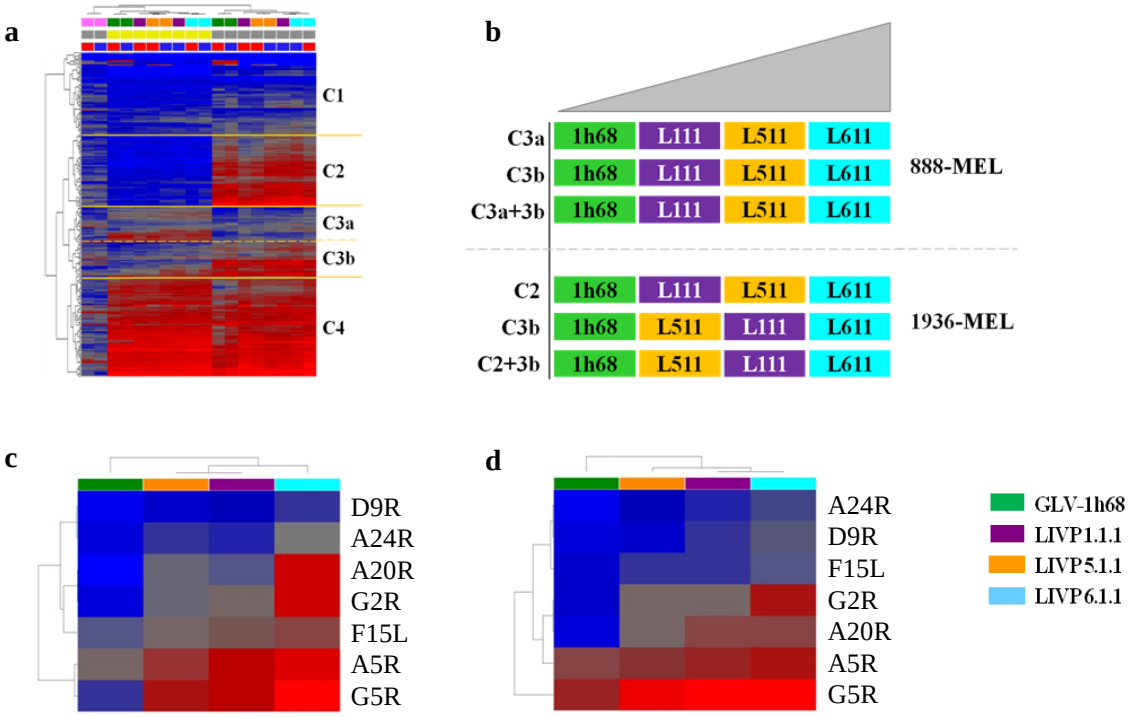

Figure 3-9: VACV ranking according to gene transcription at 2 hpi and correlation with viral replication
888-MEL and 1936-MEL cells were infected with 4 different VACV isolates (GLV-1h68, LIVP 1.1.1, LIVP 5.1.1, and LIVP 6.1.1) in separate experiments (MOI 0.01) or were treated with virus-free infection medium as negative control. Viral titers were determined by plaque assay and total RNA was isolated, amplified, purified, and labeled before generating transcriptional profiles via custom-made VACV array platforms. (a) Transcription profile incl. sub-cluster classification of 4 VACV isolates and negative control after 2 and 10 hours. (b) Transcriptional ranking of VACV isolates at 2 hpi. Transcription values at 2 hpi were averaged for each cell line considering the individual sub-clusters. Subsequently, viruses were ranked from lowest to highest mean gene transcription. (c, d) Hierarchical clustering of individual genes representing the transcriptional ranking in 888-MEL (c) and 1936-MEL (d) at 2 hpi. VACV isolate ranking from low to high in C3a: GLV-1h68, LIVP 5.1.1, LIVP 1.1.1, LIVP 6.1.1 or GLV-1h68, LIVP 1.1.1, LIVP 5.1.1, LIVP 6.1.1. *C1, C2, C3a, C3b, C4 = Cluster 1, 2, 3a, 3b, 4.

Subsequently, 7 genes from cluster C3a, whose expression corresponded with the overall early transcriptional ranking (rank 1-3, see above) were identified: *F15L*, *G2R*, *G5R*, *D9R*, *A5R*, *A20R*, and *A24R*. These viral genes encode subunits of the DNA-dependent RNA polymerase, DNA polymerase processivity factor, NTP phosphorylase, late transcription elongation factor, and a viral membrane formation protein. Hierarchical clustering based on these 7 genes was used to test whether they could segregate experiments according to VACV-specific gene transcription (Figure 3-9 c, d). Early viral gene transcription ranking (rank 1-3) was consistent with replication according to plaque forming units at 2 hpi.

3.1.3.2.2 VACV isolate-specific changes in transcription at 10 hpi

Accordingly, we concentrated on sub-clusters pointing at differences among viral isolates at 10 hpi. At this time point, gene transcription intensities in clusters C1, C2, and C3b were higher for GLV-1h68 when compared to LIVP 5.1.1. In other words, viral gene transcription ranking (rank 1-3) was inconsistent with replication according to plaque forming units at 10 hpi in these clusters (Figure 3-10 a). However, gene cluster C4 displayed strong distinctions in transcription intensity comparing GLV-1h68 with the different wt clones, in accordance with replication data at 10 hpi. In both melanoma cell lines the lowest mean transcription was observed for GLV-1h68, followed by LIVP 5.1.1 and LIVP 1.1.1 and finally by LIVP 6.1.1 (Figure 3-10 a). Consequently, we considered cluster C4 as representative of viral replication according to plaque forming units.

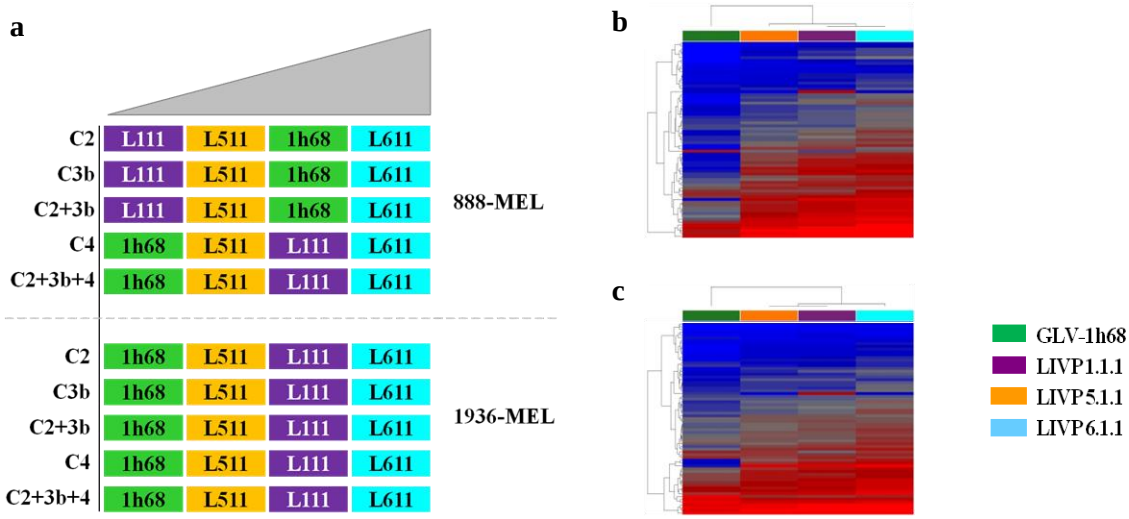

Figure 3-10: VACV ranking according to gene transcription at 10 hpi and correlation with viral replication
888-MEL and 1936-MEL cells were infected with 4 different VACV isolates (GLV-1h68, LIVP 1.1.1, LIVP 5.1.1, and LIVP 6.1.1) in separate experiments (MOI 0.01) or mock-infected (negative control). Viral titers were determined by plaque assay and transcriptional profiles generated via custom-made VACV array platforms. (a) Transcriptional ranking of VACV isolates at 10 hpi. Transcription values at 10 hpi were averaged for each cell line considering the individual sub-clusters. Subsequently, viruses were ranked from lowest to highest mean gene transcription. (b, c) Hierarchical clustering of individual genes representing the transcriptional ranking in 888-MEL (b) and 1936-MEL (c) at 10 hpi. VACV isolate ranking from low to high in C4: GLV-1h68, LIVP 5.1.1, LIVP 1.1.1, LIVP 6.1.1 or GLV-1h68, LIVP 1.1.1, LIVP 5.1.1, LIVP 6.1.1. *C1, C2, C3a, C3b, C4 = Cluster 1, 2, 3a, 3b, 4.

We identified 32 VACV genes in C4 whose expression followed the previously discussed ranking in both cell lines. Self-organizing re-clustering of 10 hpi microarray samples based on these genes demonstrated a clear gradient in transcription by the VACV isolates (Figure 3-10 b, c). Furthermore, in accordance with VACV replication data, GLV-1h68 transcription demonstrated a clear separation from all wt isolates. Functional annotations revealed that almost half of the 32 genes were involved in

DNA replication and RNA transcription and about one third in host interactions. Among the former we found genes, whose products act in dNTP synthesis (*F2L*, *J2L*, *I4L*), replication initiation, and continuance (primase/NTPase activity, ssDNA binding), as well as components of the DNA-dependent RNA polymerase.

3.1.4 Correlates between VACV and host cell transcription

To explore the relationship between host cell transcription and viral replication, we correlated viral and human gene expression at different time points. At high multiplicity of infection, VACV gene transcription levels are homogeneous according to the different temporal classes, independent of the VACV isolate utilized. We, therefore, adopted low MOI to increase the chance that subtle differences in the kinetics of transcriptional activation among viral isolates could segregate infectivity among different viruses.

3.1.4.1 Correlation between viral and human early gene transcription

We first wanted to characterize the correlation between viral and human early gene transcription (2 hpi). Therefore we used the previously identified 7 VACV genes in cluster C3a (3.1.3.2.1, viral arrays) which were most representative of early events, namely *F15L*, *G2R*, *G5R*, *D9R*, *A5R*, *A20R*, and *A24R*. These seven genes were defined as viral replication indicators (VRI) for early replication. Table 3-1 summarizes the gene names of the VRIs for GLV-1h68 (VACGL), vaccinia virus Copenhagen (COP), and vaccinia virus Western Reserve (WR) as well as their respective annotations.

Table 3-1: Gene names (in different VACV strains) and annotations of the 7 VRIs

GLV-1h68	COP	WR	Annotation
VACGL167	A5R	WR124	DNA-dependent RNA polymerase subunit rpo19
VACGL189	A20R	WR141	Viral DNA polymerase processivity factor
VACGL194	A24R	WR144	DNA-dependent RNA polymerase subunit rpo132
VACGL149	D9R	WR114	Contains mutT-like motif of NTP-phosphohydrolase for DNA repair and/or decapping function
VACGL069	F15L	WR054	Unknown
VACGL104	G2R	WR080	Late transcription elongation factor
VACGL106	G5R	WR082	Putative endonuclease/nuclease during viral DNA replication

The expression values of the 7 VRIs were averaged for each sample. The samples in turn were ranked according to average transcription level of the VRI (Figure 3-9 b).

For the human gene expression, the list of genes affected specifically by VACV infection was used. This list of virus-affected genes was developed previously by usage of a multistep filter with the human gene expression data set (3.1.1.2.1). An additional filter was applied to select only genes whose expression values were present in at least 90% of samples to avoid false-positive correlations due to missing expression values. In the end, at a 90% presence call, 400 and 370 infection-specific genes were identified for 888-MEL and 1936-MEL, respectively, and utilized for subsequent correlation analysis. Comparison between the VRI and human gene expression were performed by Pearson's correlation.

Table 3-2: Top networks and molecular functions of human genes correlating with VRI expression

Top networks	Top molecular functions
Cell cycle, cellular movement	Cell-to-cell signaling and interaction
Cell-to-cell signaling and interaction	Cellular movement
Carbohydrate and lipid metabolism	Cell morphology
Small molecule biochemistry	Cellular development
Immunological and inflammatory disease	Cellular growth and proliferation

We identified 114 human genes strongly correlating ($r \geq 0.6$) with VRI (see complete list in appendices, Table 6-1). Among them were 75 negative and 39 positive correlates. IPA revealed that these 114 genes belong to the following top networks: Cell cycle, cellular movement, cell-to-cell signaling and interaction, carbohydrate and lipid metabolism, small molecule biochemistry, as well as immunological and inflammatory disease. Besides cell cycle-related molecules we identified the subunit polymerase (RNA) II (DNA directed) polypeptide E (*POLR2E*), as well as ribosomal protein L6 (*RPL6*) within the top network both revealing a negative correlation with viral replication. The top molecular functions were cell-to-cell signaling and interaction, cellular movement, morphology, development, growth, and proliferation (Table 3-2). Canonical pathway analysis revealed an involvement in protein ubiquitination and EIF2 signaling, amongst others.

Overlay with published host factors required for infection by Mercer *et al*., 2012 [259] (based on RNAi screening of about one-third of human genes) resulted in an intersection of 3 molecules (lymphocyte-specific protein tyrosine kinase, *LCK*; proteasome (prosome, macropain) 26S subunit, non-ATPase, 2, *PSMD2;* and WNK lysine deficient protein kinase 1, *WNK1*) and showed various molecules overlapping in their functions, pathways, and networks.

3.1.5 Prediction of VACV replication

Based on the early transcriptional correlates identified in the two melanoma cell lines, we were interested in investigating their predictive strength in an independent data set including different cell lines and different viral constructs. Chen et al. [247] described, that virus replication efficiency is linked to the number of transgene insertions in a promoter-strength-dependent manner using a series of recombinant VACV strains, including GLV-1h68. Further, they demonstrated a correlation between replication efficiency of these VACV strains with antitumor efficacy and virulence. Therefore, this series of recombinant viruses appeared well-suited to test our hypothesis that a set of human genes may influence viral replication efficiency and/or permissiveness to VACV infection.

A human breast cancer (GI-101A) and a colon carcinoma (HT-29) cell line were individually infected with GLV-1h68 and five VACV recombinants (GLV-1h70, GLV-1h71, GLV-1h72, GLV-1h73, and GLV-1h74, illustrated in section 2.1.8.1) at an MOI of 0.01. Samples were taken at 2 hpi. Infections, RNA isolation, and microarray analyses were performed identically to the previous set.

For the prediction we assumed, that the transcriptional pattern of the 7 VRIs (Table 3-1; *F15L*, *G2R*, *G5R*, *D9R*, *A5R*, *A20R*, and *A24R*) reflects viral replication. Further, human melanoma genes which correlated with the average of the VRIs ($r \geq 0.5$) were assumed indicative of viral replication. We applied the same analytic criteria to the data set generated for GI-101A and HT-29. Gene transcription values of the VRIs in GI-101A and HT-29 were averaged and arranged according to value. Then, averaged viral gene expression was correlated with the respective human gene transcription (Pearson's Correlation). Correlates were included by the following criteria:

(1) r in melanoma cell lines ≥ 0.5 (absolute value)

(2) r in all cell lines must have the same algebraic sign (positive or negative) and

(3) r in GI-101A and H-T29 has to be either, at least moderate (r between -0.5 and -0.3, or between 0.3 and 0.5) in both cases, or, if one correlation is weak in one cell line, it must be strong in the other one.

a

NAME	888-MEL	1936-MEL	GI-101A	HT-29
LANCL2	0.67	0.85	0.53	0.62
HNRNPL	0.59	0.93	0.56	0.73
SNX17	0.63	0.84	0.43	0.80
TMED1	0.87	0.77	0.21	0.58
TXNRD3	0.90	0.88	0.28	0.47
ZNF69	0.66	0.79	0.36	0.34
CCL5	-0.83	-0.94	-0.42	-0.44
ATP5F1	-0.69	-0.73	-0.30	-0.67
ID2	-0.85	-0.84	-0.55	-0.23
DEK	-0.90	-0.62	-0.48	-0.24

*

strong negative correlation
strong positive correlation
moderate negative correlation
moderate positive correlation
weak negative correlation
weak positive correlation

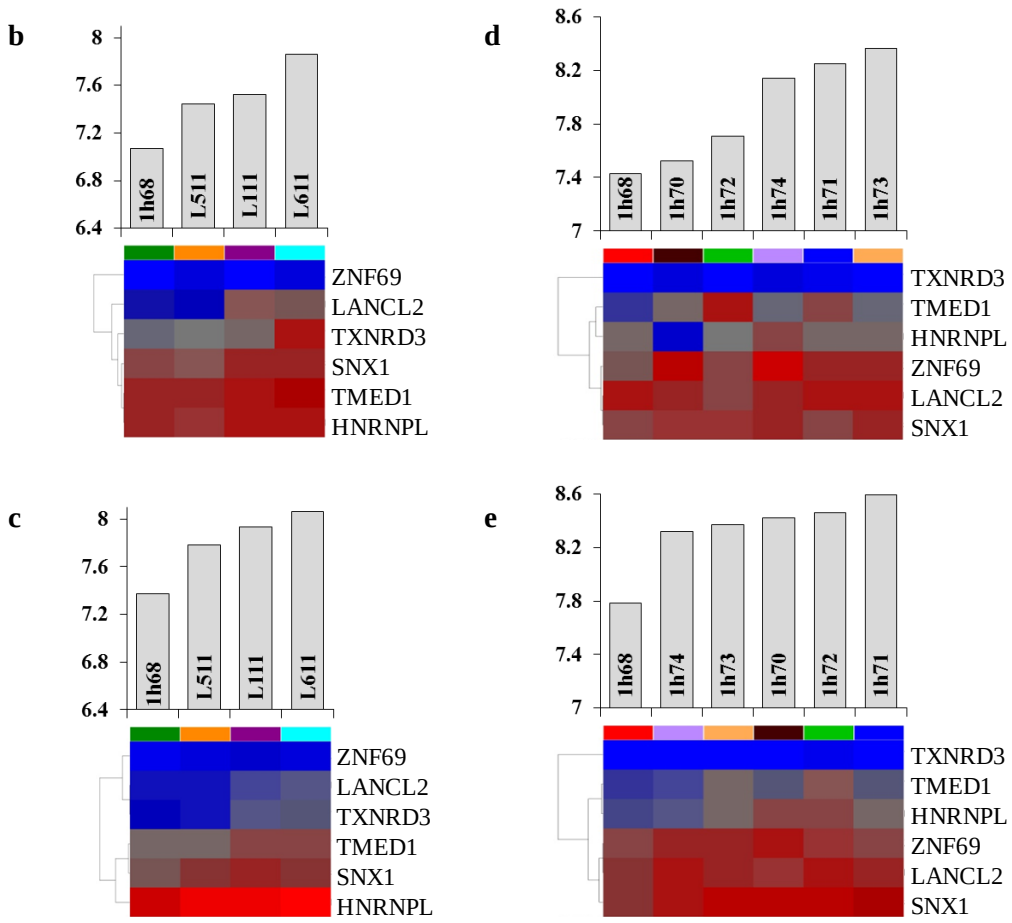

Figure 3-11: Human predictor genes of viral replication

GI-101A and HT-29 cells were infected with 6 different VACV isolates (GLV-1h68, GLV-1h70, GLV-1h71, GLV-1h72, GLV-1h73, and GLV-1h74) in separate experiments (MOI 0.01). Total RNA was isolated, amplified, purified, and labeled before generating transcriptional profiles via custom-made VACV array platforms or human whole genome (36 k) array platforms. Predictor genes were determined by the following criteria: r in melanoma cell lines ≥ 0.5 (absolute value), r in all cell lines has to have same direction (positive or negative) and r in GI-101A and HT-29 has to be either at least moderate in both cases, or if one correlation is weak in one cell line, it must be strong in the other one. (a) 10 predictors of viral replication were determined by Pearson Correlation. (b - d) Heat map of the 6 predictive positive human correlates at 2 hpi (black asterisk) in (b) 888-MEL, (c) 1936-MEL, (d) GI-101A and (e) HT-29. (b - d, bar graphs) Averaged viral gene expression of 7 VRIs at 2 hpi from cluster C3a; VRI = Viral replication indicators.

We found 10 genes (Figure 3-11 a) which matched these criteria as potential human indicators for viral replication efficiency summarized in detail in Table 3-3. The strongest positive correlations were observed for lantibiotic synthetase component C-like 2 (*LANCL2*) and heterogeneous nuclear ribonucleoprotein L (*HNRNPL*). Sortin nexin 17 (*SNX17*) transcription correlated strongly with viral early transcription in HT-29 and the melanoma cell lines and revealed a moderate correlation within GI-101A. A similar observation was made for the transmembrane emp24 protein transport domain containing 1 (*TMED1*) which showed strong correlations in all cell lines except for GI-101A, where it

only correlated weakly. Furthermore, thioredoxin reductase 3 (*TXNRD3*) and zinc finger protein 69 correlated strongly in the melanoma cell lines, moderately in HT-29, and revealed weak and moderate correlations in GI-101A, respectively. In the heat maps shown in Figure 3-11 b-e we illustrated the correlation between progressing gene expression of the 6 predictive positive human correlates (black asterisk) and the increasing VRI expression and thus viral replication (Figure 3-11 b-e, bar graphs). The transcriptional progression was more prominent in 888-MEL (Figure 3-11 b) and 1936-MEL (Figure 3-11 c) than in GI-101A (Figure 3-11 d) and HT-29 (Figure 3-11 e).

The strongest negative correlations were found for ATP synthase, H+ transporting, mitochondrial Fo complex, subunit B1 (*ATP5F1*) and chemokine (C-C motif) ligand 5 (*CCL5*).

Table 3-3: Cellular predictors of viral replication

Gene Symbol	Description
LANCL2	LanC lantibiotic synthetase component C-like 2 (bacterial) (LANCL2), mRNA.
HNRNPL	Heterogeneous nuclear ribonucleoprotein L (HNRNPL), transcript variant 1, mRNA.
SNX17	Sorting nexin 17 (SNX17), mRNA.
TMED1	Transmembrane emp24 protein transport domain containing 1 (TMED1), mRNA.
TXNRD3	Thioredoxin reductase 3 (TXNRD3), transcript variant 1, mRNA.
ZNF69	Zinc finger protein 69 (ZNF69), mRNA.
CCL5	Chemokine (C-C motif) ligand 5 (CCL5), mRNA.
ATP5F1	ATP synthase, H+ transporting, mitochondrial Fo complex, subunit B1 (ATP5F1), nuclear gene encoding mitochondrial protein, mRNA.
ID2	Inhibitor of DNA binding 2, dominant negative helix-loop-helix protein (ID2), mRNA.
DEK	DEK oncogene (DEK), transcript variant 2, mRNA.

3.2 Contributing factors to permissiveness of melanoma cell lines to oncolytic virotherapy

In the NCI-60 panel of cell lines we found that transcriptional profiles generated prior to GLV-1h68 infection did not reveal significant differences among cancer cell lines with different permissiveness to VACV infection [246]. Furthermore, we observed that the permissiveness to VACV infection was highly heterogeneous and independent of the tissue of origin [246].
In addition to that, based on the results obtained from the VACV vs. human gene expression correlation study (3.1), we concluded that transcriptional patterns are indeed important and informative but not sufficient to answer the question regarding host cell permissiveness to oncolytic vaccinia virus treatment [258]. For this reason, this follow-up study included a comprehensive evaluation and comparison of factors that might promote vaccinia virus replication and thus contribute to permissiveness of a given cell line to virus treatment.

For this study, we used a set of 15 melanoma cell lines (15-MEL) derived from patients who suffered from metastatic melanoma and were treated at the Surgery Branch of the National Cancer Institute (NCI, Bethesda, MD) [260].

3.2.1 Evaluation of general conditions for the 15-MEL study

Initially, we wanted to optimize all parameters for the final characterization of the 15 melanoma cell lines (15-MEL). For this reason, we started our experiments with two established cell lines from the NCI-60 panel of cell lines with a known level of permissiveness to infection with oncolytic VACV. HCT-116 and HCT-15 are two human colon carcinoma cell lines with high and low permissiveness to GLV-1h68 infection, respectively [246]. Therefore these two cell lines were utilized to determine the ideal experimental conditions for the analysis of the 15-MEL.

3.2.1.1 Applicability of virus-expressed fluorochromes for flow cytometric evaluation of viral replication

For flow cytometric analysis different fluorochromes with different intensities and emission/ absorption spectra can be utilized. To investigate which fluorochrome was the most suitable for our analyses, we used three VACV isolates containing different fluorescent marker gene insertions in the

same locus (*F14.5L*) of the viral genome and under the same promoter (*early/late*). The VACV isolates GLV-1h68, GLV-1h134, and GLV-1h261 express RUC-GFP (green), CBG99-mRFP1 (red), and mNeptune (far red), respectively. HCT-116 and HCT-15 cells were infected with each virus for 20 hrs at an MOI of 1. Cells were harvested, fixed, and washed before performing flow cytometric analysis. GFP, RFP, and mNeptune emissions were detected by applying specific band-pass filters. Kaluza software was used for subsequent data analysis.

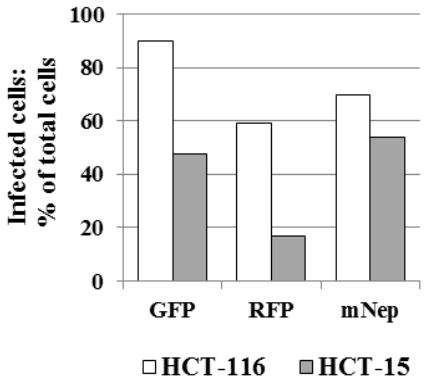

Figure 3-12: Percentage of fluorochrome-positive HCT-116 and HCT-15 cells after GLV-1h68 (GFP), GLV-1h134 (RFP), and GLV-1h261 (mNeptune) infection

Flow cytometric analysis of HCT-116 and HCT-15 revealed expectedly higher amounts of fluorochrome-positive cells for the highly permissive HCT-116 cell line for all viruses analyzed (Figure 3-12). Comparing the features of the three viruses in HCT-116 and HCT-15 we observed the following: GLV-1h68 infection resulted in an overall highest percentage of fluorochrome-positive cells and created two distinct populations of infected and uninfected cells (Figure 3-13); GLV-1h134 revealed the lowest number of positive cells with less than 20% in HCT-15 and no clear-cut separation between RFP(+) and RFP(-) cells (Figure 3-13) and was thus not included in future experiments; Finally, GLV-261 infection resulted in issues regarding clear-cut detection of mNeptune(+) cells since the extreme brightness of the fluorochrome led to a strong bleed-through of the signal through multiple channels. Therefore GLV-1h261 was considered to be ineligible for our purposes and was excluded in future analyses.

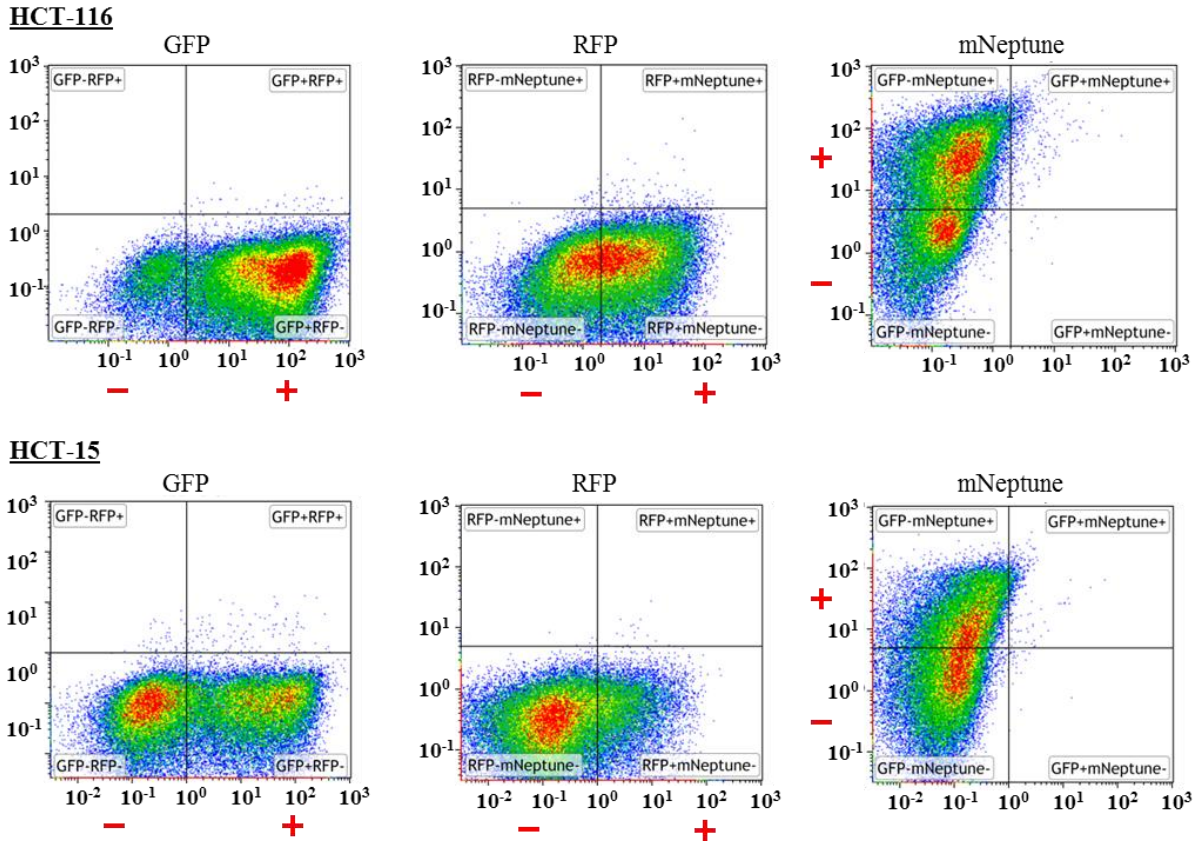

Figure 3-13: Flow cytometric evaluation of different VACV-expressed fluorochromes

HCT-116 and HCT-15 cells were infected with GLV-1h68 (GFP-expressing), GLV-1h134 (RFP-expressing), and GLV-1h261 (mNeptune-expressing) for 20 hrs at MOI 1. Dot plots of HCT-116 (top) and HCT-15 (bottom) fluorochrome-positive (+) and negative (-) cell populations after VACV infection (MOI 1); from left to right GFP, RFP, and mNeptune.

3.2.1.2 MOI-dependent infection characteristics

Next we were interested in optimizing the MOI to be used for future infection studies by testing a series of different MOIs reaching from 0.6 till a saturating MOI of 5. Therefore HCT-116 and HCT-15 cells were infected with GLV-1h68 for 20 hrs at an MOI of 0.6, 1, 2, and 5. Cells were harvested, fixed, and washed before performance of flow cytometric analysis. GFP emission was detected by using a specific band-pass filter and Kaluza software was used for subsequent data analysis.

A continuous high number of GFP(+) cells was detected for HCT-116 with 82.4% GFP(+) cells at MOI 0.6 and 96.6% at MOI 5 (Figure 3-14, white bars). For HCT-15 we observed an almost linear increase over the course of MOIs reaching from 29.9% GFP(+) cells at MOI 0.6, 44.6% at MOI 1, 64.8% at MOI 2, up to 84% at MOI 5 (Figure 3-14, grey bars).

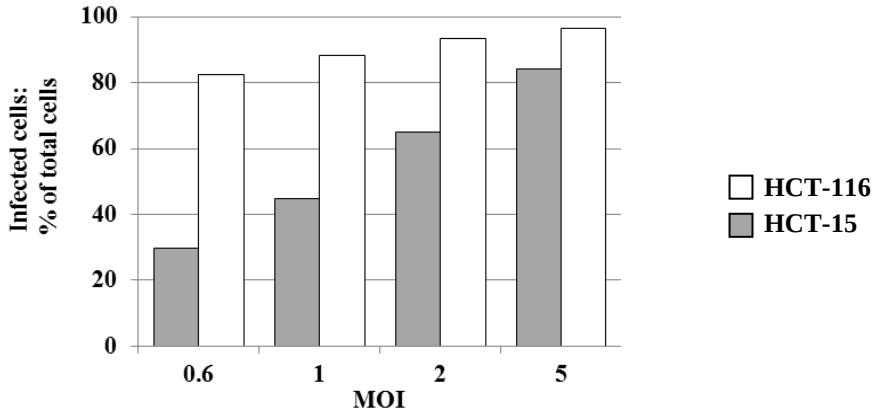

Figure 3-14: Flow cytometric evaluation of GLV-1h68 infections at different MOIs

HCT-116 and HCT-15 cells were infected with GLV-1h68 for 20 hrs at MOIs 0.6, 1, 2, and 5. Bar graph: Percentage of GFP-positive cells after GLV-1h68 infection at different MOIs.

At an MOI of 5 the differences between VACV permissiveness of HCT-116 and HCT-15 diminished. Based on that, we concluded that an MOI of 5 obscures differences in permissiveness of different cell lines due to synchronization of the infection and was therefore not appropriate for future experiments. At the same time a low MOI could result in a similar issue of having difficulties in pointing out differences between cell lines. Because of the clear difference between number of GFP(+) cells in low and highly permissive cell lines, we concluded that MOI 1 is most suitable to screen cell lines regarding variances in permissiveness and to investigate the underlying mechanisms that might contribute to causing this divergence.

3.2.2 Permissiveness of the 15-MEL panel to GLV-1h68 infection

After determination of adequate frame conditions via known NCI-60 cell lines, we screened the panel of 15 melanoma cell lines (15-MEL) and ranked them regarding their permissiveness to GLV-1h68 infection.

The 15-MEL cell lines were infected with GLV-1h68 for 20 hrs at an MOI of 1. Cells were harvested, fixed, and washed before flow cytometric analysis. GFP emission was detected by using a band-pass filter set at 513/26 nm. Kaluza software was used for subsequent data analysis. HCT-116 cells were included in all experiments as a positive control for high permissiveness. Experiments were run in two batches on different days. Lowest and highest permissive 15-MEL cell line from batch 1 were also included in the second batch. The percentage of GFP(+) cells was averaged for the double-determinants.

a

Samples	Letter
2492	A
2744	B
2155	C
2075	D
2224	E
3107	F
2448	G
2523	H
3104	I
2805	J
2458	K
2427	L
2035	M
1866	N
3025	O

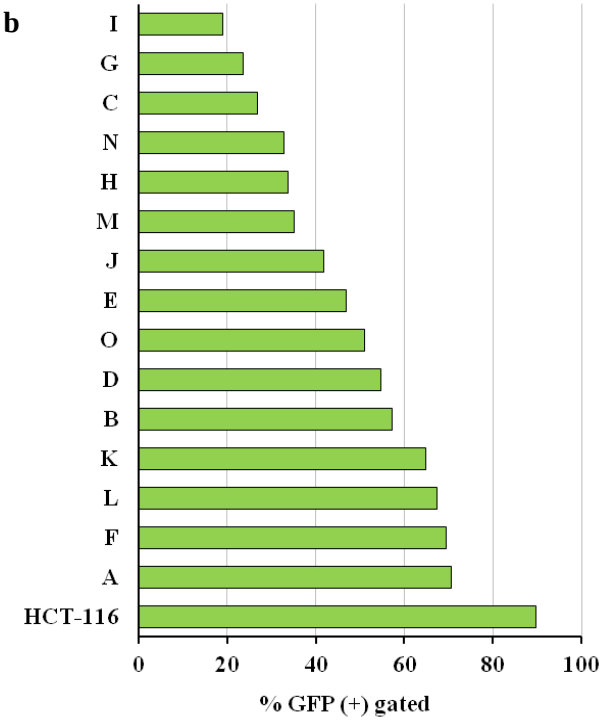

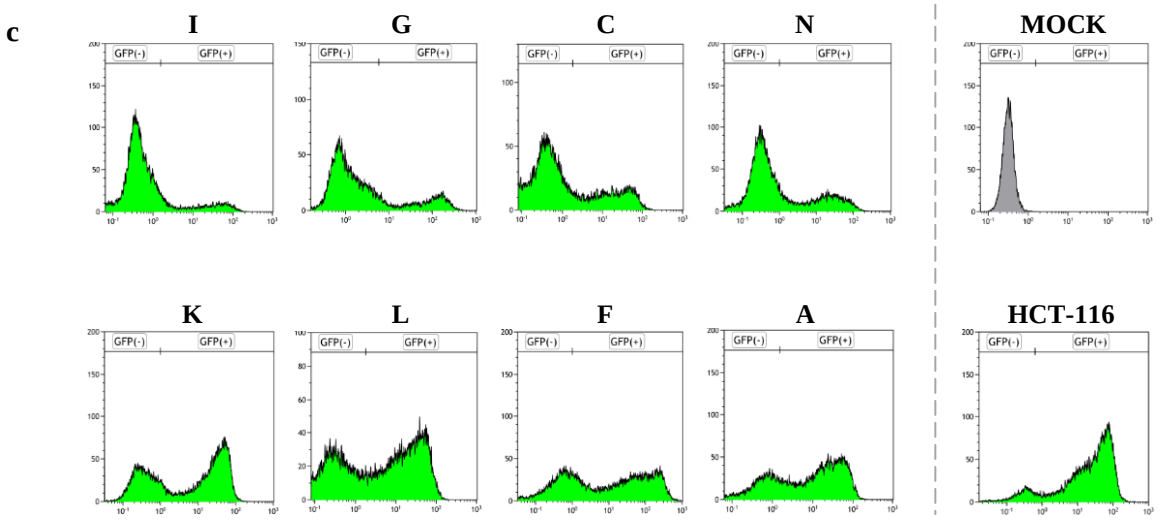

Figure 3-15: Flow cytometric screening of 15 melanoma cell lines regarding GLV-1h68 permissiveness

(a) Overview of the panel of 15 melanoma cell lines and their respective letter code. 15-MEL and HCT-116 were infected with GLV-1h68 for 20 hrs at an MOI of 1 and GFP(+) cells after VACV infection were evaluated by flow cytometry. (b) GLV-1h68 permissiveness screening and subsequent ranking of the 15-MEL including HCT-116 positive control. (c) Individual histograms of the top 4 and last 4 ranked cell lines, an exemplary mock plot, and histogram of the HCT-116 positive control.

For clarity and to facilitate inspection we assigned a letter code to the 15 melanoma cell lines from A to O (Figure 3-15 a). After screening all of the 15-MEL cell lines, we observed different permissivities throughout the panel and ranked the cell lines accordingly (Figure 3-15 b). In the

individual histograms of the 15-MEL, two peaks were visible for each cell line reflecting the uninfected GFP(-) and the infected GFP(+) populations (Figure 3-15 c). For the mock infected samples only a single GFP(-) peak was detected as shown exemplary for one of the cell lines in Figure 3-15 c. Further, almost every cell of the HCT-116 positive control revealed a positive GFP signal. The lowest permissiveness was found for the cell lines 3104 (letter I), 2448 (letter G), 2155 (letter C), and 1866 (letter N) whereas the top permissiveness was detected for 2492 (letter A), 3107 (letter F), 2427 (letter L), and 2458 (letter K).

3.2.3 Molecular biological variances associated with permissiveness to VACV treatment

3.2.3.1 Transcriptional patterns related to a VACV permissive phenotype

After screening the 15-MEL cell lines regarding their susceptibility to VACV infection, we were interested in analyzing host transcription prior to infection in order to reveal potential patterns associated with a permissive phenotype. It was published previously that transcriptional data alone are not sufficient to clearly identify overall predictors for susceptibility of cell lines to viral replication [246]. However, the comparison of transcriptional patterns of highly permissive vs. less permissive cell lines is essential to compile information for a global understanding of VACV susceptibility.

For this reason, total RNA was isolated from 15-MEL cells, amplified, purified, labeled and hybridized to single color human probe arrays. Gene expressional data analysis was assessed by Partek Genomic Suite software. Molecular networks, functions, and pathways were analyzed via IPA software. The transcriptional profiles of the four least (I, G, C, N) and the four highest (A, F, L, K) permissive cell lines were compared via analysis of variances (ANOVA) with a confidence interval of 5% ($p \leq 0.05$).

Comparing highly vs. low permissive group we detected a set of 1360 differentially expressed genes with 867 of which being mapped and analysis-ready for pathway studies via IPA. The majority of molecules were enriched in broad cellular functions such as cell cycle, cell morphology, cell growth and proliferation, as well as cell death and survival. Among the represented canonical pathways the antigen presentation pathway was the most significant one. Additionally, important canonical pathways included protein ubiquitination, cytotoxic T lymphocyte-mediated apoptosis of target cells, chondroitin sulfate biosynthesis, death receptor signaling, assembly of RNA polymerase III complex, dTMP *de novo* biosynthesis, DNA double-strand break repair by homologous recombination, and granzyme A signaling amongst others. Further, comparison between the two groups of cell lines

regarding the top up- and down-regulated molecules revealed that the majority of up-regulated molecules in the high group were nucleus-located factors (36%) whereas down-regulated molecules in this group were mainly enriched in cytoplasmic locations (32%) and the plasma membrane (35%) (Figure 3-16).

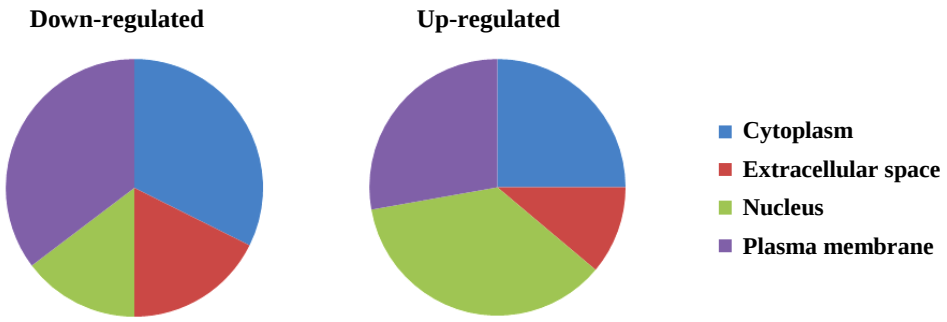

Figure 3-16: Cellular location dispersion of top up- and down-regulated molecules

Pie chart showing the percentage of top up and down-regulated molecules among intracellular locations. Gene expression values of highly vs. low permissive group of melanoma cell lines were compared via ANOVA at a p-value of 0.05 and a fold change (fc) ≥ 2 or fc ≤ -2. Molecules were interspersed throughout different cellular locations (Cytoplasm, extracellular space, nucleus, and plasma membrane) with varying fractions.

The 34 down-regulated molecules in the high group (fc ≤ -2) were distributed among the following cellular locations: Cytoplasm (32%), extracellular space (18%), nucleus (15%), and plasma membrane (35%) (Additional table 6-2). In contrast to that, the 36 up-regulated molecules in the high group (fc ≥ 2) were interspersed among the location categories as follows: Cytoplasm (25%), extracellular space (11%), nucleus (36%), and plasma membrane (28%) (Additional table 6-3).

In a next step towards understanding, the underlying mechanisms and biology behind host cell permissiveness, we compared transcriptional patterns obtained prior to infection with virus-influenced patterns that correlated with virus replication. To reveal possible connections between a pre-existing cellular make-up in permissive cell lines and actual virus-host interactions, we overlaid the results obtained previously from correlating host gene expression and viral replication in 888-MEL and 1936-MEL with the ANOVA results of the current 15-MEL transcription data.

Out of 114 early genes that correlated with viral replication in 888-MEL and 1936-MEL, seven genes were expressed significantly different between low and highly permissive groups of melanoma cell lines (Figure 3-17). Among the genes up-regulated in the low permissive group we identified WNK lysine deficient protein kinase 1 (*WNK1*), and glutamate dehydrogenase 1 (*GLUD1*). Up-regulations in the high group were observed for putative ubiquitin protein ligase E3 component n-recognin 7 (*UBR7*), the pseudogenes major histocompatibility complex, class I, L and H (*HLA-L*, *HLA-H*), as

well as the human DEK oncogene (*DEK*), which was most outstanding, since we observed previously that *DEK* was also a potential predictor for viral replication in an independent data set (Table 3-3).

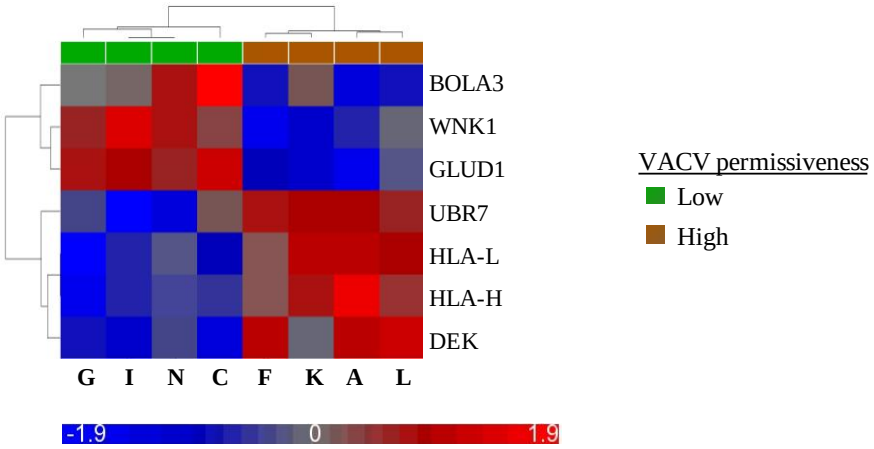

Figure 3-17: Overlay of transcriptional correlates with viral replication and base line transcription between low and high group of permissive cell lines

Transcription profile. Heatmap based on the overlay between the list of 114 human genes (888-MEL and 1936-MEL) that strongly correlated ($r \geq 0.6$) with viral replication (described in 3.1.4.1) and the gene list of 1360 genes obtained via ANOVA between 15-MEL low group (I, G, C, and N) and high group (F, K, L, A), $p \leq 0.05$. Seven genes in the 15-MEL data set passed the filtering criteria.

As described in section 3.1.4.1, the expression of 114 genes in 1936-MEL and 888-MEL correlated with viral replication, represented by the expression of seven viral replication indicators (VRIs). Out of the genes overlapping with the baseline expression of the four highly vs. four low permissive melanoma cell lines from the 15-MEL panel *WNK1*, *HLA-L*, *HLA-H*, and *DEK* revealed an inverse correlation with VACV replication, whereas the expression of the *GLUD1* and *UBR7* genes correlated positively.

3.2.3.2 MicroRNA expressional variances associated with permissiveness to VACV treatment and correlation with mRNA transcription

In a further approach, we investigated the gene expression of microRNAs (miRNAs), a member of the family of small non-protein coding RNAs. Human miRNAs are known for their role in regulation of gene expression at post-transcriptional level and account for approximately 1% of genes in humans with an average miRNA having about 100 target sites [261]. It was shown previously that vertebrate miRNAs can directly affect viral genome replication and/or gene expression by interacting with viral mRNAs or RNA genomes [262, 263]. Based on that, we considered the investigation of cellular

miRNA expression to provide valuable information regarding virus-host co-existence and in terms of host cell permissiveness to VACV infection.

Therefore, total RNA, including small RNAs, was isolated from the 15-MEL cell lines. Subsequent preparation steps included amplification of the isolated RNA, purification, miRNA-specific labeling, and hybridization to human miRNA arrays. Host miRNA expression data was evaluated via Partek Genomic Suite software. The miRNA transcription profiles of the four least (I, G, C, N) and three out of the four highest (A, F, K) permissive cell lines were compared via analysis of variances (ANOVA) with a confidence interval of 5% ($p \leq 0.05$). The chip quality for the 2427 (L) highly permissive cell line was not satisfying and therefore this cell line had to be excluded from the analysis.

A total of six miRNAs with significantly different expression patterns between low and highly permissive group were identified. We observed a strong up-regulation for *miR-32* and *miR-107* in the high group in comparison to the respective expression levels within the low group, whereas *miR-93*, *miR-29a*, *miR-148a*, and *miR-487b* on the other hand revealed a significant down-regulation (Figure 3-18).

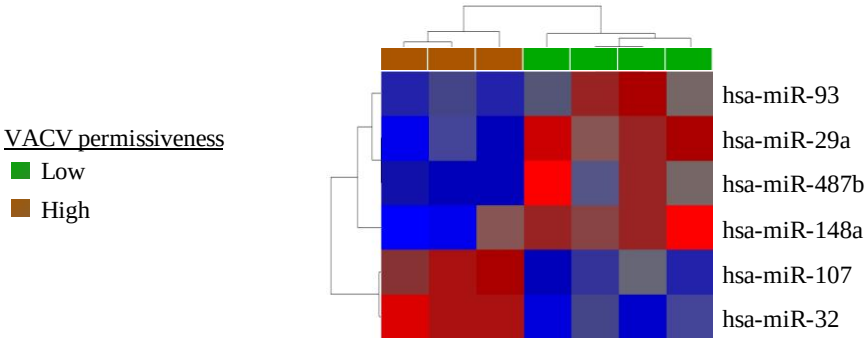

Figure 3-18: Heatmap of differentially expressed miRNAs in the low and highly permissive group
miRNA transcription profile. Heatmap based on ANOVA between 15-MEL low permissive (I, G, C, and N) and highly permissive group (F, K, A) without cell line L, $p \leq 0.05$. Six miRNAs passed the filtering criteria; hsa = homo sapiens, miR = microRNA

Moreover, we were interested to explore, whether there was a correlation between miRNA and target mRNA expression. For this reason, gene lists obtained from mRNA and miRNA ANOVAs, comparing the high and the low group, were merged. For the mRNA expression data a more stringent p-value of $p \leq 0.01$ was applied to enhance the significance of the results. 229 mRNAs passed these filter criteria and were used for comparative analyses. In addition to that, the list of the six differentially expressed miRNAs ($p \leq 0.05$) was utilized.

Table 3-4: Expressional correlation of miRNAs and target mRNAs in low vs. highly permissive cell lines

	miRNA ID	mRNA Gene Symbol	mRNA FC	FC description	Pearson correlation coefficient	p-value (pearson)	Spearman's rank correlation coefficient	p-value (spearman)
HIGH down vs LOW	hsa-mir-148a	CRTC3	1.24	HIGH up vs LOW	-0.78	0.0387	-0.82	0.0234
	hsa-mir-148a	SELT	-1.16	HIGH down vs LOW	0.85	0.0165	0.93	0.0025
	hsa-mir-148a	MAFG	-1.17	HIGH down vs LOW	0.88	0.0097	0.75	0.0522
	hsa-mir-29a	COL4A2	2.73	HIGH up vs LOW	-0.9	0.0051	-0.86	0.0137
	hsa-mir-29a	CSNK1G1	1.86	HIGH up vs LOW	-0.8	0.0315	-0.75	0.0522
	hsa-mir-93	CNOT6L	1.57	HIGH up vs LOW	-0.84	0.0193	-0.82	0.0234
	hsa-mir-93	RUNX3	2.63	HIGH up vs LOW	-0.81	0.0255	-0.82	0.0234
	hsa-mir-93	FBXO31	1.51	HIGH up vs LOW	-0.74	0.056	-0.82	0.0234
	hsa-mir-93	AAK1	-1.26	HIGH down vs LOW	0.81	0.026	0.79	0.0362
HIGH up vs LOW	hsa-mir-107	WNK1	-1.21	HIGH down vs LOW	-0.92	0.0035	-0.93	0.0025
	hsa-mir-107	GLUD1	-1.57	HIGH down vs LOW	-0.86	0.0122	-0.61	0.1482
	hsa-mir-107	CNOT6L	1.57	HIGH up vs LOW	0.79	0.0363	0.64	0.1194
	hsa-mir-107	PTPLB	1.32	HIGH up vs LOW	0.84	0.017	0.75	0.0522
	hsa-mir-32	SELT	-1.16	HIGH down vs LOW	-0.85	0.0152	-0.93	0.0025
	hsa-mir-32	WDR81	1.47	HIGH up vs LOW	0.76	0.0475	0.68	0.0938
	hsa-mir-32	PMEPA1	2.18	HIGH up vs LOW	0.88	0.0092	0.86	0.0137

With help of Partek Genomic Suite software miRNAs were assigned to their respective target genes and expression data correlated via Pearson correlation as well as Spearman's rank test. Results were filtered by correlation coefficient $r \geq 0.5$ or $r \leq -0.5$ and by p-value ($p \leq 0.05$ in at least one of the two correlation tests, Spearman and/or Pearson). After removal of duplicates we identifies a set of 16 combinations to not only match the predicted miRNA-target mRNA profile, but also correlate directly or inversely in their transcription level (Table 3-4). Out of the six miRNAs differentially expressed between low and high group, five revealed predicted targets among the 16 identified miRNA-mRNA pairs. Only *miR-487b* did not match with any of the targets within the range of the applied filtering criteria. The selenoprotein T (*SELT*) and CCR4-NOT transcription complex subunit 6-like (*CNOT6L*) showed correlation with two out of the six miRNAs, *miR148a*/ *miR-32*, and *miR93*/ *miR107*, respectively. Interestingly, the messages *WNK1* and *GLUD1*, both targets of *miR-107*, were identified previously among the seven correlates with viral replication (Figure 3-17). In addition to that, *GLUD1* and *WNK1* expression (down-regulated in the high group) correlated inversely with *miR-107* expression.

The individual miRNA-mRNA pairings, including direction of expression (high vs. low), Pearson correlation coefficient and p-value as well as Spearman rank correlation coefficient plus p-value are summarized in table 3-4.

3.2.3.3 Copy number variations associated with permissiveness

The human genome reveals a considerable degree of variation in sequence and structure which, amongst other effects, can predispose individuals for developing diseases such as cancer. Furthermore, copy number variations can affect an individual's response to therapy [264]. On the other hand, copy number variants can also be beneficial to individuals, like in case of the *CCL3L1* gene, where bearing extra copies results in a lower susceptibility to the human immunodeficiency virus (HIV) and acquired immunodeficiency syndrome (AIDS) [265].

For this reason, in a final experiment we screened the panel of 15-MEL cell lines at chromosomal level for segmental DNA gains and losses. Copy number aberrations were evaluated via high-resolution array comparative genomic hybridization (aCGH). Genomic DNA from human advanced melanoma cell lines (15-MEL) and from PBMC references was isolated, fragmented, labeled, purified, and hybridized to Agilent 2 × 105 K arrays. Copy number variations (CNVs) were analyzed via Partek Genomic Suite software.

Chromosomal aberrations found in the 15-MEL cell lines (Figure 3-19 a) were in accordance with the results described by Spivey *et al*. for these cell lines [260]. In the present study, our focus was to investigate differences in permissiveness of cell lines, therefore we only considered eight out of the 15-MEL cell lines for subsequent analysis, four with low and four featuring high permissiveness to GLV-1h68 infection.

At first, the CGH profiles of the four least (I, G, C, N) and the four highest (A, F, K, L) permissive cell lines were compared in their cyto-band pattern regarding amplifications, deletions, and unchanged regions.

Figure 3-19 b and c summarize chromosomal aberrations of the highly and low permissive group of cell lines, respectively, displayed in the form of copy number classification plots (Figure 3-19 b, c, left panel) and sample histogram plots (Figure 3-19 b, c, right panel).

Comparison of chromosomal aberrations of highly and low permissive group revealed that overall chromosomal gains were more frequent in the low group than in the high one (Figure 3-19 b, c). The most prominent chromosomal gains were observed in chromosomal regions 1q, 2, 3, 7, 12p, 15p, 17q, and 22q within the low group, but were not present or at least not to that extent within the high group. In contrast, we observed chromosomal losses in the low group in regions 9q and 16q (Figure 3-19 b, c).

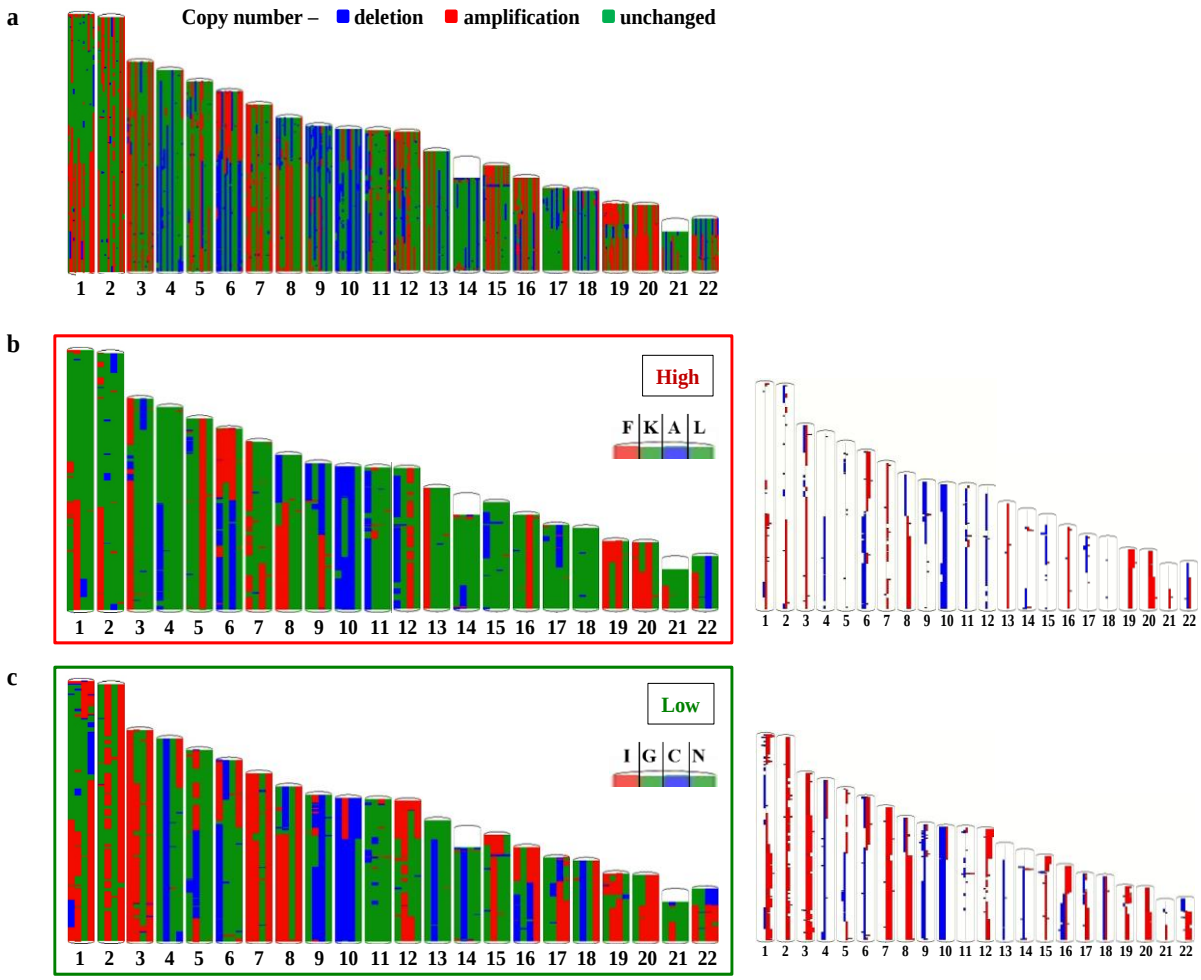

Figure 3-19: Plots of autosomal aberrations of all 15-MEL cell lines as well as of the four highly vs. four low permissive cell lines

High-resolution aCGH of human melanoma cell lines (15-MEL). Genomic DNA from 15-MEL and PBMC references was isolated, fragmented, labeled, purified, and hybridized to human CGH microarrays. CNVs were analyzed via Partek Genomic Suite software. Segments are defined by amplifications (red), deletions (blue), and unchanged regions with respect to diploid reference (green). (a) Whole genome view of autosomal aberrations of the 15 melanoma cell lines. Individual samples are represented as vertical lines. (b, left) Autosome copy number classification plot for the four highly permissive cell lines. Vertical lines represent from left to right cell lines: F, K, A, L (letter code, Figure 3-15 a) in each chromosome; indicated in the graphic legend. (b, right) Sample histogram plots (high group). Region heights are determined by the number of abnormal samples. (c, left) Autosome copy number classification plot for the four low permissive cell lines. Vertical lines represent from left to right cell lines: I, G, C, N in each chromosome. (c, right) Sample histogram plots (low group).

Subsequently, we wanted to validate the segmental differences between the high and low group, observed within the chromosomal plots (Figure 3-19 b, c) statistically via analysis of variances (ANOVA) at two different confidence intervals (1% and 0.5%). For the analysis of CNVs, chromosomal regions were annotated with corresponding gene symbols. At a p-value ≤ 0.01 a total of 5,252 genes were found, whereas analysis at $p \leq 0.005$ resulted in the identification of 2,940 genes. Out of these 2,940 identified genes, 2,652 were mapped and analysis-ready for ingenuity pathway

analysis (IPA). Network analyses revealed an enrichment of these genes in the following networks: Cell cycle and signaling, nucleic acid metabolism, small molecule biochemistry, metabolic disease, infectious disease, cell morphology, as well as cellular assembly and organization. When exploring disease-related as well as molecular and cellular functions, we found a major involvement in metabolic disease, hypersensitivity response, and inflammatory response as well as in multiple cellular functions (Table 3-5).

Table 3-5: Top bio functions of CNVs between low and highly permissive group

Diseases and Disorders	Molecular and Cellular Functions
Metabolic Disease	Cellular Growth and Proliferation
Endocrine System Disorders	Cellular Development
Gastrointestinal Disease	Cellular Movement
Hypersensitivity Response	Cell-To-Cell Signaling and Interaction
Inflammatory Response	Cell Death and Survival

Furthermore, we performed canonical pathway analysis with this gene list, illustrated in the form of a bar chart, with down-regulations and up-regulations being displayed as stacked green and red bars, respectively (Figure 3-20). Comparative analyses were performed comparing high vs. low group; therefore, all following results, which contain directional data, are shown from the perspective of the high group.

We discovered a variety of pathways of the cellular immune response which showed by trend an enrichment of up-regulated molecules in the highly permissive group. Among these pathways was for example the cytokine-mediated communication between immune cells, including a set of up-regulated interleukins, namely *IL-1A* and *1B*, *IL-2*, *IL-3*, *IL-5*, *IL-6*, *IL-10*, *IL-13*, *IL-21*, *IL-24*, and *IL-32*. Most outstanding was the pronounced up-regulation of *IL-24* of more than 4-fold within the highly permissive group. This was in contrast to the visually observed differences between low and high group (Figure 3-19) since *IL-24* mapped within the IL-10 family cluster to chromosome 1q [266] which showed amplifications in the low group. In addition to that, several other pathways of the cellular immune response were detected, such as the crosstalk between dendritic cells and natural killer cells, granzyme A signaling, TREM1 Signaling, and iNOS signaling amongst others (Figure 3-20). Furthermore, we found an enrichment of molecules in intracellular and second messenger signaling, cellular growth and proliferation, as well as apoptosis signaling. In addition to that, we identified an involvement in pathways with role in interferon induction, antiviral response, and PI3K/AKT signaling. Finally, based on the results obtained with expression and miRNA analysis we explored the copy number status of *WNK1*. The *WNK1* gene is located in the tip of the p-arm of chromosome 12, which shows partially amplified regions within the low group of cell lines (Figure 3-19). In fact, when looking at the copy number data, in accordance with mRNA and miRNA results, we found that *WNK1* was amplified in all 4 low permissive cell lines, but was unchanged in 3 of the highly permissive ones.

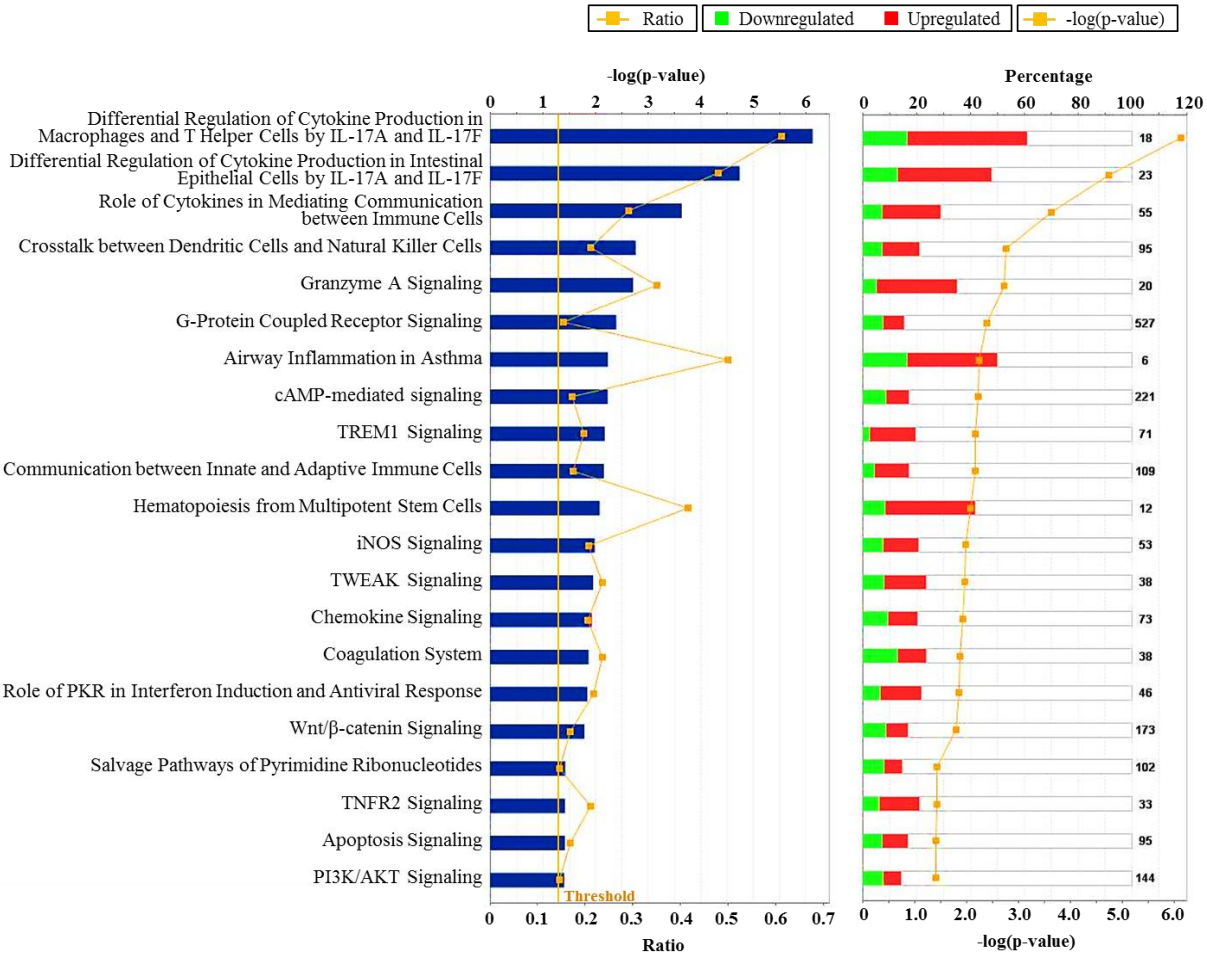

Figure 3-20: Canonical pathways of genes present within segmental differences between low and highly permissive group

Genomic DNA from samples and references was isolated, fragmented, labeled, purified, and hybridized to human CGH microarrays. CNVs were analyzed and segmental differences between groups determined via Partek Genomic Suite software. Canonical pathway analysis is based on genes present within segments with copy number variations comparing high and low permissive group (ANOVA, $p \leq 0.005$). Data are shown from the high group's perspective. Top canonical pathways of 2,940 genes present within segmental differences between groups (left) and stacked bar graph of down-regulated (green) and up regulated-molecules (red).

Finally, we compared the CNVs determined via aCGH and gene expressional differences identified via microarray and analyzed those regarding overlaps and correlations. Therefore, statistical stringency was adjusted accordingly. For the gene list obtained from the aCGH ANOVA we applied a cut-off of $p \leq 0.01$, whereas for the gene expression ANOVA a cut-off of $p \leq 0.05$ was chosen. The overlay of those two gene lists led to an intersection of 254 genes. IPA analysis indicated an involvement of these molecules in cancer, cellular development, tumor morphology, DNA replication, recombination, and repair, nucleic acid metabolism, small molecule biochemistry, cell cycle, as well as cell death and survival. In addition, we observed an involvement in the canonical pathways granzyme A signaling, assembly of RNA polymerase III complex, and DNA double-strand repair by homologous recombination, which were also found previously among the canonical pathways of gene transcriptional patterns.

4 Discussion

Despite tremendous advances in cancer research, many cancers especially at advanced stages still reveal a poor prognosis. Because of the heterogeneity of the disease, it remains extremely challenging or near-impossible to find a universal cure. Standard cancer treatments at present still lack specificity and durable efficacy for most acute cancers. This is supported by recent studies in which evidence of tolerance to chemotherapy [267] and targeted therapy [268, 269] is seen. Additionally, most types of metastatic cancers cannot be cured with current treatment options. Therefore, development of novel therapeutic approaches continues on the basis of cancer cell similarities postulated as the hallmarks of cancer [2, 3].

Within the last decade oncolytic virotherapy has emerged as a promising approach in cancer treatment. Oncolytic viruses feature an intrinsic or acquired (genetic engineering) tumor tropism, leading to a tumor-specific viral life-cycle and eventually to lysis of the infected cancer cell [59, 60]. Huge progress has been made in engineering oncolytic viruses with enhanced safety, specificity, oncolytic efficacy, and reduced toxicity [270, 271], which ultimately made the approval of the first oncolytic virus for cancer therapy in 2005 possible [83]. In addition to their oncolytic capabilities, oncolytic viruses can serve as vehicles for the delivery of therapeutic transgenes, whose tumor-specific expression then further enhances the antitumor activity of the virus [69, 72, 78, 272, 273] and opens up opportunities for personalized treatment. However, the factors contributing to virus-mediated tumor regression and therapeutic outcome are not yet fully understood. Immune-mediated oncolysis following viral infection [66], destruction of the tumor vasculature [68, 69] and direct viral oncolysis [65] are debated as possible mechanisms. We previously observed that the kinetics of *in vitro* viral replication correlates with *in vivo* oncolytic function [101]. Therefore, in this study we investigated whether cellular parameters of different molecular biological levels could contribute to or predict VACV replication *in vitro*, thereby typifying a permissive phenotype.

The LIVP derived oncolytic VACV strain GLV-1h68 [102] has been characterized extensively and its antitumor effect demonstrated for many solid cancers [98, 99, 102, 274-277]. Recently, a series of VACV wild-type (wt) clones, derived from a mixed population of the GLV-1h68 parental strain, were characterized regarding replication efficiency, toxicity and therapeutic effect in nude mice (unpublished). Three isolates which showed natural attenuation due to mutations in virulence-related genes were used in this study (LIVP 1.1.1, LIVP 5.1.1, and LIVP 6.1.1.).

In the first part of this work we analyzed the transcription of distinct viral preparations *in vitro* to identify potential markers for permissiveness of cancer cells to VACV infection.

Although cell culture provides enormous benefits, its limitations have to be considered. It has been documented previously that time in culture can alter the gene expression profile of cells drastically [278, 279]. Accordingly, we observed that the gene expression profile of uninfected control samples

greatly varied according to culture time. This variation resulted in a lack of segregation between infected and uninfected samples. However, a multistep filter could determine a list of genes affected specifically by VACV infection.

It has been reported that VACV infection causes major alterations in cell function and metabolism [280], and results in a massive interference with host DNA, RNA, and protein synthesis [93]. Guerra *et al.* [163] classified mRNAs which showed an altered expression pattern after VACV infection of HeLa cells into distinct groups, depending on their kinetics of gene activation or repression. Concordantly, we identified distinct categories of virus-affected genes, involved in broad cellular functions such as cell death, cellular growth and proliferation, post-translational modification, protein synthesis and folding, and DNA replication, recombination and repair. Expectedly, these genes revealed a drastic up- or down-regulation after 48 hours which was similar independent of the viral strain utilized. We, therefore, postulate that initial events, at an early stage of infection can provide more valuable information regarding permissiveness of a given cell line to VACV infection. For this reason, we focused our analysis mainly on data obtained at 2 hpi and 10 hpi.

In parallel to host gene expression, viral gene expression was analyzed to get better insight over the interplay between VACV and its host. Furthermore, VACV gene expression was evaluated as a parameter representative of viral replication. Recently, we showed that GFP-marker gene expression of GLV-1h68 correlates with the respective viral copy number in A375, DU-145, and A549 cells [246]. Similar results were observed in this study, when comparing GLV-1h68 and wt LIVP gene expression and replication, suggesting that viral gene transcription is a valid indicator for viral replication.

VACV messages belong to one of the three temporal expression classes: early, intermediate and late-stage, detectable at 20, 100, and 140 min after infection, respectively [127]. The transcriptional pattern, that we obtained by using a customized VACV array platform, for samples taken prior to infection as well as 2 and 10 hrs after infection with GLV-1h68 and the three wt isolates, reflected the different expression classes and pointed out expressional variances and similarities between the isolates. We observed that viral transcripts formed four different clusters, each with a characteristic time-specific expression pattern. Early after infection (2 hpi), we found a pronounced expression of VACV immune-modulating factors in cluster C4, such as double-stranded RNA binding protein E3, Toll/IL1-receptor inhibitors A46 and A52, and soluble interferon-gamma receptor-like protein B8, amongst others. This is in accordance with current literature, stating that VACV host immune evasion-related genes are expressed in the first stage of infection to secure progeny production [210]. Related to that, we further observed an accumulation of highly expressed structural components and factors involved in particle formation within cluster C2 at a later time point (10 hpi) which depicts the progression in the viral infection cycle.

Using viral array platforms, we identified a group of genes which could be classified as early-stage genes by their gene transcriptional pattern. Comparing the averaged gene expression of those early genes within the different VACV isolates, we found that LIVP 6.1.1 showed the highest mean levels of gene transcription, followed by LIVP 1.1.1 and LIVP 5.1.1, and finally by the attenuated

GLV-1h68 strain. Plaque assay analysis revealed comparable results when looking at viral titers. Similarly, Chen *et al*. [247] observed in a series of recombinant derivatives of GLV-1h68 that viral replication efficiency was proportionate to the number of removed foreign expression cassettes from the GLV-1h68 genome, suggesting that the additional transcriptional and translational load of the inserted transgenes slow down VACV replication. Furthermore, they revealed a positive correlation between replication efficiency *in vitro* and in respective tumor xenografts, as well as an association of virus replication efficiency with antitumor activity [247]. We therefore hypothesize that viral replication is one of the key elements in understanding the biology and underlying mechanisms that form a responsive phenotype.

Little is known about the supportive or inhibitory influence of host cellular factors on VACV replication and in what way interactions between VACV and its host could contribute to the permissiveness of a host cell to infection. For this reason, we first analyzed viral transcripts that featured a strong correlation between their isolate-specific gene transcriptional and replication level, and thus are representative for viral replication. We referred to those genes as viral replication indicators (VRIs). Out of the seven VRIs identified (*F15L*, *G2R*, *G5R*, *D9R*, *A5R*, *A20R*, and *A24R*) five are clearly involved in viral replication or transcription. Among them, we found subunits of the DNA-dependent RNA polymerase, DNA polymerase processivity factor, NTP phosphorylase, and a late transcription elongation factor. It has been reported previously that the DNA polymerase processivity factor A20 interacts with other VACV DNA replication and transcription relevant proteins (D4, D5, E9, and H5) [244]. Poxviruses, like VACV, carry out their entire life cycle, including DNA replication, transcription, and translation, within ER-derived sub-compartments in the cytoplasm of its host cell. In particular, it has been shown that certain cellular factors are required for post-replicative transcription [182, 186, 198, 281]. However, a participation of host factors in viral early gene transcription or DNA replication remains poorly understood. Even though VACV provides all factors and enzymes directly required for DNA and early RNA synthesis packaged within the virus particle, host gene products might affect the efficiency and outcome of the syntheses by either providing a framework or through facilitating molecular interactions and/or transport of components.

In a next step, averaged VRI expression was correlated with the list of human genes obtained via multistep filter, reflecting those genes whose expression is affected specifically due to virus infection. Correlation analysis revealed that 114 human transcripts strongly correlated with VRI expression. These 114 human gene correlates presented a cellular involvement in cell cycle, cell-to-cell signaling and interaction, cellular movement, carbohydrate and lipid metabolism, as well as immunological and inflammatory disease. Among the molecules present in the top network, we found, amongst others *POLR2E* which is a subunit of eukaryotic RNA polymerase II complex, but is also a component of DNA-dependant RNA polymerases I and III. It has been demonstrated that POLR2E interacts with virus proteins [282, 283] and plays a role in viral reproduction and transcription [284]. Moreover, older studies suggest a connection between RNA polymerase II levels and VACV replication

efficiency [285]. However, the fact that *POL2E* expression correlated inversely with VACV replication might indicate that this correlation reflects part of the host gene expressional suppression rather than a contribution to viral reproduction. The 114 human gene correlates further included factors involved in the protein ubiquitination pathway. The conjugation of ubiquitin/ubiquitin-like (Ub/Ubl) molecules to target protein substrates regulates various cellular processes, such as protein turnover, protein targeting, transcription, cell cycle, regulation of cell signal transduction, antigen presentation, and DNA repair [286, 287]. Recent reports highlight the importance of ubiquitination and proteasomal degradation for efficient reproduction and replication of orthopoxviruses [288, 289]. Inhibitors of proteasome and ubiquitin-activating enzyme (E1) potently prevent VACV replication, the formation of viral factories [288], as well as the expression of postreplicative genes [289]. Very recently, Mercer *et al.* [259] published, that proteasomes and ubiquitination act on different steps in early VACV infection. They demonstrated that proteasomes were involved in core breakdown and DNA release, whereas ubiquitination was required for replication of released DNA. However, the exact factors of the Ub/Ubl system that interact with the virus and underlying mechanisms of contribution to replication progression still remain to be further investigated.

In our data set of human correlates with viral replication we found at least six out of 114 molecules to be involved in protein ubiquitination or proteasomal function, including ubiquitin protein ligase E3 component n-recognin 7 (*UBR7*), ubiquitin-conjugating enzyme E2D 4 (*UBE2D4*), cullin 1 (*CUL1*), and proteasome (prosome, macropain) 26S subunit, non-ATPase, 2 (*PSMD2*). In addition to that, *UBR7* was present among the seven intersecting molecules of 114 human correlates and the gene list obtained comparing the low vs. highly permissive group of 15-MEL cell lines, revealing a strong up-regulation within the highly permissive group. Therefore, in accordance with other studies, we concluded that the host proteasome and ubiquitination system is vital, not only in terms of its role in viral replication, but also for a probable contribution to host cell permissiveness to VACV infection.

Additionally, we merged our list of 114 genes, identified through correlation analysis of human gene and VRI expression (thus viral replication), with the 188 genes hit list of host factors required for infection by Mercer *et al*. [259], obtained via RNAi screening. Stunningly, we found three perfect matches and a variety of related molecules between the two data sets, which in turn have been acquired out of thousands of genes each. Among the three perfect matches was *PSMD2*, which supports the importance of the proteasome for viral reproduction once more.

Another molecule of interest which was also present in both data sets is WNK lysine-deficient protein kinase 1 (*WNK1*). WNK 1 belongs to a small family of WNK serine-threonine protein kinases that feature an atypical kinase active site [290, 291] and regulate downstream processes through both kinase activity-dependent and -independent mechanisms [291]. WNK kinases have regulatory functions in ion homeostasis, but are also involved in cell signaling and other processes. The WNK1 protein is a substrate of Akt kinase [292], which in turn has been demonstrated to be related to susceptibility of human cancer cells to infection and killing by oncolytic myxoma virus [293]. Furthermore, activation of the PI3K/Akt kinase pathway plays a role in VACV reproduction [294].

In this study, we discovered that *WNK1* features differences between low and highly permissive cell lines on several molecular biological levels. As mentioned before, we identified *WNK1* among the 114 genes that correlated with viral replication in 888-MEL and 1936-MEL and observed that *WNK1* expression correlated inversely with viral replication. Subsequently, we identified *WNK1* among the seven overlapping molecules between 114 human correlates and the gene list obtained comparing low vs. highly permissive group of 15-MEL cell lines, featuring a down-regulation within the highly permissive group. Furthermore, using miRNA array, we identified six miRNAs to be expressed significantly different between low and highly permissive group. Among them was *miR-107*, which targets *WNK1* messages. Pearson correlation analysis as well as Spearman's rank correlation between *miR-107* and *WNK-1* expression levels revealed a highly significant inverse correlation ($r \leq -0.92$, $p \leq 0.005$), with *WNK1* being down-regulated and *miR-107* being up-regulated in the highly permissive group. Finally, copy number analysis showed, that the *WNK1* gene, located in the tip of chromosome 12, featured amplifications within the low permissive group.

In summary, we found that low *WNK1* levels, confirmed via base line mRNA transcription, miRNA expression, and CNV analysis, correlate with increased permissiveness. Additionally, low *WNK1* expression levels correlate with viral replication efficiency. Taken together, our data suggests that low levels of *WNK1* contribute to the appearance of a permissive phenotype.

Of special interest was also to investigate the predictive strength of the early transcriptional correlates, identified in the two melanoma cell lines (1936-MEL and 888-MEL). A human breast cancer (GI-101A) and a colon carcinoma (HT-29) cell line were used for this purpose and individually infected with GLV-1h68 and five VACV recombinants (GLV-1h70, GLV-1h71, GLV-1h72, GLV-1h73, and GLV-1h74). Applying the same conditions, ten genes could be validated in an independent data set. These included heterogeneous nuclear ribonucleoprotein L (HNRNPL), amongst others. Proteins of the hnRNP family feature wide ranging functions [295-297] and shuttle between the nucleus and the cytoplasm [298]. It has been reported previously that members of the hnRNP family may participate in vaccinia virus late transcription [198, 199] as well as in the replication of other viruses [299]. Functions assigned to hnRNP L include, but are not limited to, an involvement in transport of intronless mRNAs [300, 301], a role in HCV IRES-mediated mRNA translation [302], as well as in mRNA stability. Moreover, Bartel *et al*. [243] identified, via comparative proteome analysis, heterogeneous nuclear ribonucleoproteins B1 and M among a set of modulated human proteins after vaccinia virus IHDW-infection. It is therefore conceivable that hnRNP proteins not only play a role in VACV mRNA transcription, but might also influence VACV replication efficacy and thus contribute to permissiveness of a host cell to VACV infection.

Furthermore, strong negative correlations were detected for ATP synthase, H+ transporting, mitochondrial Fo complex, subunit B1 (ATP5F1) and chemokine (C-C motif) ligand 5 (CCL5). The down-regulation of mitochondrial ATPase expression is considered as a hallmark of several human carcinomas [303, 304]. Therefore, one could speculate about an association between the degree of ATP5F1 down-regulation and permissiveness to VACV treatment. The chemotactic cytokine

CCL5/RANTES in turn is known for its antiviral activity [305]. Yu *et al*. [99] demonstrated, through immune-related protein antigen profiling, a down-regulation of RANTES in pancreatic xenografts in nude mice upon GLV-1h68 infection. An inverse correlation between VACV replication and CCL5 expression could therefore indicate an immune evasion strategy, thereby providing a conductive environment for viral amplification. We further identified DEK oncogene among the ten predictors which also featured an inverse correlation with viral replication. In contrast to that, we observed an up-regulation of DEK in the highly permissive group. Although, *DEK* showed an inverse correlation with viral replication, it features positive expression in comparison with the PBMC reference (log2 ratios between 1.3 and 2.3). One reasonable explanation for this observation could be that DEK acts as a negative regulator of viral replication, where lower levels lead to a more efficient viral propagation. It has been published before, that DEK binds to DNA in a site-specific manner and acts in transcriptional regulation and signal transduction [306]. For HIV it has been demonstrated, that the DEK protein might be involved in the suppression of viral transcription through binding of promoter elements [307]. Additionally, it was shown that DEK decreases the replication efficiency of chromatin-associated DNA [308]. Based on that, our theory of an inhibitory role of DEK in VACV reproduction seems legitimate. An up-regulation of DEK has been shown in several tumors, including melanoma [309], which represents one possible cause for the high baseline expression levels within the highly permissive group. It is conceivable that DEK might be important in initial signaling cascades upon viral infection and is down-regulated thereafter to prevent inhibitory effects on viral replication.

In addition to comparative analysis between host gene expression of infected cells and viral replication, we investigated differences in base line transcription levels, miRNA expression levels, as well as copy number variations in low and highly permissive melanoma cell lines. Our aim was to identify factors of different molecular levels in terms of contribution to composing a permissive phenotype.

Gene transcriptional data suggest that differences between low and highly permissive group are at least in part due to variances in global cellular functions, such as cell cycle, cell growth and proliferation, as well as cell death and survival. We also observed differences in the ubiquitination pathway, which is consistent with our previous results and underlines the importance of this pathway in VACV replication and permissiveness.

When comparing the cellular location dispersion of the top up-regulated vs. the top down-regulated molecules ($fc \geq 2$ and $fc \leq -2$) between high and low group, we observed that a great percentage of up-regulated factors (high group) was located in the nucleus. More than half of these up-regulated nuclear factors featured transcription-regulating function (Additional Table 6-3). It was reported previously, that VACV is able to recruit nuclear host proteins to sites of viral replication upon infection for the use in viral processes [310]. A co-localization of a human transcription factor, namely YY1, with viral replication complexes in the cytoplasm has already been demonstrated in the

past [311]. We therefore hypothesized, that an increased pool of human transcription factors and regulators as well as other nuclear factors, might be beneficial for VACV replication.

Furthermore, we analyzed differences in baseline miRNA expression between low and highly permissive group.

In brief, miRNAs are short non-coding, highly conserved RNA molecules that are able to modulate and control gene expression on a post-transcriptional level through imperfect base pairing with the 3'UTR of target mRNAs. Small RNA-induced effects include RNA degradation, destabilization, or translational inhibition, resulting in regulation of cellular gene expression [312] as well as in antiviral mechanisms [313], among other processes. There is evidence that cellular miRNAs can directly impair viral genome replication and/or gene expression through interaction with viral messages or their RNA genomes [262, 263, 314, 315]. Our results revealed that a set of four miRNAs featured baseline down-regulation in the highly permissive group compared to the low one, namely *miR-93*, *miR-29a*, *miR-487b*, and *miR-148a*. It has been published previously that *miR-29a*, upon HIV-1 infection, influences *Nef* expression (critical for progression of HIV-1 infection) and inhibits replication of HIV-1 [316]. Furthermore, Ostsuka *et al*. [317] demonstrated that the VSV transcript encoding the viral phosphoprotein (P protein) is targeted by *miR-93*, resulting in a decrease of VSV replication. Since viruses are capable to alter the cellular miRNA expression profile [318], it seems reasonable, that these changes not only include immediate antiviral miRNAs, but also exploit the regulatory function of cellular miRNAs to inhibit or promote host gene translation. In our data set we identified a list of human miRNA-mRNA pairings whose expression correlated inversely with strong statistical significance. For example the runt-related transcription factor 3 (*RUNX3*) shows a strong up-regulation in the highly permissive group, whereas, at the same time, its targeting miRNA *miR-93* was down-regulated. Moreover, these data further support the role of human transcription factors for viral replication, as discussed above. Similar results were observed for *WNK1* and *miR-107* expression, also described before.

Finally, copy number variations (CNVs) between low and highly permissive group were evaluated. Structural genomic variants, caused by amplifications and deletions of genomic segments, lead to alterations in the copy number. These genetic variations often change the level of gene expression which in turn can contribute to disease development, especially cancer formation. However, the relationship between aberrations in gene copy number and respective gene expression is not clear-cut and remains to be elucidated. In addition to that, the effects of CNVs in non-expressed regions are even harder to interpret [319].

In this study, when investigating differences in the chromosomal aberration pattern between low and highly permissive group, we observed frequent segmental amplifications within the low permissive group, whereas the same regions were mostly unchanged in the high group. Following annotation with gene symbols, analysis of variances (ANOVA) between low and high group resulted in a list of 2,652 genes located in the chromosomal regions that varied in-between the two groups. Ingenuity

pathway analyses revealed an involvement of these genes in broad cellular functions such as cell cycle, cell-to-cell signaling, cell growth and proliferation, as well as in disease related signaling, including metabolic disease, infectious disease, and inflammatory response. Investigating the canonical pathways supported by those genes, we found enrichment in a variety of pathways of the cellular immune response such as cytokine-mediated communication between immune cells, crosstalk between dendritic cells and NK cells, granzyme A signaling and others. Interestingly, we observed a discrepancy between copy number and gene expression data. While copy number classification plots indicate gene amplifications interspersed throughout most chromosomes in the low group, gene expression data reveal an up-regulation of genes predominantly within the high group which suggests that in this case CNVs do not lead to a gene dosage effect.

Typically, it was assumed that the immune system would hinder virus spread through viral clearance and thus limit the efficacy of oncolytic virotherapy (OV). However, recent studies revealed that OV can actually stimulate antitumor immunity, thereby acting similar to a cancer immunotherapeutic agent [66, 79, 320]. To what extent pre-existing, not virus-induced immune-related pathways contribute to antitumor activity or permissiveness to virus infection is not clear. It was reported previously, that in cell culture a pre-treatment of human fibroblasts with interferon-γ did not block VACV replication. For our study it has to be considered that all results were obtained from *in vitro* samples which can only provide limited insights regarding host cell immunity.

In summary, we identified several parameters that may be useful for the ultimate understanding of how VACV and host cells interact. We observed that a subset of VACV early transcripts is mostly associated with variability in permissiveness of cell lines to VACV infection. Among them, we identified viral transcripts that correlated strictly with viral replication at 2 hpi respectively as judged by the functional plaque forming units assay. Further, we identified a set of human genes which are likely to affect viral replication, with a subset revealing predictive potential regarding VACV replicative efficiency in an independent data set.

Furthermore, we discovered variances between low and highly permissive cell lines on different molecular biological levels, including gene transcription, miRNA expression, and DNA copy number.

Although more comprehensive studies will be needed to validate these findings, the discovery of host factors which influence viral replication could provide valuable information about host cell permissiveness to oncolytic virotherapy and therapeutic efficiency. For future studies, investigation of virus-host interaction in animal models and different tumor types appears to be appropriate to get better insight over the communication between virus and host in terms of host permissiveness to OV. The ability to predict response to VACV treatment through convenient screening procedures could facilitate to determine whether OV is effective in a patient. Moreover, knowledge about factors that limit or promote virus replication and host cell permissiveness could help engineering novel oncolytic viruses that are capable to circumvent inhibitory effects or feature more efficient oncolytic activity, respectively.

5 References

1. World Health Organisation, I.A.f.R.o.C., *World Cancer Report*. 2008: Lyon.
2. Hanahan, D. and R.A. Weinberg, *The hallmarks of cancer.* Cell, 2000. **100**(1): p. 57-70.
3. Hanahan, D. and R.A. Weinberg, *Hallmarks of cancer: the next generation.* Cell, 2011. **144**(5): p. 646-74.
4. Hecht, S.S., *Tobacco smoke carcinogens and lung cancer.* J Natl Cancer Inst, 1999. **91**(14): p. 1194-210.
5. Colditz, G.A., T.A. Sellers, and E. Trapido, *Epidemiology - identifying the causes and preventability of cancer?* Nat Rev Cancer, 2006. **6**(1): p. 75-83.
6. Peto, J., *Cancer epidemiology in the last century and the next decade.* Nature, 2001. **411**(6835): p. 390-5.
7. Boyle, P., et al., *European Code Against Cancer and scientific justification: third version (2003).* Ann Oncol, 2003. **14**(7): p. 973-1005.
8. Herceg, Z. and P. Hainaut, *Genetic and epigenetic alterations as biomarkers for cancer detection, diagnosis and prognosis.* Mol Oncol, 2007. **1**(1): p. 26-41.
9. Croce, C.M., *Oncogenes and cancer.* N Engl J Med, 2008. **358**(5): p. 502-11.
10. Weinberg, R.A., *How cancer arises.* Sci Am, 1996. **275**(3): p. 62-70.
11. Vousden, K.H. and X. Lu, *Live or let die: the cell's response to p53.* Nat Rev Cancer, 2002. **2**(8): p. 594-604.
12. Greenblatt, M.S., et al., *Mutations in the p53 tumor suppressor gene: clues to cancer etiology and molecular pathogenesis.* Cancer Res, 1994. **54**(18): p. 4855-78.
13. Schmitt, C.A., et al., *Dissecting p53 tumor suppressor functions in vivo.* Cancer Cell, 2002. **1**(3): p. 289-98.
14. Weinberg, R.A., *The retinoblastoma protein and cell cycle control.* Cell, 1995. **81**(3): p. 323-30.
15. Liggett, W.H., Jr. and D. Sidransky, *Role of the p16 tumor suppressor gene in cancer.* J Clin Oncol, 1998. **16**(3): p. 1197-206.
16. Kaino, M., *Alterations in the tumor suppressor genes p53, RB, p16/MTS1, and p15/MTS2 in human pancreatic cancer and hepatoma cell lines.* J Gastroenterol, 1997. **32**(1): p. 40-6.
17. Greider, C.W. and E.H. Blackburn, *Telomeres, telomerase and cancer.* Sci Am, 1996. **274**(2): p. 92-7.
18. Iorio, M.V. and C.M. Croce, *microRNA involvement in human cancer.* Carcinogenesis, 2012. **33**(6): p. 1126-33.
19. Calin, G.A. and C.M. Croce, *MicroRNA signatures in human cancers.* Nat Rev Cancer, 2006. **6**(11): p. 857-66.
20. Calin, G.A. and C.M. Croce, *MicroRNA-cancer connection: the beginning of a new tale.* Cancer Res, 2006. **66**(15): p. 7390-4.
21. Calin, G.A., et al., *MicroRNA profiling reveals distinct signatures in B cell chronic lymphocytic leukemias.* Proc Natl Acad Sci U S A, 2004. **101**(32): p. 11755-60.
22. Calin, G.A., et al., *Human microRNA genes are frequently located at fragile sites and genomic regions involved in cancers.* Proc Natl Acad Sci U S A, 2004. **101**(9): p. 2999-3004.
23. Lu, J., et al., *MicroRNA expression profiles classify human cancers.* Nature, 2005. **435**(7043): p. 834-8.
24. Pharoah, P.D., et al., *Association studies for finding cancer-susceptibility genetic variants.* Nat Rev Cancer, 2004. **4**(11): p. 850-60.
25. Lindor, N.M., et al., *Concise handbook of familial cancer susceptibility syndromes - second edition.* J Natl Cancer Inst Monogr, 2008(38): p. 1-93.
26. Armstrong, B.K. and A. Kricker, *The epidemiology of UV induced skin cancer.* J Photochem Photobiol B, 2001. **63**(1-3): p. 8-18.

27. Gandini, S., et al., *Meta-analysis of risk factors for cutaneous melanoma: I. Common and atypical naevi.* Eur J Cancer, 2005. **41**(1): p. 28-44.
28. Gandini, S., et al., *Meta-analysis of risk factors for cutaneous melanoma: II. Sun exposure.* Eur J Cancer, 2005. **41**(1): p. 45-60.
29. Gandini, S., et al., *Meta-analysis of risk factors for cutaneous melanoma: III. Family history, actinic damage and phenotypic factors.* Eur J Cancer, 2005. **41**(14): p. 2040-59.
30. IARC, *The association of use of sunbeds with cutaneous malignant melanoma and other skin cancers: A systematic review.* Int J Cancer, 2007. **120**(5): p. 1116-22.
31. Whiteman, D.C., et al., *Melanocytic nevi, solar keratoses, and divergent pathways to cutaneous melanoma.* J Natl Cancer Inst, 2003. **95**(11): p. 806-12.
32. Gray-Schopfer, V., C. Wellbrock, and R. Marais, *Melanoma biology and new targeted therapy.* Nature, 2007. **445**(7130): p. 851-7.
33. Qi, M. and E.A. Elion, *MAP kinase pathways.* J Cell Sci, 2005. **118**(Pt 16): p. 3569-72.
34. Cohen, C., et al., *Mitogen-actived protein kinase activation is an early event in melanoma progression.* Clin Cancer Res, 2002. **8**(12): p. 3728-33.
35. Satyamoorthy, K., et al., *Constitutive mitogen-activated protein kinase activation in melanoma is mediated by both BRAF mutations and autocrine growth factor stimulation.* Cancer Res, 2003. **63**(4): p. 756-9.
36. Davies, H., et al., *Mutations of the BRAF gene in human cancer.* Nature, 2002. **417**(6892): p. 949-54.
37. Gray-Schopfer, V.C., S. da Rocha Dias, and R. Marais, *The role of B-RAF in melanoma.* Cancer Metastasis Rev, 2005. **24**(1): p. 165-83.
38. Sharma, A., et al., *Mutant V599EB-Raf regulates growth and vascular development of malignant melanoma tumors.* Cancer Res, 2005. **65**(6): p. 2412-21.
39. Bhatt, K.V., et al., *Adhesion control of cyclin D1 and p27Kip1 levels is deregulated in melanoma cells through BRAF-MEK-ERK signaling.* Oncogene, 2005. **24**(21): p. 3459-71.
40. Gray-Schopfer, V.C., et al., *Cellular senescence in naevi and immortalisation in melanoma: a role for p16?* Br J Cancer, 2006. **95**(4): p. 496-505.
41. Satyamoorthy, K. and M. Herlyn, *p16INK4A and familial melanoma.* Methods Mol Biol, 2003. **222**: p. 185-95.
42. Omholt, K., et al., *Mutations of PIK3CA are rare in cutaneous melanoma.* Melanoma Res, 2006. **16**(2): p. 197-200.
43. Wu, H., V. Goel, and F.G. Haluska, *PTEN signaling pathways in melanoma.* Oncogene, 2003. **22**(20): p. 3113-22.
44. Stahl, J.M., et al., *Deregulated Akt3 activity promotes development of malignant melanoma.* Cancer Res, 2004. **64**(19): p. 7002-10.
45. Levy, C., M. Khaled, and D.E. Fisher, *MITF: master regulator of melanocyte development and melanoma oncogene.* Trends Mol Med, 2006. **12**(9): p. 406-14.
46. Omholt, K., et al., *Cytoplasmic and nuclear accumulation of beta-catenin is rarely caused by CTNNB1 exon 3 mutations in cutaneous malignant melanoma.* Int J Cancer, 2001. **92**(6): p. 839-42.
47. Worm, J., et al., *Genetic and epigenetic alterations of the APC gene in malignant melanoma.* Oncogene, 2004. **23**(30): p. 5215-26.
48. Schaffer, J.V. and J.L. Bolognia, *The melanocortin-1 receptor: red hair and beyond.* Arch Dermatol, 2001. **137**(11): p. 1477-85.
49. van den Hurk, K., et al., *Genetics and epigenetics of cutaneous malignant melanoma: A concert out of tune.* Biochim Biophys Acta, 2012. **1826**(1): p. 89-102.
50. Sabatino, M., et al., *Conservation of genetic alterations in recurrent melanoma supports the melanoma stem cell hypothesis.* Cancer Res, 2008. **68**(1): p. 122-31.
51. Wang, E., et al., *Clonal persistence and evolution during a decade of recurrent melanoma.* J Invest Dermatol, 2006. **126**(6): p. 1372-7.
52. Pollock, R.E. and D.L. Morton, *surgical oncology*, in *Holland-Frei Cancer Medicine, 7th edition*. 2006, BC Decker.
53. Dougan, M. and G. Dranoff, *Immune therapy for cancer.* Annu Rev Immunol, 2009. **27**: p. 83-117.

54. Huo, Q., N. Zhang, and Q. Yang, *Epstein-Barr virus infection and sporadic breast cancer risk: a meta-analysis.* PLoS One, 2012. **7**(2): p. e31656.
55. Epstein, M.A., *Epstein-Barr virus as the cause of a human cancer.* Nature, 1978. **274**(5673): p. 740.
56. Thompson, M.P. and R. Kurzrock, *Epstein-Barr virus and cancer.* Clin Cancer Res, 2004. **10**(3): p. 803-21.
57. zur Hausen, H., *Cervical carcinoma and human papillomavirus: on the road to preventing a major human cancer.* J Natl Cancer Inst, 2001. **93**(4): p. 252-3.
58. Schiffman, M., et al., *Human papillomavirus and cervical cancer.* Lancet, 2007. **370**(9590): p. 890-907.
59. Zeh, H.J. and D.L. Bartlett, *Development of a replication-selective, oncolytic poxvirus for the treatment of human cancers.* Cancer Gene Ther, 2002. **9**(12): p. 1001-12.
60. Guo, Z.S., S.H. Thorne, and D.L. Bartlett, *Oncolytic virotherapy: molecular targets in tumor-selective replication and carrier cell-mediated delivery of oncolytic viruses.* Biochim Biophys Acta, 2008. **1785**(2): p. 217-31.
61. Dock, G., *The influence of complicating diseases upon leukaemia.* American Journal of the Medical Sciences, 1904. **127**(4): p. 563-592.
62. Moore, A.E., *Viruses with oncolytic properties and their adaptation to tumors.* Ann N Y Acad Sci, 1952. **54**(6): p. 945-52.
63. Kelly, E. and S.J. Russell, *History of oncolytic viruses: genesis to genetic engineering.* Mol Ther, 2007. **15**(4): p. 651-9.
64. Roberts, M.S., et al., *Naturally occurring viruses for the treatment of cancer.* Discov Med, 2006. **6**(36): p. 217-22.
65. Weibel, S., et al., *Viral-mediated oncolysis is the most critical factor in the late-phase of the tumor regression process upon vaccinia virus infection.* BMC Cancer, 2011. **11**: p. 68.
66. Prestwich, R.J., et al., *The case of oncolytic viruses versus the immune system: waiting on the judgment of Solomon.* Hum Gene Ther, 2009. **20**(10): p. 1119-32.
67. Shtrichman, R. and T. Kleinberger, *Adenovirus type 5 E4 open reading frame 4 protein induces apoptosis in transformed cells.* J Virol, 1998. **72**(4): p. 2975-82.
68. Tysome, J.R., N.R. Lemoine, and Y. Wang, *Combination of anti-angiogenic therapy and virotherapy: arming oncolytic viruses with anti-angiogenic genes.* Curr Opin Mol Ther, 2009. **11**(6): p. 664-9.
69. Frentzen, A., et al., *Anti-VEGF single-chain antibody GLAF-1 encoded by oncolytic vaccinia virus significantly enhances antitumor therapy.* Proc Natl Acad Sci U S A, 2009. **106**(31): p. 12915-20.
70. Guffey, M.B., et al., *Engineered herpes simplex virus expressing bacterial cytosine deaminase for experimental therapy of brain tumors.* Cancer Gene Ther, 2007. **14**(1): p. 45-56.
71. Schepelmann, S. and C.J. Springer, *Viral vectors for gene-directed enzyme prodrug therapy.* Curr Gene Ther, 2006. **6**(6): p. 647-70.
72. McCart, J.A., et al., *Complex interactions between the replicating oncolytic effect and the enzyme/prodrug effect of vaccinia-mediated tumor regression.* Gene Ther, 2000. **7**(14): p. 1217-23.
73. Seubert, C.M., et al., *Enhanced tumor therapy using vaccinia virus strain GLV-1h68 in combination with a beta-galactosidase-activatable prodrug seco-analog of duocarmycin SA.* Cancer Gene Ther, 2011. **18**(1): p. 42-52.
74. Zhang, X., et al., *Treatment of radioresistant stem-like esophageal cancer cells by an apoptotic gene-armed, telomerase-specific oncolytic adenovirus.* Clin Cancer Res, 2008. **14**(9): p. 2813-23.
75. Boisgerault, N., F. Tangy, and M. Gregoire, *New perspectives in cancer virotherapy: bringing the immune system into play.* Immunotherapy, 2010. **2**(2): p. 185-99.
76. Errington, F., et al., *Reovirus activates human dendritic cells to promote innate antitumor immunity.* J Immunol, 2008. **180**(9): p. 6018-26.
77. Errington, F., et al., *Inflammatory tumour cell killing by oncolytic reovirus for the treatment of melanoma.* Gene Ther, 2008. **15**(18): p. 1257-70.

78. Kim, J.H., et al., *Systemic armed oncolytic and immunologic therapy for cancer with JX-594, a targeted poxvirus expressing GM-CSF.* Mol Ther, 2006. **14**(3): p. 361-70.
79. Prestwich, R.J., et al., *Oncolytic viruses: a novel form of immunotherapy.* Expert Rev Anticancer Ther, 2008. **8**(10): p. 1581-8.
80. Prestwich, R.J., et al., *Immunotherapeutic potential of oncolytic virotherapy.* Lancet Oncol, 2008. **9**(7): p. 610-2.
81. http://www.clinicaltrials.gov/, U.S. National Library of Medicine, National Institutes of Health.
82. Donnelly, O.G., et al., *Recent clinical experience with oncolytic viruses.* Curr Pharm Biotechnol, 2011. **13**(9): p. 1834-41.
83. Garber, K., *China approves world's first oncolytic virus therapy for cancer treatment.* J Natl Cancer Inst, 2006. **98**(5): p. 298-300.
84. Hendrickson, R.C., et al., *Orthopoxvirus genome evolution: the role of gene loss.* Viruses, 2010. **2**(9): p. 1933-67.
85. Emerson, G.L., et al., *The phylogenetics and ecology of the orthopoxviruses endemic to North America.* PLoS One, 2009. **4**(10): p. e7666.
86. Werden, S.J., M.M. Rahman, and G. McFadden, *Poxvirus host range genes.* Adv Virus Res, 2008. **71**: p. 135-71.
87. Riedel, S., *Edward Jenner and the history of smallpox and vaccination.* Proc (Bayl Univ Med Cent), 2005. **18**(1): p. 21-5.
88. Fenner, F., *The global eradication of smallpox.* Med J Aust, 1980. **1**(10): p. 455-5.
89. Fenner, F., et al., *Smallpox and its Eradication*, in *WHO*. 1988: Geneva.
90. Baxby, D., *The origins of vaccinia virus.* J Infect Dis, 1977. **136**(3): p. 453-5.
91. Smith, G.L. and B. Moss, *Infectious poxvirus vectors have capacity for at least 25 000 base pairs of foreign DNA.* Gene, 1983. **25**(1): p. 21-8.
92. Falkner, F.G. and B. Moss, *Transient dominant selection of recombinant vaccinia viruses.* J Virol, 1990. **64**(6): p. 3108-11.
93. Moss, B., *Poxviridae: The Viruses and their Replication*. Fields Virology, ed. D.M.K.P.M. Howley. 2007, Philadelphia: Lippincott Williams & Wilkins.
94. McFadden, G., *Poxvirus tropism.* Nat Rev Microbiol, 2005. **3**(3): p. 201-13.
95. McCart, J.A., et al., *Systemic cancer therapy with a tumor-selective vaccinia virus mutant lacking thymidine kinase and vaccinia growth factor genes.* Cancer Res, 2001. **61**(24): p. 8751-7.
96. Buller, R.M., et al., *Decreased virulence of recombinant vaccinia virus expression vectors is associated with a thymidine kinase-negative phenotype.* Nature, 1985. **317**(6040): p. 813-5.
97. Puhlmann, M., et al., *Vaccinia as a vector for tumor-directed gene therapy: biodistribution of a thymidine kinase-deleted mutant.* Cancer Gene Ther, 2000. **7**(1): p. 66-73.
98. Gentschev, I., et al., *Regression of human prostate tumors and metastases in nude mice following treatment with the recombinant oncolytic vaccinia virus GLV-1h68.* J Biomed Biotechnol, 2010. **2010**: p. 489759.
99. Yu, Y.A., et al., *Regression of human pancreatic tumor xenografts in mice after a single systemic injection of recombinant vaccinia virus GLV-1h68.* Mol Cancer Ther, 2009. **8**(1): p. 141-51.
100. Kirn, D.H., et al., *Enhancing poxvirus oncolytic effects through increased spread and immune evasion.* Cancer Res, 2008. **68**(7): p. 2071-5.
101. Worschech, A., et al., *Systemic treatment of xenografts with vaccinia virus GLV-1h68 reveals the immunologic facet of oncolytic therapy.* BMC Genomics, 2009. **10**: p. 301.
102. Zhang, Q., et al., *Eradication of solid human breast tumors in nude mice with an intravenously injected light-emitting oncolytic vaccinia virus.* Cancer Res, 2007. **67**(20): p. 10038-46.
103. Advani, S.J., et al., *Preferential replication of systemically delivered oncolytic vaccinia virus in focally irradiated glioma xenografts.* Clin Cancer Res, 2012. **18**(9): p. 2579-90.
104. Lun, X.Q., et al., *Efficacy of systemically administered oncolytic vaccinia virotherapy for malignant gliomas is enhanced by combination therapy with rapamycin or cyclophosphamide.* Clin Cancer Res, 2009. **15**(8): p. 2777-88.

105. Guse, K., V. Cerullo, and A. Hemminki, *Oncolytic vaccinia virus for the treatment of cancer.* Expert Opin Biol Ther, 2011. **11**(5): p. 595-608.
106. Garon, C.F., E. Barbosa, and B. Moss, *Visualization of an inverted terminal repetition in vaccinia virus DNA.* Proc Natl Acad Sci U S A, 1978. **75**(10): p. 4863-7.
107. Baroudy, B.M., S. Venkatesan, and B. Moss, *Incompletely base-paired flip-flop terminal loops link the two DNA strands of the vaccinia virus genome into one uninterrupted polynucleotide chain.* Cell, 1982. **28**(2): p. 315-24.
108. DeLange, A.M. and G. McFadden, *Efficient resolution of replicated poxvirus telomeres to native hairpin structures requires two inverted symmetrical copies of a core target DNA sequence.* J Virol, 1987. **61**(6): p. 1957-63.
109. Merchlinsky, M., *Mutational analysis of the resolution sequence of vaccinia virus DNA: essential sequence consists of two separate AT-rich regions highly conserved among poxviruses.* J Virol, 1990. **64**(10): p. 5029-35.
110. Cyrklaff, M., et al., *Cryo-electron tomography of vaccinia virus.* Proc Natl Acad Sci U S A, 2005. **102**(8): p. 2772-7.
111. Roberts, K.L. and G.L. Smith, *Vaccinia virus morphogenesis and dissemination.* Trends Microbiol, 2008. **16**(10): p. 472-9.
112. Goebel, S.J., et al., *The complete DNA sequence of vaccinia virus.* Virology, 1990. **179**(1): p. 247-66, 517-63.
113. Schmidt, F.I., C.K. Bleck, and J. Mercer, *Poxvirus host cell entry.* Curr Opin Virol, 2012. **2**(1): p. 20-7.
114. Hsiao, J.C., C.S. Chung, and W. Chang, *Vaccinia virus envelope D8L protein binds to cell surface chondroitin sulfate and mediates the adsorption of intracellular mature virions to cells.* J Virol, 1999. **73**(10): p. 8750-61.
115. Chiu, W.L., et al., *Vaccinia virus 4c (A26L) protein on intracellular mature virus binds to the extracellular cellular matrix laminin.* J Virol, 2007. **81**(5): p. 2149-57.
116. Chung, C.S., et al., *A27L protein mediates vaccinia virus interaction with cell surface heparan sulfate.* J Virol, 1998. **72**(2): p. 1577-85.
117. Hsiao, J.C., C.S. Chung, and W. Chang, *Cell surface proteoglycans are necessary for A27L protein-mediated cell fusion: identification of the N-terminal region of A27L protein as the glycosaminoglycan-binding domain.* J Virol, 1998. **72**(10): p. 8374-9.
118. Lin, C.L., et al., *Vaccinia virus envelope H3L protein binds to cell surface heparan sulfate and is important for intracellular mature virion morphogenesis and virus infection in vitro and in vivo.* J Virol, 2000. **74**(7): p. 3353-65.
119. Vanderplasschen, A. and G.L. Smith, *A novel virus binding assay using confocal microscopy: demonstration that the intracellular and extracellular vaccinia virions bind to different cellular receptors.* J Virol, 1997. **71**(5): p. 4032-41.
120. White, J.M., et al., *Structures and mechanisms of viral membrane fusion proteins: multiple variations on a common theme.* Crit Rev Biochem Mol Biol, 2008. **43**(3): p. 189-219.
121. Mercer, J. and A. Helenius, *Virus entry by macropinocytosis.* Nat Cell Biol, 2009. **11**(5): p. 510-20.
122. Mercer, J., et al., *Vaccinia virus strains use distinct forms of macropinocytosis for host-cell entry.* Proc Natl Acad Sci U S A, 2010. **107**(20): p. 9346-51.
123. Senkevich, T.G., et al., *Poxvirus multiprotein entry-fusion complex.* Proc Natl Acad Sci U S A, 2005. **102**(51): p. 18572-7.
124. Moss, B., *Poxvirus cell entry: how many proteins does it take?* Viruses, 2012. **4**(5): p. 688-707.
125. Carter, G.C., et al., *Vaccinia virus cores are transported on microtubules.* J Gen Virol, 2003. **84**(Pt 9): p. 2443-58.
126. Mallardo, M., S. Schleich, and J. Krijnse Locker, *Microtubule-dependent organization of vaccinia virus core-derived early mRNAs into distinct cytoplasmic structures.* Mol Biol Cell, 2001. **12**(12): p. 3875-91.
127. Baldick, C.J., Jr. and B. Moss, *Characterization and temporal regulation of mRNAs encoded by vaccinia virus intermediate-stage genes.* J Virol, 1993. **67**(6): p. 3515-27.
128. Cairns, J., *The initiation of vaccinia infection.* Virology, 1960. **11**: p. 603-23.

129. Tolonen, N., et al., *Vaccinia virus DNA replication occurs in endoplasmic reticulum-enclosed cytoplasmic mini-nuclei.* Mol Biol Cell, 2001. **12**(7): p. 2031-46.
130. Boyle, K. and P. Traktman, *Poxviruses*, in *Viral Genome Replication*, C.E. Cameron, M. Götte, and K.D. Raney, Editors. 2009, Springer Science+Business Media LLC: New York. p. 225-248.
131. Traktman, P., M. Kelvin, and S. Pacheco, *Molecular genetic analysis of vaccinia virus DNA polymerase mutants.* J Virol, 1989. **63**(2): p. 841-6.
132. McDonald, W.F., V. Crozel-Goudot, and P. Traktman, *Transient expression of the vaccinia virus DNA polymerase is an intrinsic feature of the early phase of infection and is unlinked to DNA replication and late gene expression.* J Virol, 1992. **66**(1): p. 534-47.
133. Challberg, M.D. and P.T. Englund, *The effect of template secondary structure on vaccinia DNA polymerase.* J Biol Chem, 1979. **254**(16): p. 7820-6.
134. Challberg, M.D. and P.T. Englund, *Purification and properties of the deoxyribonucleic acid polymerase induced by vaccinia virus.* J Biol Chem, 1979. **254**(16): p. 7812-9.
135. Hamilton, M.D. and D.H. Evans, *Enzymatic processing of replication and recombination intermediates by the vaccinia virus DNA polymerase.* Nucleic Acids Res, 2005. **33**(7): p. 2259-68.
136. Stanitsa, E.S., L. Arps, and P. Traktman, *Vaccinia virus uracil DNA glycosylase interacts with the A20 protein to form a heterodimeric processivity factor for the viral DNA polymerase.* J Biol Chem, 2006. **281**(6): p. 3439-51.
137. Punjabi, A., et al., *Clustered charge-to-alanine mutagenesis of the vaccinia virus A20 gene: temperature-sensitive mutants have a DNA-minus phenotype and are defective in the production of processive DNA polymerase activity.* J Virol, 2001. **75**(24): p. 12308-18.
138. Klemperer, N., et al., *The A20R protein is a stoichiometric component of the processive form of vaccinia virus DNA polymerase.* J Virol, 2001. **75**(24): p. 12298-307.
139. Boyle, K.A., L. Arps, and P. Traktman, *Biochemical and genetic analysis of the vaccinia virus d5 protein: Multimerization-dependent ATPase activity is required to support viral DNA replication.* J Virol, 2007. **81**(2): p. 844-59.
140. Evans, E., et al., *The vaccinia virus D5 protein, which is required for DNA replication, is a nucleic acid-independent nucleoside triphosphatase.* J Virol, 1995. **69**(9): p. 5353-61.
141. Lin, Y.C., et al., *Vaccinia virus DNA ligase recruits cellular topoisomerase II to sites of viral replication and assembly.* J Virol, 2008. **82**(12): p. 5922-32.
142. Paran, N., et al., *Cellular DNA ligase I is recruited to cytoplasmic vaccinia virus factories and masks the role of the vaccinia ligase in viral DNA replication.* Cell Host Microbe, 2009. **6**(6): p. 563-9.
143. Tseng, M., et al., *DNA binding and aggregation properties of the vaccinia virus I3L gene product.* J Biol Chem, 1999. **274**(31): p. 21637-44.
144. Rochester, S.C. and P. Traktman, *Characterization of the single-stranded DNA binding protein encoded by the vaccinia virus I3 gene.* J Virol, 1998. **72**(4): p. 2917-26.
145. D'Costa, S.M., et al., *Vaccinia H5 is a multifunctional protein involved in viral DNA replication, postreplicative gene transcription, and virion morphogenesis.* Virology, 2010. **401**(1): p. 49-60.
146. Senkevich, T.G., E.V. Koonin, and B. Moss, *Predicted poxvirus FEN1-like nuclease required for homologous recombination, double-strand break repair and full-size genome formation.* Proc Natl Acad Sci U S A, 2009. **106**(42): p. 17921-6.
147. Garcia, A.D., et al., *Quaternary structure and cleavage specificity of a poxvirus holliday junction resolvase.* J Biol Chem, 2006. **281**(17): p. 11618-26.
148. Culyba, M.J., et al., *DNA branch nuclease activity of vaccinia A22 resolvase.* J Biol Chem, 2007. **282**(48): p. 34644-52.
149. Grubisha, O. and P. Traktman, *Genetic analysis of the vaccinia virus I6 telomere-binding protein uncovers a key role in genome encapsidation.* J Virol, 2003. **77**(20): p. 10929-42.
150. Cassetti, M.C., et al., *DNA packaging mutant: repression of the vaccinia virus A32 gene results in noninfectious, DNA-deficient, spherical, enveloped particles.* J Virol, 1998. **72**(7): p. 5769-80.

151. Lin, S., W. Chen, and S.S. Broyles, *The vaccinia virus B1R gene product is a serine/threonine protein kinase.* J Virol, 1992. **66**(5): p. 2717-23.
152. Wiebe, M.S. and P. Traktman, *Poxviral B1 kinase overcomes barrier to autointegration factor, a host defense against virus replication.* Cell Host Microbe, 2007. **1**(3): p. 187-97.
153. Nichols, R.J., M.S. Wiebe, and P. Traktman, *The vaccinia-related kinases phosphorylate the N' terminus of BAF, regulating its interaction with DNA and its retention in the nucleus.* Mol Biol Cell, 2006. **17**(5): p. 2451-64.
154. Pogo, B.G., M. O'Shea, and P. Freimuth, *Initiation and termination of vaccinia virus DNA replication.* Virology, 1981. **108**(1): p. 241-8.
155. Pogo, B.G., *Changes in parental vaccinia virus DNA after viral penetration into cells.* Virology, 1980. **101**(2): p. 520-4.
156. Boyle, K.A., et al., *Evaluation of the role of the vaccinia virus uracil DNA glycosylase and A20 proteins as intrinsic components of the DNA polymerase holoenzyme.* J Biol Chem, 2011. **286**(28): p. 24702-13.
157. McCraith, S., et al., *Genome-wide analysis of vaccinia virus protein-protein interactions.* Proc Natl Acad Sci U S A, 2000. **97**(9): p. 4879-84.
158. Moyer, R.W. and R.L. Graves, *The mechanism of cytoplasmic orthopoxvirus DNA replication.* Cell, 1981. **27**(2 Pt 1): p. 391-401.
159. Stuart, D., et al., *The target DNA sequence for resolution of poxvirus replicative intermediates is an active late promoter.* J Virol, 1991. **65**(1): p. 61-70.
160. Hu, F.Q. and D.J. Pickup, *Transcription of the terminal loop region of vaccinia virus DNA is initiated from the telomere sequences directing DNA resolution.* Virology, 1991. **181**(2): p. 716-20.
161. Harrison, S.C., et al., *Discovery of antivirals against smallpox.* Proc Natl Acad Sci U S A, 2004. **101**(31): p. 11178-92.
162. Traktman, P. 2012; Available from: www.mcw.edu/microbiology/PaulaTraktman.htm.
163. Guerra, S., et al., *Cellular gene expression survey of vaccinia virus infection of human HeLa cells.* J Virol, 2003. **77**(11): p. 6493-506.
164. Walsh, D. and I. Mohr, *Viral subversion of the host protein synthesis machinery.* Nat Rev Microbiol, 2011. **9**(12): p. 860-75.
165. Yang, Z., et al., *Simultaneous high-resolution analysis of vaccinia virus and host cell transcriptomes by deep RNA sequencing.* Proc Natl Acad Sci U S A, 2010. **107**(25): p. 11513-8.
166. Boone, R.F. and B. Moss, *Sequence complexity and relative abundance of vaccinia virus mRNA's synthesized in vivo and in vitro.* J Virol, 1978. **26**(3): p. 554-69.
167. Davison, A.J. and B. Moss, *Structure of vaccinia virus early promoters.* J Mol Biol, 1989. **210**(4): p. 749-69.
168. Broyles, S.S. and B.S. Fesler, *Vaccinia virus gene encoding a component of the viral early transcription factor.* J Virol, 1990. **64**(4): p. 1523-9.
169. Gershon, P.D. and B. Moss, *Early transcription factor subunits are encoded by vaccinia virus late genes.* Proc Natl Acad Sci U S A, 1990. **87**(11): p. 4401-5.
170. Cassetti, M.A. and B. Moss, *Interaction of the 82-kDa subunit of the vaccinia virus early transcription factor heterodimer with the promoter core sequence directs downstream DNA binding of the 70-kDa subunit.* Proc Natl Acad Sci U S A, 1996. **93**(15): p. 7540-5.
171. Broyles, S.S. and B. Moss, *DNA-dependent ATPase activity associated with vaccinia virus early transcription factor.* J Biol Chem, 1988. **263**(22): p. 10761-5.
172. Yang, Z. and B. Moss, *Interaction of the vaccinia virus RNA polymerase-associated 94-kilodalton protein with the early transcription factor.* J Virol, 2009. **83**(23): p. 12018-26.
173. Yuen, L. and B. Moss, *Oligonucleotide sequence signaling transcriptional termination of vaccinia virus early genes.* Proc Natl Acad Sci U S A, 1987. **84**(18): p. 6417-21.
174. Deng, L. and S. Shuman, *Vaccinia NPH-I, a DExH-box ATPase, is the energy coupling factor for mRNA transcription termination.* Genes Dev, 1998. **12**(4): p. 538-46.
175. Christen, L.M., et al., *Vaccinia virus nucleoside triphosphate phosphohydrolase I is an essential viral early gene transcription termination factor.* Virology, 1998. **245**(2): p. 360-71.

176. Hagler, J. and S. Shuman, *A freeze-frame view of eukaryotic transcription during elongation and capping of nascent mRNA.* Science, 1992. **255**(5047): p. 983-6.
177. Gershon, P.D., et al., *Poly(A) polymerase and a dissociable polyadenylation stimulatory factor encoded by vaccinia virus.* Cell, 1991. **66**(6): p. 1269-78.
178. Yang, Z., et al., *Expression profiling of the intermediate and late stages of poxvirus replication.* J Virol, 2011. **85**(19): p. 9899-908.
179. Vos, J.C., M. Sasker, and H.G. Stunnenberg, *Vaccinia virus capping enzyme is a transcription initiation factor.* EMBO J, 1991. **10**(9): p. 2553-8.
180. Rosales, R., et al., *Purification and identification of a vaccinia virus-encoded intermediate stage promoter-specific transcription factor that has homology to eukaryotic transcription factor SII (TFIIS) and an additional role as a viral RNA polymerase subunit.* J Biol Chem, 1994. **269**(19): p. 14260-7.
181. Sanz, P. and B. Moss, *Identification of a transcription factor, encoded by two vaccinia virus early genes, that regulates the intermediate stage of viral gene expression.* Proc Natl Acad Sci U S A, 1999. **96**(6): p. 2692-7.
182. Katsafanas, G.C. and B. Moss, *Vaccinia virus intermediate stage transcription is complemented by Ras-GTPase-activating protein SH3 domain-binding protein (G3BP) and cytoplasmic activation/proliferation-associated protein (p137) individually or as a heterodimer*. J Biol Chem, 2004. **279**(50): p. 52210-7.
183. Solomon, S., et al., *Distinct structural features of caprin-1 mediate its interaction with G3BP-1 and its induction of phosphorylation of eukaryotic translation initiation factor 2alpha, entry to cytoplasmic stress granules, and selective interaction with a subset of mRNAs.* Mol Cell Biol, 2007. **27**(6): p. 2324-42.
184. Bertholet, C., et al., *Vaccinia virus produces late mRNAs by discontinuous synthesis.* Cell, 1987. **50**(2): p. 153-62.
185. Schwer, B., et al., *Discontinuous transcription or RNA processing of vaccinia virus late messengers results in a 5' poly(A) leader.* Cell, 1987. **50**(2): p. 163-9.
186. Knutson, B.A., et al., *Vaccinia virus intermediate and late promoter elements are targeted by the TATA-binding protein.* J Virol, 2006. **80**(14): p. 6784-93.
187. Knutson, B.A., J. Oh, and S.S. Broyles, *Downregulation of vaccinia virus intermediate and late promoters by host transcription factor YY1*. J Gen Virol, 2009. **90**(Pt 7): p. 1592-9.
188. Xiang, Y., et al., *Transcription elongation activity of the vaccinia virus J3 protein in vivo is independent of poly(A) polymerase stimulation.* Virology, 2000. **269**(2): p. 356-69.
189. Condit, R.C. and E.G. Niles, *Regulation of viral transcription elongation and termination during vaccinia virus infection.* Biochim Biophys Acta, 2002. **1577**(2): p. 325-36.
190. Broyles, S.S., *Vaccinia virus transcription.* J Gen Virol, 2003. **84**(Pt 9): p. 2293-303.
191. Davison, A.J. and B. Moss, *Structure of vaccinia virus late promoters.* J Mol Biol, 1989. **210**(4): p. 771-84.
192. Broyles, S. and B.A. Knutson, *Poxvirus transcription.* Future Virology, 2010. **5**(5): p. 639-650.
193. Hooda-Dhingra, U., C.L. Thompson, and R.C. Condit, *Detailed phenotypic characterization of five temperature-sensitive mutants in the 22- and 147-kilodalton subunits of vaccinia virus DNA-dependent RNA polymerase*. J Virol, 1989. **63**(2): p. 714-29.
194. Keck, J.G., C.J. Baldick, Jr., and B. Moss, *Role of DNA replication in vaccinia virus gene expression: a naked template is required for transcription of three late trans-activator genes.* Cell, 1990. **61**(5): p. 801-9.
195. Passarelli, A.L., G.R. Kovacs, and B. Moss, *Transcription of a vaccinia virus late promoter template: requirement for the product of the A2L intermediate-stage gene.* J Virol, 1996. **70**(7): p. 4444-50.
196. Kovacs, G.R. and B. Moss, *The vaccinia virus H5R gene encodes late gene transcription factor 4: purification, cloning, and overexpression.* J Virol, 1996. **70**(10): p. 6796-802.
197. Gunasinghe, S.K., A.E. Hubbs, and C.F. Wright, *A vaccinia virus late transcription factor with biochemical and molecular identity to a human cellular protein.* J Biol Chem, 1998. **273**(42): p. 27524-30.

198. Wright, C.F., B.W. Oswald, and S. Dellis, *Vaccinia virus late transcription is activated in vitro by cellular heterogeneous nuclear ribonucleoproteins.* J Biol Chem, 2001. **276**(44): p. 40680-6.
199. Dellis, S., et al., *Protein interactions among the vaccinia virus late transcription factors.* Virology, 2004. **329**(2): p. 328-36.
200. Shchelkunov, S.N., *[Evasion of mammalian organism defense systems by orthopoxviruses]*. Mol Biol (Mosk), 2011. **45**(1): p. 30-43.
201. Bowie, A., et al., *A46R and A52R from vaccinia virus are antagonists of host IL-1 and toll-like receptor signaling.* Proc Natl Acad Sci U S A, 2000. **97**(18): p. 10162-7.
202. Chang, H.W., J.C. Watson, and B.L. Jacobs, *The E3L gene of vaccinia virus encodes an inhibitor of the interferon-induced, double-stranded RNA-dependent protein kinase.* Proc Natl Acad Sci U S A, 1992. **89**(11): p. 4825-9.
203. Myskiw, C., et al., *Vaccinia virus E3 suppresses expression of diverse cytokines through inhibition of the PKR, NF-kappaB, and IRF3 pathways.* J Virol, 2009. **83**(13): p. 6757-68.
204. Davies, M.V., et al., *The E3L and K3L vaccinia virus gene products stimulate translation through inhibition of the double-stranded RNA-dependent protein kinase by different mechanisms.* J Virol, 1993. **67**(3): p. 1688-92.
205. Mossman, K., et al., *Species specificity of ectromelia virus and vaccinia virus interferon-gamma binding proteins.* Virology, 1995. **208**(2): p. 762-9.
206. Colamonici, O.R., et al., *Vaccinia virus B18R gene encodes a type I interferon-binding protein that blocks interferon alpha transmembrane signaling.* J Biol Chem, 1995. **270**(27): p. 15974-8.
207. Shchelkunov, S.N., *[Immunomodulatory proteins of orthopoxviruses]*. Mol Biol (Mosk), 2003. **37**(1): p. 41-53.
208. Born, T.L., et al., *A poxvirus protein that binds to and inactivates IL-18, and inhibits NK cell response.* J Immunol, 2000. **164**(6): p. 3246-54.
209. Alcami, A., et al., *Blockade of chemokine activity by a soluble chemokine binding protein from vaccinia virus.* J Immunol, 1998. **160**(2): p. 624-33.
210. Seet, B.T., et al., *Poxviruses and immune evasion.* Annu Rev Immunol, 2003. **21**: p. 377-423.
211. Hilleman, M.R., *Strategies and mechanisms for host and pathogen survival in acute and persistent viral infections.* Proc Natl Acad Sci U S A, 2004. **101 Suppl 2**: p. 14560-6.
212. Hay, S. and G. Kannourakis, *A time to kill: viral manipulation of the cell death program.* J Gen Virol, 2002. **83**(Pt 7): p. 1547-64.
213. Roulston, A., R.C. Marcellus, and P.E. Branton, *Viruses and apoptosis.* Annu Rev Microbiol, 1999. **53**: p. 577-628.
214. Zhai, D., et al., *Vaccinia virus protein F1L is a caspase-9 inhibitor.* J Biol Chem, 2010. **285**(8): p. 5569-80.
215. Geada, M.M., et al., *Movements of vaccinia virus intracellular enveloped virions with GFP tagged to the F13L envelope protein.* J Gen Virol, 2001. **82**(Pt 11): p. 2747-60.
216. Rietdorf, J., et al., *Kinesin-dependent movement on microtubules precedes actin-based motility of vaccinia virus.* Nat Cell Biol, 2001. **3**(11): p. 992-1000.
217. Hollinshead, M., et al., *Vaccinia virus utilizes microtubules for movement to the cell surface.* J Cell Biol, 2001. **154**(2): p. 389-402.
218. Boone, R.F. and B. Moss, *Methylated 5'-terminal sequences of vaccinia virus mRNA species made in vivo at early and late times after infection.* Virology, 1977. **79**(1): p. 67-80.
219. Venkatesan, S., A. Gershowitz, and B. Moss, *Modification of the 5' end of mRNA. Association of RNA triphosphatase with the RNA guanylyltransferase-RNA (guanine-7-)methyltransferase complex from vaccinia virus.* J Biol Chem, 1980. **255**(3): p. 903-8.
220. McMahon, R., I. Zaborowska, and D. Walsh, *Noncytotoxic inhibition of viral infection through eIF4F-independent suppression of translation by 4EGi-1.* J Virol, 2011. **85**(2): p. 853-64.
221. Walsh, D., *Manipulation of the host translation initiation complex eIF4F by DNA viruses.* Biochem Soc Trans, 2010. **38**(6): p. 1511-6.
222. Jackson, R.J., C.U. Hellen, and T.V. Pestova, *The mechanism of eukaryotic translation initiation and principles of its regulation.* Nat Rev Mol Cell Biol, 2010. **11**(2): p. 113-27.

223. Walsh, D., et al., *Eukaryotic translation initiation factor 4F architectural alterations accompany translation initiation factor redistribution in poxvirus-infected cells.* Mol Cell Biol, 2008. **28**(8): p. 2648-58.
224. Katsafanas, G.C. and B. Moss, *Colocalization of transcription and translation within cytoplasmic poxvirus factories coordinates viral expression and subjugates host functions.* Cell Host Microbe, 2007. **2**(4): p. 221-8.
225. Zaborowska, I., et al., *Recruitment of host translation initiation factor eIF4G by the Vaccinia Virus ssDNA-binding protein I3.* Virology, 2012. **425**(1): p. 11-22.
226. Parrish, S. and B. Moss, *Characterization of a second vaccinia virus mRNA-decapping enzyme conserved in poxviruses.* J Virol, 2007. **81**(23): p. 12973-8.
227. Parrish, S., W. Resch, and B. Moss, *Vaccinia virus D10 protein has mRNA decapping activity, providing a mechanism for control of host and viral gene expression.* Proc Natl Acad Sci U S A, 2007. **104**(7): p. 2139-44.
228. Cudmore, S., et al., *Actin-based motility of vaccinia virus.* Nature, 1995. **378**(6557): p. 636-8.
229. Newsome, T.P., N. Scaplehorn, and M. Way, *SRC mediates a switch from microtubule- to actin-based motility of vaccinia virus.* Science, 2004. **306**(5693): p. 124-9.
230. Scaplehorn, N., et al., *Grb2 and Nck act cooperatively to promote actin-based motility of vaccinia virus.* Curr Biol, 2002. **12**(9): p. 740-5.
231. Frischknecht, F., et al., *Actin-based motility of vaccinia virus mimics receptor tyrosine kinase signalling.* Nature, 1999. **401**(6756): p. 926-9.
232. Moreau, V., et al., *A complex of N-WASP and WIP integrates signalling cascades that lead to actin polymerization.* Nat Cell Biol, 2000. **2**(7): p. 441-8.
233. Snapper, S.B., et al., *N-WASP deficiency reveals distinct pathways for cell surface projections and microbial actin-based motility.* Nat Cell Biol, 2001. **3**(10): p. 897-904.
234. Komano, J., et al., *Inhibiting the Arp2/3 complex limits infection of both intracellular mature vaccinia virus and primate lentiviruses.* Mol Biol Cell, 2004. **15**(12): p. 5197-207.
235. Newsome, T.P., et al., *Abl collaborates with Src family kinases to stimulate actin-based motility of vaccinia virus.* Cell Microbiol, 2006. **8**(2): p. 233-41.
236. Humphries, A.C., et al., *Clathrin potentiates vaccinia-induced actin polymerization to facilitate viral spread.* Cell Host Microbe, 2012. **12**(3): p. 346-59.
237. McNulty, S., et al., *The host phosphoinositide 5-phosphatase SHIP2 regulates dissemination of vaccinia virus.* J Virol, 2011. **85**(14): p. 7402-10.
238. Blasco, R. and B. Moss, *Extracellular vaccinia virus formation and cell-to-cell virus transmission are prevented by deletion of the gene encoding the 37,000-Dalton outer envelope protein.* J Virol, 1991. **65**(11): p. 5910-20.
239. Husain, M. and B. Moss, *Role of receptor-mediated endocytosis in the formation of vaccinia virus extracellular enveloped particles.* J Virol, 2005. **79**(7): p. 4080-9.
240. Husain, M. and B. Moss, *Vaccinia virus F13L protein with a conserved phospholipase catalytic motif induces colocalization of the B5R envelope glycoprotein in post-Golgi vesicles.* J Virol, 2001. **75**(16): p. 7528-42.
241. Chen, Y., et al., *Vaccinia virus p37 interacts with host proteins associated with LE-derived transport vesicle biogenesis.* Virol J, 2009. **6**: p. 44.
242. Grosshans, B.L., D. Ortiz, and P. Novick, *Rabs and their effectors: achieving specificity in membrane traffic.* Proc Natl Acad Sci U S A, 2006. **103**(32): p. 11821-7.
243. Bartel, S., et al., *Proteome analysis of vaccinia virus IHD-W-infected HEK 293 cells with 2-dimensional gel electrophoresis and MALDI-PSD-TOF MS of on solid phase support N-terminally sulfonated peptides.* Virol J, 2011. **8**: p. 380.
244. Van Vliet, K., et al., *Poxvirus proteomics and virus-host protein interactions.* Microbiol Mol Biol Rev, 2009. **73**(4): p. 730-49.
245. Zhang, L., et al., *Analysis of vaccinia virus-host protein-protein interactions: validations of yeast two-hybrid screenings.* J Proteome Res, 2009. **8**(9): p. 4311-8.
246. Ascierto, M.L., et al., *Permissivity of the NCI-60 cancer cell lines to oncolytic Vaccinia Virus GLV-1h68.* BMC Cancer, 2011. **11**(1): p. 451.
247. Chen, N.G., et al., *Replication efficiency of oncolytic vaccinia virus in cell cultures prognosticates the virulence and antitumor efficacy in mice.* J Transl Med, 2011. **9**: p. 164.

248. Simon, R., et al., *Analysis of gene expression data using BRB-ArrayTools.* Cancer Inform, 2007. **3**: p. 11-7.
249. Eisen, M.B., et al., *Cluster analysis and display of genome-wide expression patterns.* Proc Natl Acad Sci U S A, 1998. **95**(25): p. 14863-8.
250. Ruutu, M., et al., *Effect of confluence state and passaging on global cancer gene expression pattern in oral carcinoma cell lines.* Anticancer Res, 2004. **24**(5A): p. 2627-31.
251. Ascierto, M.L., et al., *Permissivity of the NCI-60 cancer cell lines to oncolytic Vaccinia Virus GLV-1h68.* BMC Cancer, 2011. **11**: p. 451.
252. Ranz, J.M. and C.A. Machado, *Uncovering evolutionary patterns of gene expression using microarrays.* Trends Ecol Evol, 2006. **21**(1): p. 29-37.
253. Gresham, D., M.J. Dunham, and D. Botstein, *Comparing whole genomes using DNA microarrays.* Nat Rev Genet, 2008. **9**(4): p. 291-302.
254. Raman, T., et al., *Quality control in microarray assessment of gene expression in human airway epithelium.* BMC Genomics, 2009. **10**: p. 493.
255. Jin, P., et al., *Selection and validation of endogenous reference genes using a high throughput approach.* BMC Genomics, 2004. **5**(1): p. 55.
256. Lagos-Quintana, M., et al., *Identification of novel genes coding for small expressed RNAs.* Science, 2001. **294**(5543): p. 853-8.
257. Zeng, Y., R. Yi, and B.R. Cullen, *MicroRNAs and small interfering RNAs can inhibit mRNA expression by similar mechanisms.* Proc Natl Acad Sci U S A, 2003. **100**(17): p. 9779-84.
258. Reinboth, J., et al., *Correlates between host and viral transcriptional program associated with different oncolytic vaccinia virus isolates.* Hum Gene Ther Methods, 2012.
259. Mercer, J., et al., *RNAi Screening Reveals Proteasome- and Cullin3-Dependent Stages in Vaccinia Virus Infection.* Cell Rep, 2012.
260. Spivey, T.L., et al., *The stable traits of melanoma genetics: an alternate approach to target discovery.* BMC Genomics, 2012. **13**: p. 156.
261. Brennecke, J., et al., *Principles of microRNA-target recognition.* PLoS Biol, 2005. **3**(3): p. e85.
262. Ghosh, Z., B. Mallick, and J. Chakrabarti, *Cellular versus viral microRNAs in host-virus interaction.* Nucleic Acids Res, 2009. **37**(4): p. 1035-48.
263. Russo, A. and N. Potenza, *Antiviral effects of human microRNAs and conservation of their target sites.* FEBS Lett, 2011. **585**(16): p. 2551-5.
264. Vucic, E.A., et al., *Copy Number Variations in the Human Genome and Strategies for Analysis*, in *Genetic Variations: Methods and Protocols*, M.R. Barnes and G. Breed, Editors. 2010, Springer Science + Business Media, LLC: London. p. 103-117.
265. Gonzalez, E., et al., *The influence of CCL3L1 gene-containing segmental duplications on HIV-1/AIDS susceptibility.* Science, 2005. **307**(5714): p. 1434-40.
266. Patani, N., et al., *Tumour suppressor function of MDA-7/IL-24 in human breast cancer.* Cancer Cell Int, 2010. **10**: p. 29.
267. Sun, Y., et al., *Treatment-induced damage to the tumor microenvironment promotes prostate cancer therapy resistance through WNT16B.* Nat Med, 2012. **18**(9): p. 1359-68.
268. Kwak, E.L., et al., *Anaplastic lymphoma kinase inhibition in non-small-cell lung cancer.* N Engl J Med, 2010. **363**(18): p. 1693-703.
269. Sequist, L.V., et al., *Genotypic and histological evolution of lung cancers acquiring resistance to EGFR inhibitors.* Sci Transl Med, 2011. **3**(75): p. 75ra26.
270. Wong, H.H., N.R. Lemoine, and Y. Wang, *Oncolytic Viruses for Cancer Therapy: Overcoming the Obstacles.* Viruses, 2010. **2**(1): p. 78-106.
271. Hernandez-Alcoceba, R., *Recent advances in oncolytic virus design.* Clin Transl Oncol, 2011. **13**(4): p. 229-39.
272. Kim, J.H., et al., *Relaxin expression from tumor-targeting adenoviruses and its intratumoral spread, apoptosis induction, and efficacy.* J Natl Cancer Inst, 2006. **98**(20): p. 1482-93.
273. Chalikonda, S., et al., *Oncolytic virotherapy for ovarian carcinomatosis using a replication-selective vaccinia virus armed with a yeast cytosine deaminase gene.* Cancer Gene Ther, 2008. **15**(2): p. 115-25.

274. Gentschev, I., et al., *Efficient Colonization and Therapy of Human Hepatocellular Carcinoma (HCC) Using the Oncolytic Vaccinia Virus Strain GLV-1h68.* PLoS One, 2011. **6**(7): p. e22069.
275. Kelly, K.J., et al., *Novel oncolytic agent GLV-1h68 is effective against malignant pleural mesothelioma.* Hum Gene Ther, 2008. **19**(8): p. 774-82.
276. Lin, S.F., et al., *Treatment of anaplastic thyroid carcinoma in vitro with a mutant vaccinia virus.* Surgery, 2007. **142**(6): p. 976-83; discussion 976-83.
277. Yu, Z., et al., *Oncolytic vaccinia therapy of squamous cell carcinoma.* Mol Cancer, 2009. **8**: p. 45.
278. Zaitseva, M., B.J. Vollenhoven, and P.A. Rogers, *In vitro culture significantly alters gene expression profiles and reduces differences between myometrial and fibroid smooth muscle cells.* Mol Hum Reprod, 2006. **12**(3): p. 187-207.
279. Neumann, E., et al., *Cell culture and passaging alters gene expression pattern and proliferation rate in rheumatoid arthritis synovial fibroblasts.* Arthritis Res Ther, 2010. **12**(3): p. R83.
280. Buller, R.M. and G.J. Palumbo, *Poxvirus pathogenesis.* Microbiol Rev, 1991. **55**(1): p. 80-122.
281. Zhu, M., T. Moore, and S.S. Broyles, *A cellular protein binds vaccinia virus late promoters and activates transcription in vitro.* J Virol, 1998. **72**(5): p. 3893-9.
282. Cheong, J.H., et al., *Human RPB5, a subunit shared by eukaryotic nuclear RNA polymerases, binds human hepatitis B virus X protein and may play a role in X transactivation.* EMBO J, 1995. **14**(1): p. 143-50.
283. Dorjsuren, D., et al., *RMP, a novel RNA polymerase II subunit 5-interacting protein, counteracts transactivation by hepatitis B virus X protein.* Mol Cell Biol, 1998. **18**(12): p. 7546-55.
284. UniProt. Available from: http://www.uniprot.org/uniprot/P19388.
285. Wilton, S. and S. Dales, *Relationship between RNA polymerase II and efficiency of vaccinia virus replication.* J Virol, 1989. **63**(4): p. 1540-8.
286. Weissman, A.M., *Themes and variations on ubiquitylation.* Nat Rev Mol Cell Biol, 2001. **2**(3): p. 169-78.
287. Pickart, C.M. and D. Fushman, *Polyubiquitin chains: polymeric protein signals.* Curr Opin Chem Biol, 2004. **8**(6): p. 610-6.
288. Teale, A., et al., *Orthopoxviruses require a functional ubiquitin-proteasome system for productive replication.* J Virol, 2009. **83**(5): p. 2099-108.
289. Satheshkumar, P.S., et al., *Inhibition of the ubiquitin-proteasome system prevents vaccinia virus DNA replication and expression of intermediate and late genes.* J Virol, 2009. **83**(6): p. 2469-79.
290. Xu, B., et al., *WNK1, a novel mammalian serine/threonine protein kinase lacking the catalytic lysine in subdomain II.* J Biol Chem, 2000. **275**(22): p. 16795-801.
291. McCormick, J.A. and D.H. Ellison, *The WNKs: atypical protein kinases with pleiotropic actions.* Physiol Rev, 2011. **91**(1): p. 177-219.
292. Vitari, A.C., et al., *WNK1, the kinase mutated in an inherited high-blood-pressure syndrome, is a novel PKB (protein kinase B)/Akt substrate.* Biochem J, 2004. **378**(Pt 1): p. 257-68.
293. Wang, G., et al., *Infection of human cancer cells with myxoma virus requires Akt activation via interaction with a viral ankyrin-repeat host range factor.* Proc Natl Acad Sci U S A, 2006. **103**(12): p. 4640-5.
294. Soares, J.A., et al., *Activation of the PI3K/Akt pathway early during vaccinia and cowpox virus infections is required for both host survival and viral replication.* J Virol, 2009. **83**(13): p. 6883-99.
295. Krecic, A.M. and M.S. Swanson, *hnRNP complexes: composition, structure, and function.* Curr Opin Cell Biol, 1999. **11**(3): p. 363-71.
296. Dreyfuss, G., et al., *hnRNP proteins and the biogenesis of mRNA.* Annu Rev Biochem, 1993. **62**: p. 289-321.

297. Chaudhury, A., P. Chander, and P.H. Howe, *Heterogeneous nuclear ribonucleoproteins (hnRNPs) in cellular processes: Focus on hnRNP E1's multifunctional regulatory roles.* RNA. **16**(8): p. 1449-62.
298. Pinol-Roma, S. and G. Dreyfuss, *Shuttling of pre-mRNA binding proteins between nucleus and cytoplasm.* Nature, 1992. **355**(6362): p. 730-2.
299. Li, Z. and P.D. Nagy, *Diverse roles of host RNA binding proteins in RNA virus replication.* RNA Biol. **8**(2): p. 305-15.
300. Guang, S., A.M. Felthauser, and J.E. Mertz, *Binding of hnRNP L to the pre-mRNA processing enhancer of the herpes simplex virus thymidine kinase gene enhances both polyadenylation and nucleocytoplasmic export of intronless mRNAs.* Mol Cell Biol, 2005. **25**(15): p. 6303-13.
301. Liu, X. and J.E. Mertz, *HnRNP L binds a cis-acting RNA sequence element that enables intron-dependent gene expression.* Genes Dev, 1995. **9**(14): p. 1766-80.
302. Hwang, B., et al., *hnRNP L is required for the translation mediated by HCV IRES.* Biochem Biophys Res Commun, 2009. **378**(3): p. 584-8.
303. Cuezva, J.M., et al., *The bioenergetic signature of cancer: a marker of tumor progression.* Cancer Res, 2002. **62**(22): p. 6674-81.
304. Willers, I.M. and J.M. Cuezva, *Post-transcriptional regulation of the mitochondrial H(+)-ATP synthase: a key regulator of the metabolic phenotype in cancer.* Biochim Biophys Acta. **1807**(6): p. 543-51.
305. Glass, W.G., H.F. Rosenberg, and P.M. Murphy, *Chemokine regulation of inflammation during acute viral infection.* Curr Opin Allergy Clin Immunol, 2003. **3**(6): p. 467-73.
306. Fu, G.K., G. Grosveld, and D.M. Markovitz, *DEK, an autoantigen involved in a chromosomal translocation in acute myelogenous leukemia, binds to the HIV-2 enhancer.* Proc Natl Acad Sci U S A, 1997. **94**(5): p. 1811-5.
307. Sitwala, K.V., N. Mor-Vaknin, and D.M. Markovitz, *Minireview: DEK and gene regulation, oncogenesis and AIDS.* Anticancer Res, 2003. **23**(3A): p. 2155-8.
308. Alexiadis, V., et al., *The protein encoded by the proto-oncogene DEK changes the topology of chromatin and reduces the efficiency of DNA replication in a chromatin-specific manner.* Genes Dev, 2000. **14**(11): p. 1308-12.
309. Grottke, C., et al., *Identification of differentially expressed genes in human melanoma cells with acquired resistance to various antineoplastic drugs.* Int J Cancer, 2000. **88**(4): p. 535-46.
310. Oh, J. and S.S. Broyles, *Host cell nuclear proteins are recruited to cytoplasmic vaccinia virus replication complexes.* J Virol, 2005. **79**(20): p. 12852-60.
311. Broyles, S.S., et al., *Transcription factor YY1 is a vaccinia virus late promoter activator.* J Biol Chem, 1999. **274**(50): p. 35662-7.
312. Kim, V.N., *MicroRNA biogenesis: coordinated cropping and dicing.* Nat Rev Mol Cell Biol, 2005. **6**(5): p. 376-85.
313. Waterhouse, P.M., M.B. Wang, and T. Lough, *Gene silencing as an adaptive defence against viruses.* Nature, 2001. **411**(6839): p. 834-42.
314. Cullen, B.R., *Viruses and microRNAs: RISCy interactions with serious consequences.* Genes Dev, 2011. **25**(18): p. 1881-94.
315. Skalsky, R.L. and B.R. Cullen, *Viruses, microRNAs, and host interactions.* Annu Rev Microbiol, 2010. **64**: p. 123-41.
316. Ahluwalia, J.K., et al., *Human cellular microRNA hsa-miR-29a interferes with viral nef protein expression and HIV-1 replication.* Retrovirology, 2008. **5**: p. 117.
317. Otsuka, M., et al., *Hypersusceptibility to vesicular stomatitis virus infection in Dicer1-deficient mice is due to impaired miR24 and miR93 expression.* Immunity, 2007. **27**(1): p. 123-34.
318. Yeung, M.L., et al., *Changes in microRNA expression profiles in HIV-1-transfected human cells.* Retrovirology, 2005. **2**: p. 81.
319. Klopocki, E. and S. Mundlos, *Copy-number variations, noncoding sequences, and human phenotypes.* Annu Rev Genomics Hum Genet, 2011. **12**: p. 53-72.
320. Pol, J.G., J. Rességuier, and B.D. Lichty, *Oncolytic viruses: a step into cancer immunotherapy.* Dovepress, Dove Medical Press Ltd, 2012. **2012:4**: p. 1-21.

6 Appendices

6.1 Additional Tables

Table 6-1: 888-MEL and 1936-MEL host correlates with VACV replication (via VRI expression).

Gene Symbol	Description
AKAP8	A kinase (PRKA) anchor protein 8 (AKAP8), mRNA.
AKR1B1	aldo-keto reductase family 1, member B1 (aldose reductase) (AKR1B1), mRNA.
ANAPC11	anaphase promoting complex subunit 11 (ANAPC11), transcript variant 4, mRNA.
ANAPC13	anaphase promoting complex subunit 13 (ANAPC13), transcript variant 1, mRNA.
ANK3	ankyrin 3, node of Ranvier (ankyrin G) (ANK3), transcript variant 1, mRNA.
ANKRD13D	ankyrin repeat domain 13 family, member D (ANKRD13D), transcript variant 1, mRNA.
ARFIP2	ADP-ribosylation factor interacting protein 2 (ARFIP2), mRNA.
ATP5F1	ATP synthase, H+ transporting, mitochondrial Fo complex, subunit B1 (ATP5F1), nuclear gene encoding mitochondrial protein, mRNA.
ATP5I	ATP synthase, H+ transporting, mitochondrial Fo complex, subunit E (ATP5I), nuclear gene encoding mitochondrial protein, transcript variant 1, mRNA.
BLVRB	biliverdin reductase B (flavin reductase (NADPH)) (BLVRB), mRNA.
BOLA3	bolA homolog 3 (E. coli) (BOLA3), transcript variant 2, mRNA.
C7orf42	chromosome 7 open reading frame 42 (C7orf42), mRNA.
CARD16	caspase recruitment domain family, member 16 (CARD16), transcript variant 1, mRNA.
CCL5	chemokine (C-C motif) ligand 5 (CCL5), mRNA.
CDC34	cell division cycle 34 homolog (S. cerevisiae) (CDC34), mRNA.
CHKB	choline kinase beta (CHKB), mRNA.
CSRNP2	cysteine-serine-rich nuclear protein 2 (CSRNP2), mRNA.
CST3	cystatin C (CST3), mRNA.
CSTB	cystatin B (stefin B) (CSTB), mRNA.
CUL1	cullin 1 (CUL1), mRNA.
DEK	DEK oncogene (DEK), transcript variant 2, mRNA.
DENND1C	DENN/MADD domain containing 1C (DENND1C), mRNA.
DGCR2	DiGeorge syndrome critical region gene 2 (DGCR2), transcript variant 3, mRNA.
EFHD1	EF-hand domain family, member D1 (EFHD1), transcript variant 1, mRNA.
EIF2AK4	eukaryotic translation initiation factor 2 alpha kinase 4 (EIF2AK4), mRNA.
ENTPD6	ectonucleoside triphosphate diphosphohydrolase 6 (putative) (ENTPD6), transcript variant 2, mRNA.
EZH2	enhancer of zeste homolog 2 (Drosophila) (EZH2), transcript variant 2, mRNA.
FAHD1	fumarylacetoacetate hydrolase domain containing 1 (FAHD1), nuclear gene encoding mitochondrial protein, transcript variant 2, mRNA.
FTHL3	ferritin, heavy polypeptide-like 3 (FTHL3), non-coding RNA.
FTSJD2	FtsJ methyltransferase domain containing 2
GADD45B	growth arrest and DNA-damage-inducible, beta (GADD45B), mRNA.
GLUD1	glutamate dehydrogenase 1 (GLUD1), nuclear gene encoding mitochondrial protein, mRNA.
GMFG	Glia maturation factor, gamma

GRB2	growth factor receptor-bound protein 2 (GRB2), transcript variant 2, mRNA.
GUSB	glucuronidase, beta (GUSB), mRNA.
HLA-DPB1	major histocompatibility complex, class II, DP beta 1 (HLA-DPB1), mRNA.
HLA-H	major histocompatibility complex, class I, H (pseudogene) (HLA-H), non-coding RNA.
HLA-L	major histocompatibility complex, class I, L, pseudogene (HLA-L), non-coding RNA.
HORMAD1	HORMA domain containing 1 (HORMAD1), mRNA.
ID2	inhibitor of DNA binding 2, dominant negative helix-loop-helix protein (ID2), mRNA.
ITPKA	inositol 1,4,5-trisphosphate 3-kinase A (ITPKA), mRNA.
KIAA0913	KIAA0913
KLF14	Kruppel-like factor 14 (KLF14), mRNA.
LANCL2	LanC lantibiotic synthetase component C-like 2 (bacterial) (LANCL2), mRNA.
LCK	lymphocyte-specific protein tyrosine kinase (LCK), transcript variant 1, mRNA.
LILRA2	leukocyte immunoglobulin-like receptor, subfamily A (with TM domain), member 2 (LILRA2), transcript variant 2, mRNA.
LIPA	lipase A, lysosomal acid, cholesterol esterase (LIPA), transcript variant 2, mRNA.
LOC100289224	PREDICTED: hypothetical protein LOC100289224 (LOC100289224), mRNA.
LOC388948	hypothetical LOC388948 (LOC388948), non-coding RNA.
LRRFIP2	leucine rich repeat (in FLII) interacting protein 2 (LRRFIP2), transcript variant 1, mRNA.
LSM4	LSM4 homolog, U6 small nuclear RNA associated (S. cerevisiae) (LSM4), mRNA.
LUC7L3	LUC7-like 3 (S. cerevisiae)
LYN	v-yes-1 Yamaguchi sarcoma viral related oncogene homolog (LYN), transcript variant 2, mRNA.
M6PR	mannose-6-phosphate receptor (cation dependent) (M6PR), mRNA.
METRNL	meteorin, glial cell differentiation regulator-like (METRNL), mRNA.
MGRN1	mahogunin, ring finger 1 (MGRN1), transcript variant 4, mRNA.
MLL5	myeloid/lymphoid or mixed-lineage leukemia 5 (trithorax homolog, Drosophila) (MLL5), transcript variant 2, mRNA.
MMP25	matrix metallopeptidase 25 (MMP25), mRNA.
MRPL41	mitochondrial ribosomal protein L41 (MRPL41), nuclear gene encoding mitochondrial protein, mRNA.
MRPS11	mitochondrial ribosomal protein S11 (MRPS11), nuclear gene encoding mitochondrial protein, transcript variant 1, mRNA.
NAPSB	napsin B aspartic peptidase pseudogene (NAPSB), non-coding RNA.
NDUFA8	NADH dehydrogenase (ubiquinone) 1 alpha subcomplex, 8, 19kDa (NDUFA8), nuclear gene encoding mitochondrial protein, mRNA.
NDUFS3	NADH dehydrogenase (ubiquinone) Fe-S protein 3, 30kDa (NADH-coenzyme Q reductase) (NDUFS3), nuclear gene encoding mitochondrial protein, mRNA.
NHP2L1	NHP2 non-histone chromosome protein 2-like 1 (S. cerevisiae) (NHP2L1), transcript variant 2, mRNA.
PAPD7	PAP associated domain containing 7 (PAPD7), transcript variant 2, mRNA.
PC	pyruvate carboxylase (PC), nuclear gene encoding mitochondrial protein, transcript variant 1, mRNA.
PDCD6	programmed cell death 6 (PDCD6), mRNA.
PLXDC2	plexin domain containing 2 (PLXDC2), mRNA.
PNPLA6	Patatin-like phospholipase domain containing 6
POLR2E	polymerase (RNA) II (DNA directed) polypeptide E, 25kDa (POLR2E), mRNA.
PPIAL4G	peptidylprolyl isomerase A (cyclophilin A)-like 4G (PPIAL4G), mRNA.
PREP	prolyl endopeptidase (PREP), mRNA.
PSMD2	proteasome (prosome, macropain) 26S subunit, non-ATPase, 2 (PSMD2), mRNA.
PWP1	PWP1 homolog (S. cerevisiae) (PWP1), mRNA.

RGS2	regulator of G-protein signaling 2, 24kDa (RGS2), mRNA.
RIMS2	Regulating synaptic membrane exocytosis protein 2 (Rab3-interacting molecule 2) (RIM 2). [Source:Uniprot/SWISSPROT;Acc:Q9UQ26]
RNPEPL1	arginyl aminopeptidase (aminopeptidase B)-like 1 (RNPEPL1), mRNA.
RPL12	ribosomal protein L12 (RPL12), mRNA.
RPL6	ribosomal protein L6 (RPL6), transcript variant 1, mRNA.
RPN2	ribophorin II (RPN2), transcript variant 1, mRNA.
SF3B2	splicing factor 3b, subunit 2, 145kDa (SF3B2), mRNA.
SLC38A9	Solute carrier family 38, member 9
SNX10	sorting nexin 10 (SNX10), mRNA.
SNX17	sorting nexin 17 (SNX17), mRNA.
SPHAR	S-phase response (cyclin related) (SPHAR), mRNA.
STARD7	StAR-related lipid transfer (START) domain containing 7 (STARD7), mRNA.
STOM	stomatin (STOM), transcript variant 1, mRNA.
TMED1	transmembrane emp24 protein transport domain containing 1 (TMED1), mRNA.
TMEM134	transmembrane protein 134 (TMEM134), transcript variant 2, mRNA.
TNFAIP3	tumor necrosis factor, alpha-induced protein 3 (TNFAIP3), mRNA.
TOMM22	translocase of outer mitochondrial membrane 22 homolog (yeast) (TOMM22), nuclear gene encoding mitochondrial protein, mRNA.
TP53I13	tumor protein p53 inducible protein 13 (TP53I13), mRNA.
TRPM2	transient receptor potential cation channel, subfamily M, member 2 (TRPM2), mRNA.
TXNRD3	thioredoxin reductase 3 (TXNRD3), transcript variant 1, mRNA.
UBE2D4	ubiquitin-conjugating enzyme E2D 4 (putative) (UBE2D4), mRNA.
UBR7	ubiquitin protein ligase E3 component n-recognin 7 (putative) (UBR7), transcript variant 3, mRNA.
UROS	uroporphyrinogen III synthase (UROS), mRNA.
VGF	VGF nerve growth factor inducible (VGF), mRNA.
WBP2	WW domain binding protein 2 (WBP2), mRNA.
WDR18	WD repeat domain 18 (WDR18), mRNA.
WNK1	WNK lysine deficient protein kinase 1 (WNK1), transcript variant 3, mRNA.
XP_945475.1	PREDICTED: similar to ribosomal protein S3a [Source:RefSeq_peptide_predicted;Acc:XP_940681]
YTHDF2	YTH domain family, member 2 (YTHDF2), transcript variant 3, mRNA.
YWHAB	tyrosine 3-monooxygenase/tryptophan 5-monooxygenase activation protein, beta polypeptide (YWHAB), transcript variant 2, mRNA.
ZFAND2A	zinc finger, AN1-type domain 2A (ZFAND2A), mRNA.
ZNF69	zinc finger protein 69 (ZNF69), mRNA.
-	EmptyWell
-	Unknown
-	Unknown
-	HLA CLASS I HISTOCOMPATIBILITY ANTIGEN, ALPHA CHAIN F PRECURSOR (HLA F ANTIGEN) (LEUKOCYTE ANTIGEN F) (CDA12)
-	EmptyWell
-	Unknown
-	Unknown
-	Unknown

Table 6-2: Gene expression ANOVA, low vs. highly permissive group; Top down-regulated molecules (fc ≥ -2)

Gene symbol	Entrez Gene Name	Fold Change	Location	Type(s)
CHST9	carbohydrate (N-acetylgalactosamine 4-0) sulfotransferase 9	-4.529	Cytoplasm	enzyme
HPGD	hydroxyprostaglandin dehydrogenase 15-(NAD)	-4.431	Cytoplasm	enzyme
IGF2BP1	insulin-like growth factor 2 mRNA binding protein 1	-3.315	Cytoplasm	translation regulator
PRKAA2	protein kinase, AMP-activated, alpha 2 catalytic subunit	-3	Cytoplasm	kinase
B3GALT1	UDP-Gal:betaGlcNAc beta 1,3-galactosyltransferase, polypeptide 1	-2.879	Cytoplasm	enzyme
TDO2	tryptophan 2,3-dioxygenase	-2.848	Cytoplasm	enzyme
ZFP106	zinc finger protein 106 homolog (mouse)	-2.463	Cytoplasm	other
DYNC1I1	dynein, cytoplasmic 1, intermediate chain 1	-2.438	Cytoplasm	other
PEX5L	peroxisomal biogenesis factor 5-like	-2.118	Cytoplasm	ion channel
RAB6B	RAB6B, member RAS oncogene family	-2.001	Cytoplasm	enzyme
NDRG2	NDRG family member 2	-2.001	Cytoplasm	other
MGP	matrix Gla protein	-12.49	ES	other
SERPINA3	serpin peptidase inhibitor, clade A (alpha-1 antiproteinase, antitrypsin), member 3	-6.977	ES	other
RNASE1	ribonuclease, RNase A family, 1 (pancreatic)	-4.19	ES	enzyme
SPP1	secreted phosphoprotein 1	-3.093	ES	cytokine
SEMA3E	sema domain, immunoglobulin domain (Ig), short basic domain, secreted, (semaphorin) 3E	-3.018	ES	other
PDGFD	platelet derived growth factor D	-2.32	ES	growth factor
LDOC1	leucine zipper, down-regulated in cancer 1	-3.726	Nucleus	other
AKAP6	A kinase (PRKA) anchor protein 6	-3.258	Nucleus	other
SATB1	SATB homeobox 1	-2.807	Nucleus	TR
PHF10	PHD finger protein 10	-2.303	Nucleus	other
H1F0	H1 histone family, member 0	-2.126	Nucleus	other
CLDN1	claudin 1	-7.607	PM	other
CD22	CD22 molecule	-4.322	PM	other
SORCS1	sortilin-related VPS10 domain containing receptor 1	-3.622	PM	transporter
ANK2	ankyrin 2, neuronal	-3.555	PM	other
SLC45A2	solute carrier family 45, member 2	-3.406	PM	other
GHR	growth hormone receptor	-3.373	PM	TMR
SLC7A2	solute carrier family 7 (cationic amino acid transporter, y+ system), member 2	-3.249	PM	transporter
MERTK	c-mer proto-oncogene tyrosine kinase	-3.006	PM	kinase
SLC26A4	solute carrier family 26, member 4	-2.569	PM	transporter
ATP1B1	ATPase, Na+/K+ transporting, beta 1 polypeptide	-2.312	PM	transporter
SYT17	synaptotagmin XVII	-2.088	PM	other
ACVR1C	activin A receptor, type IC	-2.031	PM	kinase

*PM = plasma membrane, ES = extracellular space, TR = transcription regulator, TMR = transmembrane receptor

Table 6-3: Gene expression ANOVA, low vs. highly permissive group; Top up-regulated molecules (fc ≥ 2)

Gene symbol	Entrez Gene Name	Fold Change	Location	Type(s)
ALDH1A3	aldehyde dehydrogenase 1 family, member A3	2.119	Cytoplasm	enzyme
GBP4	guanylate binding protein 4	2.184	Cytoplasm	enzyme
DOCK9	dedicator of cytokinesis 9	2.624	Cytoplasm	other
PSMB9	proteasome (prosome, macropain) subunit, beta type, 9 (large multifunctional peptidase 2)	2.796	Cytoplasm	peptidase
AGPAT9	1-acylglycerol-3-phosphate O-acyltransferase 9	2.965	Cytoplasm	enzyme
LRRK1	leucine-rich repeat kinase 1	2.975	Cytoplasm	kinase
CASP1	caspase 1, apoptosis-related cysteine peptidase	3.334	Cytoplasm	peptidase
AS3MT	arsenic (+3 oxidation state) methyltransferase	4.143	Cytoplasm	enzyme
KDELC1	KDEL (Lys-Asp-Glu-Leu) containing 1	4.919	Cytoplasm	other
PTHLH	parathyroid hormone-like hormone	2.311	ES	other
COL4A1	collagen, type IV, alpha 1	2.682	ES	other
COL4A2	collagen, type IV, alpha 2	2.733	ES	other
TFPI2	tissue factor pathway inhibitor 2	6.12	ES	other
KLF5	Kruppel-like factor 5 (intestinal)	2.072	Nucleus	TR
TCF19	transcription factor 19	2.083	Nucleus	TR
IRX3	iroquois homeobox 3	2.102	Nucleus	TR
RAD50	RAD50 homolog (S. cerevisiae)	2.122	Nucleus	enzyme
PPM1E	protein phosphatase, Mg2+/Mn2+ dependent, 1E	2.128	Nucleus	phosphatase
HIST1H4A	histone cluster 1, H4a	2.141	Nucleus	other
TBX3	T-box 3	2.268	Nucleus	TR
E2F7	E2F transcription factor 7	2.284	Nucleus	TR
EHD2	EH-domain containing 2	2.368	Nucleus	other
RUNX2	runt-related transcription factor 2	2.489	Nucleus	TR
RUNX3	runt-related transcription factor 3	2.627	Nucleus	TR
CENPV	centromere protein V	5.248	Nucleus	other
MX2	myxovirus (influenza virus) resistance 2 (mouse)	8.228	Nucleus	enzyme
KCNH1	potassium voltage-gated channel, subfamily H (eag-related), member 1	2.057	PM	ion channel
SCARA3	scavenger receptor class A, member 3	2.126	PM	TMR
PMEPA1	prostate transmembrane protein, androgen induced 1	2.179	PM	other
LAT	linker for activation of T cells	2.199	PM	other
HLA-F	major histocompatibility complex, class I, F	2.229	PM	TMR
ITGA5	integrin, alpha 5 (fibronectin receptor, alpha polypeptide)	2.242	PM	other
HLA-B	major histocompatibility complex, class I, B	2.454	PM	TMR
ANPEP	alanyl (membrane) aminopeptidase	3.031	PM	peptidase
ADAM19	ADAM metallopeptidase domain 19	3.311	PM	peptidase
ODZ3	odz, odd Oz/ten-m homolog 3 (Drosophila)	5.559	PM	other

*PM = plasma membrane, ES = extracellular space, TR = transcription regulator, TMR = transmembrane receptor

6.2 List of Figures

6.3 List of Tables

6.4 List of Abbreviations

%	percent
°C	degree celsius
aCGH	array comparative genomic hybridization
Ad	adenovirus
AIDS	acquired immunodeficiency syndrome
ANOVA	analysis of variances
AP-2	adaptor protein 2
APC	adenomatous polyposis coli
aRNA	amplified ribonucleic acid
Arp	actin-related proteins
ATP5F1	ATP synthase, H+ transporting, mitochondrial Fo complex, subunit B1
AT-rich	adenosin-thymidine-rich
Bcl-2	B-cell leukemia/lymphoma 2
BOLA3	bolA homolog 3 (E. coli)
bp	basepairs
BRAF	v-raf murine sarcoma viral oncogene homolog B1
C1, 2, 3a, 3b, 4	cluster 1, 2, 3a, 3b, 4
Caprin-1	cytoplasmic activation/proliferation-associated protein 1
CBG	click beetle green
CCL3L1	chemokine (C-C motif) ligand 3-like 1
CCL5	chemokine (C-C motif) ligand 5
CDK	cyclin-dependent kinase
cDNA	copy deoxyribonucleic acid
CEV	cell-associated enveloped virus
CIP	calf intestinal alkaline phosphatase
CNOT6L	CCR4-NOT transcription complex subunit 6-like
CNVs	copy number variations
CO_2	carbon dioxide
COP	vaccinia virus Copenhagen
cryo-EM	cryo-electron microscopy
CUL1	cullin 1
Cy3	cyanine 3
Cy5	cyanine 5
d(A)	deoxyadenosine
Da	dalton
DEK	DEK oncogene
DNA	deoxyribonucleic acid
dNTP	deoxyribonucleotide triphosphate
ds	double-stranded
dT	deoxythymidine
dTMP	deoxythymidine monophosphate
DTT	dithiothreitol

E. coli	Escherichia coli
EEV	extracellular enveloped virus
EFC	entry/fusion complex
EGFR	epidermal growth factor receptor
eIF (4F, 4E, 4G)	eukaryotic initiation factor (4F, 4E, 4G)
eIF2α	eukaryotic initiation factor 2
ER	endoplasmic reticulum
ERK	extracellular signal-regulated kinase
etc.	*et cetera*
fc	fold change
Fig	figure
FSC	forward scatter channel
g	gram
G3BP	Ras-GTPase activating protein SH3-domain-binding protein
GDEPT	gene-directed enzyme prodrug therapy
GFP	green fluorescent protein
GLUD1	glutamate dehydrogenase 1
Grb2	growth factor receptor-bound protein 2
gusA	β-glucoronidase
H_2O	water
HA	hemagglutinin
HCV	hepatitis C virus
HindIII	*Haemophilus influenzae*dIII
HIV	human immunodeficiency virus
HLA-H	major histocompatibility complex, class I, H (pseudogene)
HLA-L	major histocompatibility complex, class I, L (pseudogene)
hnRNP A2/B1	heterogeneous nuclear ribonucleoprotein A2/B1
HNRNPL	heterogeneous nuclear ribonucleoprotein L
hpi	hours post infection
hr/ hrs	hour/ hours
HRAS	v-Ha-ras Harvey rat sarcoma viral oncogene homolog
hsa	homo sapiens
HSV-1	herpes simplex type-1
hyb	hybridization
IARC	International Agency for Research on Cancer
ID2	inhibitor of DNA binding 2, dominant negative helix-loop-helix protein
IEV	intracellular enveloped virus
IFN	interferon
IL	interleukine
IL-2 (IL-1A, IL-24 etc.)	interleukin 2 (interleikine 1A, interleukine 24 etc.)
IMV	intracellular mature virus
INR	initiator element
IPA	Ingenuity Pathway Analysis
IR	ionizing radiation
IRAK2	interleukin-1 receptor-associated kinase-like 2
IRES	internal ribosome entry site

ITR	inverted terminal repeats
IV	immature virion
IVT	in vitro transcription
k	kilo
KRAS	v-Ki-ras2 Kirsten rat sarcoma viral oncogene homolog
l	liter
lacZ	β-galactosidase
LANCL2	LanC lantibiotic synthetase component C-like 2 (bacterial)
LIVP	Lister strain, Institute of Viral Preparations (Moscow, Russia)
M	molar
m7G cap	7-methylguanosine cap
MALDI-PSD-TOF MS	matrix-assisted laser desorption/ionization - post source decay - time-of-flight mass spectrometer
MAPK	mitogen-activated protein kinase
MART-1	melanoma-associated antigen recognized by T cells-1
MC1-R	melanocortin-1 receptor
MEK	mitogen-activated protein kinase kinase 1
MEL	melanoma
min	minutes
miRNA or miR	microRNA
MITF	microphthalmia-associated transcription factor
ml	milliliter
mm	millimeter
mM	millimolar
MOI	multiplicity of infection
mRNA	messenger ribonucleic acid
MV	mature virion
MVA	modified vaccinia virus Ankara
MyD88	Myeloid differentiation primary response gene (88)
NCI	National Cancer Institute
Nck	non-catalytic region of tyrosine kinase adaptor protein 1
NDV	Newcastle disease virus
NF-κB	nuclear factor-κB
NF-κB	nuclear factor kappa B
NIH	National Institutes of Health
nm	nanometer
NPH I	nucleotide phosphohydrolase I
NRAS	neuroblastoma RAS viral (v-ras) oncogene homolog
nt	nucleotide
NTP	ribonucleotide triphosphate
NYVAC	New York vaccinia virus
OAS	2’,5’-oligoadenylate synthetase
ORF	open reading frame
OV	oncolytic virus
p	p-value
P(e/l)	early-late promoter

p137	cytoplasmic activation/proliferation-associated protein 1
p15	cyclin-dependent kinase inhibitor 2B
p16	cyclin-dependent kinase inhibitor 2A
p53	protein 53
PBMCs	peripheral blood mononuclear cells
PCA	principal components analysis
PCR	polymerase chain reaction
pfu	plaque forming units
pH	negative decimal logarithm of the hydrogen ion activity
PI(3)K	phosphoinositide-3-OH kinase
PKB or Akt	effector protein kinase B
PKR	protein kinase R
POLR2E	polymerase (RNA) II (DNA directed) polypeptide E, 25kDa
PR	post-replicative
PSMD2	proteasome (prosome, macropain) 26S subunit, non-ATPase, 2
PTEN	phosphate and tensin homologue
r	correlation coefficient
RAP94	RNA polymerase-associated protein of 94 kDa
RB	retino blastoma
RFP	red fluorescent protein
RGP	Radial-growth-phase
RIN	RNA integrity number
RNA	ribonucleic acid
rpm	rounds per minute
RPO	DNA-dependent RNA polymerase
RQS	RNA quality score
rRNA	ribosomal ribonucleic acid
RT	room temperature
rtfr	human transferin receptor
RUC	Renilla luciferase
RUNX3	runt-related transcription factor 3
SD	standard deviation
SELT	selenoprotein T
SHIP-2	SH2-containing 5'-inositol phosphatase 2
SNX17	Sorting nexin 17
SSB protein	single-stranded DNA binding protein
SSC	side scatter channel
ssDNA	single-stranded deoxyribonucleic acid
TBP	TATA binding protein
TF	transcription factor
TFIIS	eukaryotic transcription elongation factor SII
TGN	trans-Golgi network
TIL	tumor infiltrating lymphocytes
TIR	Toll/IL-1 receptor
TK	thymidine kinase
TLR	Toll-like receptor

TMED1	transmembrane emp24 protein transport domain containing 1
TNF	tumor necrosis factor
TRAF6	TNF receptor associated factor 6
TREM1	triggering receptor expressed on myeloid cells 1
ttRNA	total ribonucleic acid
TXNRD3	thioredoxin reductase 3
U	units
Ub/Ubl	ubiquitin/ubiquitin-like
UBE2D4	ubiquitin-conjugating enzyme E2D 4
UBR7	ubiquitin protein ligase E3 component n-recognin 7 (putative)
UTR	untranslated region
UV	ultra violet
VACV	vaccinia virus
VEGF	vascular endothelial growth factor
VETF	vaccinia virus early transcription factor
VGP	vertical-growth-phase
VITF	vaccinia virus intermediate transcription factor
VLTF	vaccinia virus late transcription factor
VPEF/FAM21	vaccinia virus penetration factor
VRI	viral replication indicator
VSV	vesicular stomatitis virus
WASP	Wiskott-Aldrich syndrome protein
WHO	World Health Organisation
WIP	WASP interacting protein
WNK1	WNK lysine deficient protein kinase 1
WR	vaccinia virus Western Reserve
wt	Wild-type
Y2H	yeast-two-hybrid
YY1	YinYang 1
ZNF69	zinc finger protein 69
ß	beta
γ	gamma
µg	microgram
µl	microliter

6.5 Eidesstattliche Erklärung

Hiermit versichere ich, dass ich die vorliegende Dissertation selbstständig und nur mit den angegebenen Quellen und Hilfsmitteln angefertigt habe.

Ich erkläre weiterhin, dass diese Dissertation weder in dieser noch in anderer Form bereits in einem anderen Prüfungsverfahren vorgelegt wurde.

Zuvor habe ich neben dem akademischen Grad “Diplombiologin, Univ.” keine akademischen Grade erworben oder zu erwerben versucht.

Bethesda, den _____

_____

(Jennifer Reinboth)

6.6 Publication List

Reinboth J, Ascierto ML, Chen NG, Zhang Q, Yu YA, Aguilar RJ, Carretero R, Worschech A, Zhao Y, Wang E, Marincola FM, Szalay AA.
Correlates Between Host and Viral Transcriptional Program Associated with Different Oncolytic Vaccinia Virus Isolates. Hum Gene Ther Methods, 2012 Oct 17.

Tomei S, Adams S, Uccellini L, Bedognetti D, De Giorgi V, Erdenebileg N, Ascierto ML, **Reinboth J**, Liu Q, Bevilacqua G, Wang E, Mazzanti C, Marincola FM.
Association between HRAS rs12628 and rs112587690 polymorphisms with the risk of melanoma in the North American population. Med Oncol. 2012 May 22.

Spivey TL, De Giorgi V, Zhao Y, Bedognetti D, Pos Z, Liu Q, Tomei S, Ascierto ML, Uccellini L, **Reinboth J**, Chouchane L, Stroncek DF, Wang E, Marincola FM.
The stable traits of melanoma genetics: an alternate approach to target discovery. BMC Genomics. 2012 Apr 26;13:156.

Guirado M, Gil H, Saenz-Lopez P, **Reinboth J**, Garrido F, Cozar JM, Ruiz-Cabello F, Carretero R.
Association between C13ORF31, NOD2, RIPK2 and TLR10 polymorphisms and urothelial bladder cancer. Hum Immunol. 2012 Jun;73(6):668-72

Ascierto ML, Worschech A, Yu Z, Adams S, **Reinboth J**, Chen NG, Pos Z, Roychoudhuri R, Di Pasquale G, Bedognetti D, Uccellini L, Rossano F, Ascierto PA, Stroncek DF, Restifo NP, Wang E, Szalay AA, Marincola FM.
Permissivity of the NCI-60 cancer cell lines to oncolytic Vaccinia Virus GLV-1h68. BMC Cancer. 2011 Oct 19;11:451.

Carretero R, Wang E, Rodriguez AI, **Reinboth J**, Ascierto ML, Engle AM, Liu H, Camacho FM, Marincola FM, Garrido F, Cabrera T.
Regression of melanoma metastases after immunotherapy is associated with activation of antigen presentation and interferon-mediated rejection genes. Int J Cancer. 2012 Jul 15;131(2):387-95

6.7 Conferences

- **Society for Immunotherapy of Cancer (SITC) 2010, 25th Annual Meeting**

  - attended

- **Federation of Clinical Immunology Societies (FOCIS) Meeting 2011**

  - attended

- **Society for Immunotherapy of Cancer (SITC) 2011, 26th Annual Meeting**

  - attended plus participated in the following posters:

  Jennifer Reinboth, Nanhai G. Chen, Qian Zhang, Yong A. Yu, Maria L. Ascierto, Ena Wang, Francesco M. Marincola, Aladar A. Szalay

  Influence of melanoma host cell factors on replication and early gene expression of oncolytic vaccinia virus isolates

  Qiuzhen Liu, Valeria De Giorgi, Tara L. Spivey, Zoltan Pos, Jaime Thomas, Daniela Murtas, Lorenzo Uccellini, Maria L. Ascierto, Davide Bedognetti, **Jennifer Reinboth**, Hui Liu, Ena Wang, Francesco M. Marincola

  Classification of melanoma cell lines according to immune modulatory properties

- **Society for Immunotherapy of Cancer (SITC) 2012, 27th Annual Meeting**

  - attended plus participated in the following posters:

  Jennifer Reinboth, Maria L. Ascierto, Nanhai G. Chen, Qian Zhang, Yong A. Yu, Ena Wang, Francesco M. Marincola, Aladar A. Szalay

  Correlation between human and oncolytic vaccinia virus transcriptional profile

  Maria L. Ascierto, Cathy Schechterly, Davide Bedognetti, Valeria De Giorgi, **Jennifer Reinboth**, Sara Tomei, Lorenzo Uccelini, Quizhen Liu, Ena Wang, Harvey Alter, Andrea De Maria, Francesco M. Marincola

  Effect of HCV viraemia on NK cells (chosen for oral presentation)

  Sara Tomei, Sara Civini, Davide Bedognetti, Valeria De Giorgi, **Jennifer Reinboth**, Maria L. Ascierto, Qiuzhen Liu, Lorenzo Uccellini, Ena Wang, Francesco M. Marincola

  The immune-related role of BRAF mutation in melanoma

  Qiuzhen Liu, Sara Tomei, Maria L. Ascierto, Valeria De Giorgi, Cuilian Dai, Lorenzo Uccellini, Tara Spivey, Zoltan Pos, Jaime Thomas, **Jennifer Reinboth**, Daniela Murtas, Davide Bedognetti, Ena Wang, Francesco M. Marincola

  NOS1 overexpression by melanoma cells contributes to type I IFNα signal dysfunction in immune cells

Acknowledgments

First of all I would like to thank my supervisor Prof. Dr. Szalay for giving me the opportunity to work on this fascinating and exciting project and for making it possible for me to carry out my studies at the National Institutes of Health in Bethesda, Maryland as well as at Genelux Corporation in San Diego, California. Furthermore, I highly appreciate Prof. Szalay's continuous support, guidance and mentorship.

A special thanks to all the members of Genelux Corporation for all their support and advice. I thank Dr. Nanhai Chen, Dr. Tony Yu and Dr. Qian Zhang for their help and guidance throughout the three years of my PhD. I am very grateful to Jason for not only providing me with cells and viruses, but also for teaching me virological methods and procedures. Furthermore I'd like to thank Terry and Melody for their help with cell culture and animal experiments. I'd like to thank Alexa and Ricky for their huge help with the animal studies during my time in San Diego.
I greatly acknowledge the graduate stipend and foreign travel grant provided by Genelux Corporation.

Great appreciation to Dr. Francesco Marincola and Dr. Ena Wang at the National Institutes of Health, Bethesda Maryland for having me in their laboratory and allowing me to carry out my studies in their research group. I am very grateful for their help and support with my projects and for their expertise.

I thank Dr. Dragan Maric for his help with the flow cytometric experiments and data analysis.

I further thank our technicians Hui, Jinguo, Rongye and Helen for teaching me various methods and for helping me whenever I needed assistance.

I thank Rafael for his help with the microarray studies and his friendship.

I thank all my friends & co-workers and former colleagues at NIH not only for their help and encouragement, but also for making my time here so special. Thank you, Lorenzo for sharing your work space with me for months and months, for teaching me some basic Italian ;-) and for being such a good friend. Grazie mille, Valeria for your invaluable help with my project, your guidance and friendship; you made especially my first week during orientation so much more fun. Thank you, Maria Libera for helping me with my projects and for always cheering me up especially when we were working late hours in the lab. A very special thanks you goes to my sorellina Sara 2, I can't thank you enough for everything you have done for me in and outside from work. I'd also like to thank my big sister Sara 1, Eliane aka "Holland", Davide, Qiuzhen, Ping, Daniela, Pablo, Pia, Marianna, Barbara, Luciano, and all others – THANK YOU!

My special thanks goes to my American friends Heidi and Jaime, thank you for all the great moments we shared over the past three years. I'm really grateful to have met you.

Ich möchte mich herzlich bei allen Mitgliedern der AG Szalay in Würzburg bedanken, insbesondere bei Prof. Dr. Grummt für die Unterstützung und insbesondere für das Korrekturlesen dieser Arbeit.

Ich danke Herrn Prof. Dr. Krohne ganz herzlich für die Übernahme des Zweitgutachtens.
Frau Prof. Dr. Förster danke ich vielmals für die Übernahme des Prüfungsvorsitzes.

Allen Würzburger Freunden und Kollegen möchte ich ganz herzlich für ihre Unterstützung und Freundschaft danken. Johanna, Micha, Ivo, Caro, Rike, Barbara, Marion, Lorenz, Elisabeth, Steffi und alle anderen, vielen Dank für alles, insbesondere für die herzliche Begrüßung und Aufnahme, jedes Mal, wenn ich zu Besuch vorbei gekommen bin und ihr mir das Gefühl gegeben habt, nie weg gewesen zu sein ☺. In diesem Zusammenhang danke ich auch allen Mitgliedern der Biochemie. Ein riesengroßes Dankeschön geht an Clemens, fuer die spontane Hilfe beim Einreichen dieser Arbeit ☺.

Ein ganz besonderer Dank geht an Julia. Danke, dass du immer für mich da warst und bist, dass du in jeder Lebenslage hinter mir stehst und mich immer unterstützt egal wie viele tausend Meilen zwischen uns liegen. Ich danke Dir außerdem sehr für das Gegenlesen dieser Arbeit!

Ein riesengroßes Dankeschön gilt meinen Freunden, die mir durch zahlreiche Emails, Telefonate, Briefe und Päckchen immer wieder gezeigt haben, dass große Distanzen wahren Freundschaften nichts anhaben können ☺. Denize, meine Zwillingsschwester, ejal wie oft oder selten wir uns sehen, hören du warst mir immer eine große Stütze. Die Hessenfraktion Tobi, Mariana und Jasmina, danke für eure Jahrzehnte lange Freundschaft. Vanessa, vielen Dank für deine Unterstützung und dein stets offenes Ohr. Tanja, die dritte im Bunde, danke für alles, und für unsere nächste Re-union kommen wir nach Basel ☺. Markus, vielen Dank für die zahlreichen bereichernden Momente während der gesamten Studienzeit.

Außerdem möchte ich mich ganz herzlich bei Inge und Jürgen bedanken. Danke, dass ihr mich immer so herzlich aufnehmt, ich fühle mich bei euch immer wie zu Hause. Außerdem danke ich euch sehr für eure Hilfe beim Einreichen dieser Arbeit.

Ein ganz besonderes Dankeschön gilt meiner Familie. Ich danke meinen Eltern, Christine und Werner Reinboth, von ganzem Herzen für ihre grenzenlose Unterstützung und den Glauben an mich. Alles was ich bisher erreicht habe, habt ihr mir ermöglicht. Tausend Dank! Meiner Schwester Kerstin danke ich dafür, dass sie trotz der Entfernung immer für mich da war und mir beigestanden hat. Robert danke ich dafür, dass er mich über Emails und Fotos immer auf dem neuesten Stand im Hause Scholl gehalten hat ☺. Weiterhin möchte ich mich bei meiner Oma Bernhardine und meiner Tante Gabriele bedanken, dafür, dass ihr immer für mich da wart und an mich geglaubt habt.

Am Ende möchte ich mich bei Dir, Christian bedanken. Deine uneingeschränkte Unterstützung und deine Liebe haben mir immer wieder Kraft gegeben und mich motiviert. Die letzten drei Jahre haben uns trotz der großen Entfernung nur noch fester zusammengeschweißt. Tausend Dank!